A LOWER-BOUND LIMIT ANALYSIS SOLUTION FOR LATERAL LOAD CAPACITY OF MASONRY WALLS

A THESIS SUBMITTED TO
THE GRADUATE SCHOOL OF NATURAL AND APPLIED SCIENCES
OF
MIDDLE EAST TECHNICAL UNIVERSITY

BY

DERYA KARADENİZ

IN PARTIAL FULFILLMENT OF THE REQUIREMENTS
FOR
THE DEGREE OF MASTER OF SCIENCE
IN
EARTHQUAKE STUDIES

DECEMBER 2019

Approval of the thesis:

A LOWER-BOUND LIMIT ANALYSIS SOLUTION FOR LATERAL LOAD CAPACITY OF MASONRY WALLS

submitted by **DERYA KARADENİZ** in partial fulfillment of the requirements for the degree of **Master of Science in Earthquake Studies Department, Middle East Technical University** by,

Prof. Dr. Halil Kalıpçılar
Dean, Graduate School of **Natural and Applied Sciences** _____

Prof. Dr. Ayşegül Askan Gündoğan
Head of Department, **Earthquake Studies** _____

Prof. Dr. Murat Altuğ Erberik
Supervisor, **Earthquake Studies, METU** _____

Assoc. Prof. Dr. Mustafa Tolga Yılmaz
Co-Supervisor, **Engineering Science, METU** _____

Examining Committee Members:

Prof. Dr. Mehmet Utku
Civil Engineering, METU _____

Prof. Dr. Murat Altuğ Erberik
Earthquake Studies, METU _____

Prof. Dr. Tolga Akış
Civil Engineering, Atılım University _____

Assoc. Prof. Dr. Mustafa Tolga Yılmaz
Engineering Science, METU _____

Assist. Prof. Dr. Bekir Özer Ay
Earthquake Studies, METU _____

Date: 06.12.2019

I hereby declare that all information in this document has been obtained and presented in accordance with academic rules and ethical conduct. I also declare that, as required by these rules and conduct, I have fully cited and referenced all material and results that are not original to this work.

Name, Surname: DERYA KARADENİZ

Signature:

ABSTRACT

A LOWER-BOUND LIMIT ANALYSIS SOLUTION FOR LATERAL LOAD CAPACITY OF MASONRY WALLS

KARADENİZ, DERYA
Master of Scıence, Earthquake Studıes
Supervisor: Prof. Dr. Murat Altuğ Erberik
Co-Supervisor: Assoc. Prof. Dr. Mustafa Tolga Yılmaz

December 2019, 121 pages

Masonry exists from very past centuries around the world which is used not only for sheltering, most of historical architectural masterpieces are masonry structures. Masonry offers advantages in many areas such as easy supply of materials, easy to construct and thermal durability of materials. However, the analysis of masonry buildings is not a easy task. Various reasons such as the diversity of materials used and the lack of characteristic properties of these materials, lack of design regulations and the fact that the analysis methods used for today's reinforced concrete and steel structures are not suitable for masonry buildings complicate the analysis of masonry buildings. Because these structures are non-engineered structures, it is difficult and time-consuming to apply complex analysis methods for masonry buildings. Limit analysis is a very useful and fast method for non-engineered buildings such as masonry buildings. In this study, it is provided to obtain lateral load capacity by using lower-bound limit analysis method. Starting from a wall with no opening with the lower bound theorem based on the provision of static equilibrium and yield conditions, the walls with various openings were calculated and the maximum lateral load they were able to take was found. In this way, the openings had an effect on the lateral load capacity of the wall and a comparison was made. In addition, various properties of the

wall have been changed to support the assumptions about the masonry wall. Matlab2017b program was applied for the application of the lower-bound theorem.

Keywords: Unreinforced masonry buildings, limit analysis, lower bound theorem, lateral load capacity, Mohr Coulomb failure criteria

ÖZ

YIĞMA DUVARLARIN YATAY YÜK KAPASİTESİ İÇİN BİR ALT-SINIR LİMİT ANALİZ ÇÖZÜMÜ

KARADENİZ, DERYA
Yüksek Lisans, Deprem Çalışmaları
Tez Danışmanı: Prof. Dr. Murat Altuğ Erberik
Ortak Tez Danışmanı: Doç. Dr. Mustafa Tolga Yılmaz

Aralık 2019, 121 sayfa

Yığma yapılar dünya üzerinde ilk barınma yerleri olarak inşa edildiklerinden beri gerek kırsal bölgelerde gerekse şehirlerde hala yaygın olarak kullanılan bir yapı çeşididir. Tarihi eserlerden barınmaya kadar birçok alanda kullanılan yığma yapılar, kullanılan malzemelerin kolay tedarik edilmesi, kolay şekilde inşa edilmesi ve malzemelerin termal dayanıklılığı gibi birçok konuda avantaj sunmaktadır. Ancak yığma yapıların analizi pek de kolay olmamaktadır. Kullanılan malzemelerin çeşitliliği ve bu malzemelerin karakteristik özelliklerinin eksik olabilmesi, tasarım kurallarının eksik olabilmesi ve günümüz betonarme ve çelik yapılar için kullanılan analizlerin yığma yapılar için uygun olamaması gibi çeşitli nedenler yığma binaların analizini güçleştirmektedir. Bu yapılar çoğunlukla mühendislik yaklaşımı olmadan inşa edilen yapılar olduğu için, karmaşık analiz yöntemlerini yığma yapılar için uygulamak güç ve zaman alıcıdır. Çoğu karmaşık analiz yönteminin yanında, limit analiz yöntemi ise yığma yapılar için oldukça kullanışlı ve hızlı bir yöntemdir. Bu çalışmada yığma duvarları alt-sınır limit analiz yöntemiyle yanal yük kapasitesinin elde edilmesi sağlanmıştır. Statik dengenin ve akma koşullarının sağlanmasını temel alan alt-sınır teoremi ile düz bir duvardan başlanarak çeşitli açıklıklara sahip duvarların hesaplamaları yapılmış ve alabilecekleri maksimum yanal yük

bulunmuştur. Bu sayede açıklıkların duvarın yanal yük kapasitesine etkisi bulunmuş ve karşılaştırma yapılabilmiştir. Bunun yanı sıra duvarın çeşitli özelikleri değiştirilerek yapılan hesaplamalar sonucu yığma duvar hakkındaki varsayımların desteklenmesi sağlanmıştır. Alt-sınır teoreminin uygulanması için Matlab2017b programından yardım alınmış ve buradan alınan sonuçlar ile değerlendirme yapılmıştır.

Anahtar Kelimeler: Donatısız yığma bina, limit analiz yöntemi, alt-sınır teoremi, yanal yük kapasitesi, Mohr Coulomb yenilme kriteri

To my family for their love, endless support and encouragement

ACKNOWLEDGEMENTS

I completed this work thanks to the people who helped me and believed in me. First of all, my family is always supportive and encouraging me. They always stand by my side. I would like to thank to my family to their love and endless support.

I would like to special thanks to my supervisor Prof. Dr. Murat Altuğ Erberik for the help me to complete this thesis, encouragement, patience and wisdom of the whole study. Special thanks to Assoc. Prof. Dr. Mustafa Tolga Yılmaz, my co-supervisor, for many things he taught, helping me to spend unlimited time, and for patience and guidance throughout the work.

TABLE OF CONTENTS

LIST OF TABLES

TABLES

LIST OF FIGURES

FIGURES

LIST OF ABBREVIATIONS

ABBREVIATIONS

URM	Unreinforced masonry
MC	Mohr Coulomb

LIST OF SYMBOLS

SYMBOLS

σ	stress
ε	strain
φ	yield function
δ_F	failure load factor
δ_L	load factor of statically admissible stress field
δ_U	load factor of kinematically admissible mechanism
σ_X	normal stress in x direction
σ_Y	normal stress in y direction
τ	shear stress
σ_1	maximum principal stress
σ_2	intermediate principal stress
σ_3	minimum principal stress
τ_{yield}	yield shear stress
σ_{yield}	yield stress
σ_V	vertical compressive stress
H	distributed lateral load
Fx	forces in x direction
Fy	forces in y direction
Fs	shear force

t	thickness of the wall
St	tensile strength of material
Sc	compressive strength of material

CHAPTER 1

INTRODUCTION

1.1. General

Masonry exists from very past centuries around the world. Humankind used masonry structures not only for sheltering. Lots of historical architectural masterpieces are masonry structures. These structures remain standing over the centuries as cultural and historical monuments of human nature. People used mud and stone to create living space in early centuries. This is the beginning of masonry construction and also civil engineering. Major part of building stock around the world; especially in Europe, Asia and South America consist of masonry construction, that means major part of the population still live and probably will continue to live in the future in masonry dwellings. One of the oldest known masonry structure is the Pyramids in Egypt, that were made of stone. Taj Mahal, Roman Colesseum are also examples of stone masonry construction. Figure 1 shows examples of historical masonry structures. It is a fact that majority of the historical buildings that we encounter today are made with the greatest possible knowledge at that times and are accepted as cultural heritage (Mourad and El-Hakim, 1996)

Figure 1.1. Examples of historical masonry structures (a) the Pyramids, (b) Tac Mahal, (c) Roman Colosseum

Recent research in structural engineering have focused on the design and analysis of modern and tall buildings. The results of these studies show how to build a more durable structure. The structural damage can be minimized if engineering knowledge, material properties and analysis methods are enhanced and used correctly. However, in rural areas, there are still buildings that have not been constructed with engineering knowledge. These structures are often masonry buildings that people have constructed only with tradition and experience from previous generations. These types of buildings have been built without making necessary design, calculations and analysis. As a result, they become vulnerable to seismic loads and damage is inevitable for these structures. Since masonry is very common in rural regions, it is of great importance to conduct their analysis (Bhattacharya et al, 2014). However, detailed and complex analysis methods become irrelevant since these structures do not even have a consistent structural system and in most of the cases, it is not possible to estimate their material properties to be used in structural analysis. Therefore, simple and practical analysis tools should be used in order to obtain seismic response of non-engineered masonry structures.

1.1.1. Characteristics of Masonry Units

Masonry generally consists of units such as clay, brick, stone, concrete block, etc and mortar joints that bind these units together to form structural walls. Mortar joints generally possess low strength as opposed to masonry units. Masonry can be classified as unreinforced, confined and reinforced. Existence of reinforcement in masonry provides more tensile strength to the structure. On the other hand, strength of unreinforced masonry depends on the strength of brick and brick-mortar interface. There are many factors affecting the strength of masonry structures. The walls constructed with brick and mortar create a non-homogeneous and non-isotropic continuum. Particularly, in masonry walls formed with natural stones, joints are completely in a random composition. Thus, the analysis methods developed for the walls formed with artificial stones may not be valid for the walls created with natural stones. In addition to that, there are many factors that affect the masonry strength like

layout of the bricks, size of the bricks, thickness of the joint, freshness of the mortar used, dimensions of the wall, water absorption capacity of masonry and workmanship. Considering all these factors, the difficulties in design, analysis and response calculation of masonry structures are noteworthy (Sutcliffe et al, 2001). Since masonry structures are strong in resisting vertical and gravity loads, their behavior under lateral loads such as earthquake and wind is more critical and worth to be investigated.

1.1.2. Behavior of Masonry Structures under Earthquake Loading

Determining the seismic behavior of masonry structures is more difficult and complex than that of frame structures made of reinforced concrete and steel materials. As mentioned before, strength of masonry depends on many factors. Similarly, seismic behavior of masonry structures depends on many different properties other than the strength of masonry. Some of these are the material characteristics, geometry of the structure, wall-to-wall, wall-to-roof and wall-to-slab connections, strength of mortar and its bond with the units (Mendes and Lourenço, 2014). Masonry structures cannot behave properly in the nonlinear range, because of the absence of ductility of structure and they cannot dissipate enough energy during deformation, which causes a narrow margin of safety.

Although strength of masonry in tension and shear is low, it can exhibit sufficient resistance due to earthquake loads, if design and construction are properly managed. Up to recent times, people have been building their own structures without proper earthquake resistance. Since in the past, current technology and engineering education level were not available, masonry buildings were designed and constructed by approximate and crude methods rather than engineering basis. Those, who managed to keep their buildings stood still, transferred the knowledge they used to the next generations, and in this way, people were able to construct structures to accommodate themselves for centuries. Without using mathematical and engineering background, people created magnificent structures. The new ones with the use of engineering

information were added to these structures, which were built with traditional methods in the first place.

However, masonry structures, that have increased in number exponentially from past to present, are generally considered to be vulnerable against seismic action. The reasons for this prejudice can be stated as follows. First, there is not much information in the literature about the construction of these structures since they had been constructed in traditional manner. Second, there is a lack of consistency of relevant standardized rules in order to observe the behavior of these structures, and because of this, difficulties arise in the analysis of these structures notwithstanding the anisotropy and non-homogeneity of the material and insufficient information about the behavior of units and mortar (Lourenço, 1996). That makes masonry structures difficult to understand from structural engineering point of view.

1.1.3. Failure Mechanisms of Masonry Structures

In unreinforced masonry construction, slabs and floors distribute lateral forces to the in plane walls and the connection between the orthogonal walls leads to box action under these forces. Masonry structures exhibit two local failure modes named as in-plane and out-of-plane failure according to the direction of loading as it is seen from Figure 1.2. In addition to that, walls can be exposed to combination of these actions. In-plane elastic stiffness of masonry walls is generally more than out-of-plane elastic stiffness.

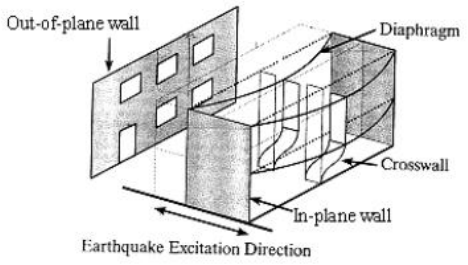

Figure 1.2. Behavior of unreinforced masonry walls under earthquake excitation (Yi,2004)

Piers and spandrels are two main components that are influenced by in plane loading and they show cracking, damage and failure accordingly. There are four types of in plane failure modes for masonry walls which are rocking, sliding, diagonal tension and toe crushing. The flexural cracks, usually occur as a result of flexural moment. Such damage occurs in the form of large horizontal cracks in the upper and lower parts of the piers. Accordingly, rigid body rotation at the corners of the piers can be seen as a result of flexural moment (Figure 1.3.a). If the shear stress applied to the system is more than the bond strength at the interface between the units and the mortar, shear sliding occurs in the pier, which is illustrated in Figure 1.3.b. Another case is the diagonal tension crack, which occurs if the principal tensile stress applied to the system exceeds the tensile strength of the wall. The mechanism of progress of this crack is to propagate from the weakest path. In a wall with weak mortar and strong unit combination, the progression of cracks is followed by the mortar head and bed joints. If the mortar and unit strength are close to each other, cracks pass through both unit and mortar which is presented in Figure 1.3.c. The last type of in-plane failure mode is toe crashing in which the principal compressive stress applied at the toe is greater than the compressive strength of the wall (Figure 1.3.d).

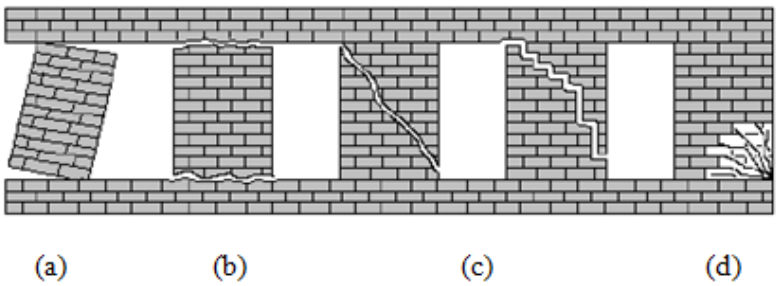

Figure 1.3. In-plane failure types of unreinforced masonry walls (a) rocking, (b) sliding, (c) diagonal tension, (d) toe crushing (Yi,2004)

Out-of-plane failure of masonry structures generally occurs as local failure or collapse because out-of-plane stiffness of walls is not as high as the in-plane stiffness. However

out-of-plane failure can be prevented by improving the connection between the walls and the floors in order to ensure box-like action of the structure. Figure 1.4 shows both out-of-plane behavior and in part in plane behavior of a typical masonry structure.

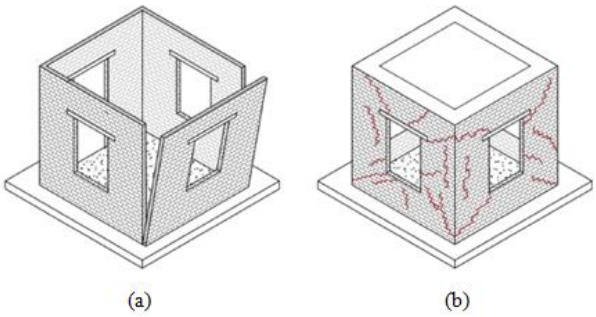

Figure 1.4. Failure types of masonry structures, (a) out-of-plane failure, (b) in-plane failure (Oyguc, 2017)

Seismic behavior of masonry structures is a critical issue that needs to be discussed and examined. As already mentioned before, accurate modeling, reliable input parameters and suitable analysis tools are essential for estimating the lateral strength of masonry structures in a correct manner. It can be possible to control which of the in-plane and out-of-plane actions on the masonry wall have priority. For example, if wall-to-wall and wall-to-diaphragm connections in a masonry structure are provided appropriately, local brittle failures, in other words out-of-plane failures, that are expected to occur as a result of seismic action, are avoided. Moreover, due to shear dominated behavior of masonry structures, in-plane mode is more pronounced in the structure if good connection details are ensured. Therefore, in analysis of a masonry structure, in-plane behavior generally dominates. In the in-plane direction, the walls are generally considered as piers and spandrels considering the door and window openings.

1.1.4. Effects of Openings in Seismic Behavior of Masonry Walls

If there are openings in masonry walls, such as doors and windows, these should be taken into account in the calculation of in-plane shear capacity of the wall. Spandrels are known to have a significant effect on the seismic behavior of masonry wall (Salmanpour et al, 2013). However, when the strength capacity of masonry walls is under concern, strength capacity of piers should be considered first rather than strength capacity of the spandrels.

If there is no opening in masonry walls, the in-plane stiffness of walls can be accurately calculated by simple mechanical formulations. On the contrary, if there are opening on walls, it becomes more complex to calculate. As the total area of openings increases, the in-plane stiffness and strength of the wall eventually decrease. Depending on the size and position of the openings, stress concentrations may occur at the corners of these openings. The aforementioned in-plane failure modes are too much influenced by the size and position of the openings as it is seen in Figure 1.5.

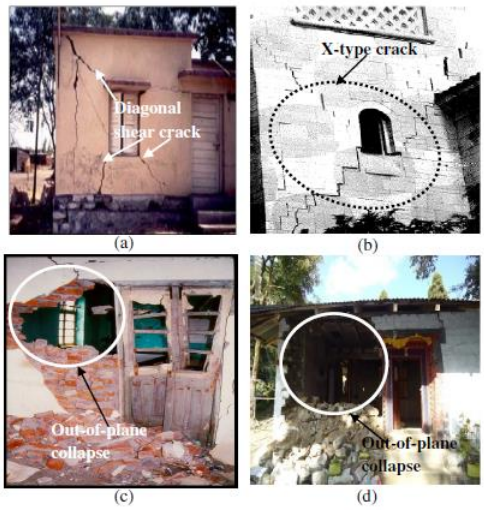

Figure 1.5. Different damage examples of masonry wall with openings, (a) diagonal shear crack, (b) X shaped crack, (c, d) Out-of-plane collapse (Nayak and Dutta, 2015)

1.2. Challenges in Analysis and Design of Masonry Structures

In today's world, design and analysis of reinforced concrete and steel structures have been made easier by developing programs and engineering knowledge. Lots of analysis methods and software programs are on the market for these types of structures. On the other hand, there are still difficulties in design, analysis, evaluation and prediction of the seismic behavior of masonry structures. First of all, since the behavior and characteristics of these structural types are very different from each other, analysis methods should also differ, as summarized in Table 1.1. While most of the analysis methods are used for reinforced concrete and steel structures, they cannot be used for masonry structures or these analysis methods yield too much computational time in the analysis of masonry. (Giordano et al, 2017).

Table 1.1. *Analysis strategies and differences of general structures and masonry structures (Giordano et al, 2017)*

	General Structures	Masonry Structures
Material/ structural components behavior in Service Limit State (SLS)	Linear elastic	Linear elastic response in compression. Very low resistance in tension (no-tension material assumption)
Material/ structural components behavior in Ultimate Limit State (ULS)	In general, it is possible to adopt elastic-plastic constitutive models in tension/ compression.	Material behavior in compression is characterized by softening branch.
Modelling	The structure (usually 3D frame) is represented by a beam finite element model	The structure is considered as a masonry continuum which, in some cases, cannot be discretized as a simple frame member
Type of analysis	Response Spectrum Analysis (RSA) is recommended by the codes and guidelines	Since elastic analysis cannot estimate the redistribution of stresses due to cracking, nonlinear methods are required.
Behavior under seismic action	Global behavior is guaranteed by proper node connections between structural elements	In case of poor wall-to-wall and wall-to-floor connections, extensive cracks and damage can lead to the collapse of the entire building

As the structural properties, construction stages and behavior under seismic action are different from each other, the design rules and analysis of masonry structures are not as standardized as reinforced concrete and steel structures. The uncertainty in the seismic behavior of masonry walls and the reasons for difficulties in design and analysis can be summarized as follows.

First, masonry walls are composite structures. Bearing elements are units (such as brick, blocks, etc) and mortar, in which the complexity is formed by the combination of unit and mortar. The main reason for the difficulties in the analysis of the masonry structures comes from this heterogeneity. Different characteristics of masonry units and mortar play crucial roles in the complexity regarding the analysis of the structure. These factors can be classified as the dimensions of the units, the quality of the mortar and unit, and the combination of these, the mechanical and material properties of the units and mortars, and the bond between unit and mortar. In addition, experimental measures of the material properties used for the analysis need to be accurate and reliable. However, the material properties for masonry units can show large variations even from sample to sample in the same batch. Another reason for the issues in structural modeling and analysis is that there is not enough material data about most of the existing masonry structures.

As mentioned earlier, most of the masonry buildings appear as residential dwellings in rural areas or as historical structures constructed in the past centuries. Lack of structural drawings, design specifications, technical reports and lack of knowledge about the materials used in construction make structural analysis of these masonry structures extremely difficult. In addition to that, another factor that causes difficulty in modeling and analysis is the load bearing system. Since these buildings were not designed and constructed by using engineering knowledge, the structural system is generally not definite and also adequate for the transfer of loads to the foundation safely. Hence modeling of the connection of the structural elements and components causes complexities and difficulties in the analysis. Although it is relatively easy to construct the model in a single wall, considering the whole structural system, the

connections of piers, spandrels, lintels and slabs with each other increase the difficulties in the analysis (Roca et al, 2005).

Generally traditional calculation methods are used for the analysis of masonry structures that are either numerical or empirical. Analysis methods and modeling strategies are mainly different from reinforced concrete and steel structures that cannot approached with the same criteria. The fact that the methods of analysis on masonry structures is limited compared to the other structures also cause a challenge for the engineers. This leads to another drawback, which is the education of engineers in the field of structural masonry. Due to the lack of new masonry structures in modern world and their usage in modern urbanization, lectures on masonry structures in engineering education are less than that of reinforced concrete and steel structures and engineers do not have much knowledge about this structural type. Therefore, it is very difficult to transfer this knowledge to the field and engineers need to train themselves when they have to deal with masonry structures (Lourenço, 1996).

1.3. Computer Programs for Masonry Structures

The challenges in analysis and modeling of masonry structures are discussed in Section 1.2. Because of these difficulties, analysis and modeling of masonry structures are not conducted by conventional strategies and methods like in the case of reinforced concrete and steel structures. Although there are lots of software programs that gives accurate and reliable results for the analysis reinforced concrete and steel structures, software programs are rare in the market to analyze masonry structures. Taking economical and reliable solutions results from modeling and analyzing of masonry structures, obtaining strength and behavior against to external forces and seismic actions and maintaining structural safety at the highest level are based on the engineering knowledge and experience rather than the software programs (Salmanpour et al, 2013).

Another reason why masonry structures cannot be analyzed with software programs easily is that material and mechanical properties of all components are not precisely

known. As mentioned before, since masonry structures consist of complex material domain which shows different properties due to heterogeneity, engineers should get the required information through laboratory tests or predict the values of these parameters. The former requires too much effort and time whereas the latter causes misleading results compared to the actual behavior.

In addition to that design, the rules and regulations of the structure and the system for example, the lintels, spandrels, the floor and their connections should be known by the engineer for using computers. The lack of this information has pushed engineers to obtain results by hand calculations instead of using software programs. It is easy and quick way to calculate the strength and seismic behavior of a masonry structure with the methods available in the literature. Lack of data, entering inputs to the programs and modeling of available information make that the computer programs is a waste of time for analysis of masonry structures and is not preferred so much. Of course, these methods are not useful for very complex masonry structures, but they provide sufficient results for single buildings and having relatively regular construction. Therefore, it is both economical, faster and more reliable to use methods provided to engineers instead of software programs. As a whole, using computer programs for analyzing and modeling of masonry structure is not an easy task so that another computational technique should be used.

1.4. Objectives and Scope

As mentioned in the previous chapters, it is unnecessary and time consuming to use complex programs for masonry structures. Since non-engineering unreinforced masonry structures do not have a specific design specification or a structural plan to use computer programs, it is not possible to analyze such structures using such programs. Instead, it is more appropriate to analyze by selecting simpler methods. The aim of this study is to obtain a practical method for estimating the lateral capacity of simple non-engineering masonry structures under a certain axial load. This allows the lateral capacity of the masonry walls to be easily achieved without having to deal with

detailed analysis methods. Load capacity, failure mechanism and behavior of unreinforced masonry under stress condition by using limit analysis method is presented in this study. By calculating the maximum capacity at the determined points of the wall without exceeding the yield criteria at any point of the wall during the collapse of the masonry walls, the maximum load on the side of the wall is calculated.

Main principle that is used is the lower bound theory to calculate ultimate load capacity of unreinforced masonry wall. The in-plane failure mode of the masonry wall is taken into consideration for the study and calculations are carried out against possible damages during this failure mode. For modeling strategy, macro modeling is chosen. Wall is considered as a single macro element. Mortar, unit and mortar-unit interface are assumed to be homogenized. The reason of assuming the wall as a single macro element is that ultimate load capacity of unreinforced masonry wall under stress condition can be calculated easier and faster by hand calculation. In addition to that, the global behavior of the building is more critical when compared to the local behavior of each component. For this reason, material properties of mortar, unit and mortar unit interface are not taken into account separately.

In order to obtain maximum lateral load, only the failure state of masonry wall is examined, and Mohr Coulomb failure criteria is obtained from the interface regions to obtain the condition of the wall just before the collapse. Lower bound limit analysis method is used in this study. Equilibrium equations of stresses are used to ensure the system to be in equilibrium state and any point in the system should not exceed the yield criteria. The boundary conditions are also taken into account and the lateral capacity of the wall is calculated.

This study is organized in 6 Chapters. In Chapter 2, analysis methods that are used to calculate masonry structures are mentioned and their use in literature is given. In Chapter 3, the limit analysis method and its application areas are explained. Three methods of limit analysis technique are explained and calculation methods are presented. Lower bound theory to be used in this study is given in detail in this chapter.

In Chapter 4, the calculation method which is developed by using the lower bound theory and the detailed procedure of the study are presented. In Chapter 5, sample walls that are calculated using the lower bound theory are examined and characteristics of these wall types are determined. The results of the experiments for the considered walls are compared with the results obtained with the calculation method in this study. In Chapter 6, summary of the study and conclusions are presented.

CHAPTER 2

LITERATURE SURVEY ON ANALYSIS TECHNIQUES FOR MASONRY STRUCTURES

2.1. Current State of Practice in Analysis Techniques

As mentioned in Section 1.3, modeling and analysis techniques of masonry structures are not handled by traditional computer programs and calculation methods as in the case of reinforced concrete and steel structures. For structural assessment purposes, the engineer needs to elaborate models of the mechanical behavior of materials. These models can vary widely from very accurate to very simplified ones. Accurate mechanical models enable to predict very closely the behavior of the analyzed structure when the loads and model parameters are known with good accuracy. These models can predict all the essential features and also many features that can be unessential in practice. At the other extreme, very simplified models produce limited and approximated information about the structural behavior. Nevertheless, this information can be enough in quantity and accuracy for engineering assessment purposes when the available data about the material properties, boundary conditions and loads is also roughly approximated. In order to analyze the masonry structures and to obtain proper results, it is necessary to choose the appropriate modeling approach and the analysis method. If all necessary data about the analysis of the system are known and the appropriate analysis method is chosen, it is easy to obtain the expected results for the masonry structure under concern.

Analysis methods can be categorized as follows: if structures such as historical buildings which is unpredictable in behavior against forces, has a complex geometry and possess material characteristics in wide variety, an accurate model can be used. This analysis model provides almost all the features of the building. If ordinary and

simple masonry structures are to be analyzed for which only global response parameters are required, it will be more convenient and practical to use simplified analyses (Orduna, 2003). Complexity of the unreinforced masonry structure makes the analysis more sophisticated.

First, the structural engineer needs to gather necessary information about the structure such as design report, plan layout, geometrical and material properties of the components. Next step is to decide the type of analysis to be used in accordance with the available structural input parameters and the required level of sophistication for the response parameters. The choices are static or dynamic analysis due to the nature of loading, and linear or nonlinear analysis due to the expected behavior of the structural model.

2.1.1. Modeling Strategies of Masonry Walls

In structural modeling phase, masonry structure should be divided into components in both macro and micro modeling approaches. Masonry wall, as mentioned earlier, is a heterogeneous medium that consist of masonry units and mortar and for the analysis of this structure, first of all, it is necessary to decide which modeling strategy should be chosen. In micro modeling approach, unit, mortar and unit-mortar interface are considered separately and the properties of each ingredient should be known. If more accurate results are required for the wall and it is expected to obtain the strength and strain states of each of these parts, it would be appropriate to select this detailed approach. However, as it can be realized, it would not be feasible to choose this modeling strategy if large structures are to be solved, as the calculations for each unit, mortar and unit-mortar interface will take too much time. Considering the large structures, micro modeling should be replaced with macro modeling because the global response of the building is more important than the local behavior of the components. In macro modeling, the heterogeneous wall is considered as a composite structure and the average strength and stresses are calculated. Therefore, when modeling complex and large structures, it would be more accurate to choose macro

modeling as the modeling method (Lourenço, 1996) In addition to micro and macro modeling techniques, a simplified micro modeling technique can be used in analysis of masonry structures. In simplified micro modeling technique, unlike other models, units are considered as continuum elements, while unit-mortar interface and mortar are considered to act together called as interface elements. On the contrary, in macro modeling technique, masonry is represented as continuum as a homogenized material. In the homogenization technique, representative element volume (REV) is used to evaluate unit, mortar and unit-mortar interface as a whole. This model combines all the elements under continuum with a fictitious orthotropic equivalent material and help to determine the behavior and limit values of the structure (Milani, 2011). Because micro-modeling is more detailed and consumes more time, it is used to analysis small structures or detailed components. This technique requires more data about the structure, however, relevant data about unit, mortar and unit-mortar interface cannot be provided all the time. In Figure 2.1, macro, micro and simplified micro modeling can be seen in detail.

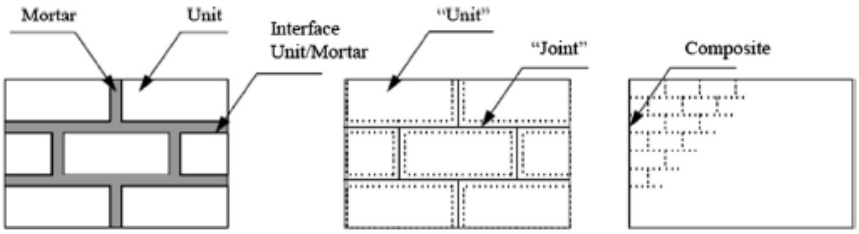

Figure 2.1. Modeling techniques of masonry, (a) detailed micro modeling, (b) simplified micro modeling, (c) macro modeling (Kamal et al, 2014)

2.1.2. Analysis Methods of Masonry Structures

After modeling the structure by choosing the right strategies, next step is analysis of the masonry structure. As mentioned before, it is not easy to analysis the structure with software programs as in reinforced concrete or steel structure. However, there

are other techniques to make analysis of masonry structure easier in literature. These analysis techniques can be classified as;

- Rigid block analysis
- Load path method
- Strut and tie method
- Equivalent frame method
- Discrete element method (DEM)
- Finite element method (FEM)
- Limit analysis method

Rigid block analysis method depends mostly on macro - micro element modeling. Rigid block analysis for masonry structure is regarded as the most practical analysis technique. Although rigid block analysis is the fastest and most practical way to analysis masonry structures and understand their behavior, there are some limitations of the method. In rigid block analysis, all failure modes cannot be demonstrated. More specifically, toe crushing and diagonal tension failure modes cannot be simulated in this method for masonry structures. The reason is that, toe crushing and diagonal tension failures are caused on masonry wall by high compressive stresses. Because wall types under high compressive stress values are not suitable for rigid body analysis, these failure types cannot be studied with rigid block analysis method. Hence, it is proper to apply this method for wall types exposed to low compressive stresses which cause rocking and sliding failure modes (Yi et al, 2006).

Second analysis method for masonry structures is the load path method. This method is very fast and easy to apply in the analysis of masonry structures, which is based on equilibrium and compatibility of the structure (Palmisano et al, 2003).

Third analysis method in the literature for masonry structures is the strut and tie method. This method was developed at the end of nineteenth century for reinforced concrete structures as an equivalent truss modeling technique. Load path method can be regarded as the extended version of the strut and tie method. Although the strut and tie method is very easy to use, there are some disadvantages. One of these is the selection of the appropriate model for the calculations. There is debate about the validity of the models. Another disadvantage is whether the engineer has full knowledge about the application or not. If it is decided to apply the strut and tie method is decided to be applied according to the chosen model, the knowledge and experience of the engineer in this method is important. If the engineer is not familiar with the approach, the technique can be a waste of time (Palmisano, 2016).

The fourth analysis method is the equivalent frame method. When using this method, walls and lintel beams are considered as discrete frame elements. The walls and beams are interconnected by rigid arms to make allowance for the real finite dimension of the wall (Roca et al, 2005). Complexities of the equivalent frame method comes mostly from the irregularities in geometry of structure, which make it hard to idealize the structure. In addition to that, limited information about the actual structure and lack of experimental tests results cause difficulties in technical aspects.

The fifth method for analysis of masonry is the discrete element method (DEM) which works by analyzing the collection of blocks in boundary states by modeling materials. The basic idea is to model the material as a discontinuum element on surfaces between different blocks. The DEM is used to model various states of non-linear behavior also containing very large displacements. In addition to that, this method is applicable to analyze the failures in static and dynamic ranges (Roca et al, 2010). The drawback of this technique is that it needs high computational effort. In addition to that, this method deals with nonlinearity and engineers should know previous failure conditions of masonry before the analysis and this information cannot be always accessible.

The last and probably the most commonly used analysis method for both masonry and other structures is the finite element method (FEM). In this method, there are three modeling strategies for masonry structures as micro modeling (brick, mortar and brick-mortar interface separately), simplified micro modeling (bricks and interface separately) and macro modeling. In finite element method, the structure is divided into meshes. Thus, the relationship between nodal forces and displacements can be established for each mesh. Equilibrium equations are written using external loads. Boundary conditions are defined. Then the system of equations is created using equilibrium equations and boundary conditions. The system is then resolved using nodal displacements. By using these displacements, strain and stress values at the nodes are obtained (Lourenço, 1996). In finite element analysis, masonry structure is subjected to incrementally increasing in-plane loading up to the ultimate state. Figure 2.2 shows the typical finite element mesh that Page and Ali (1988) stated in their study. For saving the computing time with negligible loss of accuracy, four noded quadrilateral elements are used where finer mesh has been employed near the loading point rather than more complex higher order elements.

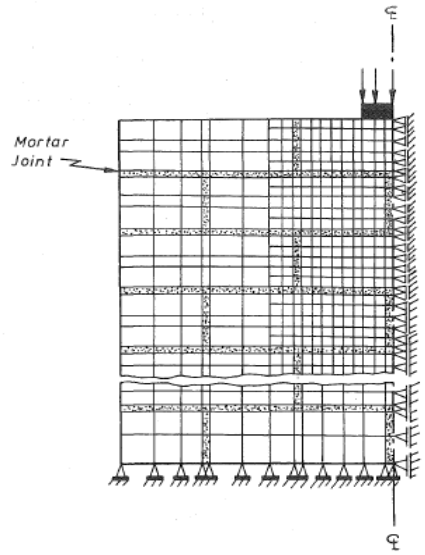

Figure 2.2. Finite element mesh (Ali and Page, 1988)

In finite element analysis, under low levels of loading, the elements are supposed to show elastic behavior and stresses are obtained according to this situation. As the load is increased, elements are accepted to show elastic-brittle behavior on condition that stresses are in tension direction, else elements are regarded as in nonlinear behavior. Two kinds of iterations are utilized to proceed from low levels to high levels of loading. One of them allows nonlinearity of the material. The other one allows the cracking to progress. Under specified loading, iterations continue as long as forces at the nodes are below the given value of tolerance. If the failure occurs, it will disperse to the entire width of the structure. The stiffness coefficient value is reduced in accordance with the failure type used. The stresses at the time the fracture occurs are distributed to other regions immediately or step by step. This dispersion depends on the type of failure the structure undergoes and the postcracking situation of the material. Repeated correction cycles for nonlinearity of material and control for failure continue until converging to a solution. These applications are repeated at each load increase mentioned above. The final failure occurs due to huge residual forces or absence of convergence when the deformations are calculated [Ali and Page, 1988].

Although finite element method is mostly used for masonry structure analysis, there are also disadvantages of this technique. First one is related to the identification of material properties of masonry structure, which is composed of brick and mortar with different material properties and different behavior under loading. Mortar joint between the units create anisotropic behavior and this makes it hard to get the actual material properties of the elements of masonry structures. The more data required, the more difficult is the method to be used for masonry structures. Because the required data may not be available or it may cause too much effort and time to obtain, method that require too much data such as finite element analysis is not always suitable for masonry structures (Mojsilovic, 2011). Another disadvantage is that finite element analysis is very time consuming and needs high computational effort. Because the analysis is conducted with step by step solution with incremental loading condition and iteration, it is not easy task to use it for large structures and it is time consuming

for practicing engineers. In addition to that, the selected parameters must be handled appropriately and carefully for these calculations. As a consequence, this method is suitable for special and important structures, but not for ordinary structures that should be analyzed frequently (Yi et al, 2006).

2.1.3. Limit Analysis Theory and Applications

Limit analysis method is successful, easy to apply to determine the ultimate capacity of masonry structures under given loading and stress state. Because masonry structures show complex behavior, limit analysis method make the analysis easier for engineers and give appropriate results about failure with minimum information about structure. Plasticity provides one of the most useful tool to calculate the approximate maximum load that structure can take. Plasticity has revealed two methods for calculating maximum approximate value. These are lower bound theorem and upper bound theorem. Although these methods will be explained in detail in the next chapters, they can be summarized as follows: Lower bound theory states that if the stresses that provide the internal equilibrium and boundary conditions of the system are lower than the yield stress value throughout the system, then collapse will not occur. The regions that meet this criterion in the lower bound theorem are called statically admissible stress fields. In upper bound theory, if the internal energy dissipation of the body is less than the work performed by the external forces, the collapse occurs. The regions that meet this criterion in the upper bound are called kinematically admissible stress fields (Davis and Selvadurai, 2009).

Limit analysis method is a simple tool and has many advantages to calculate maximum load under applied loading for masonry. Collapse mechanisms and stress distributions and ultimate strength of masonry can be determined by using limit analysis. It requires less material parameters, which hard to obtain for masonry structures, when compared to other types of analysis method. In addition, it also requires less computational time when compared to other methods, especially the finite element method. There are various types of analysis methods to be used by engineers. These methods vary

according to the type of structure and behavior made of the building analyzed. These types of analysis can be divided into two categories. First one is linear and nonlinear static analysis whereas second one is linear and nonlinear dynamic analysis. In this study, unreinforced masonry is chosen as the case study structural model. Since unreinforced masonry has a very low tensile strength and it exhibits inelastic action even under low levels of lateral load, linear analysis is not as considered a very suitable method. In addition to that, applying nonlinear analysis to unreinforced masonry structures is a very complex and time-consuming task as mentioned before. It requires intensive calculations and complex modeling techniques. Therefore, the most suitable method for calculating the maximum load that unreinforced masonry can take seems to be the limit analysis with macro block (Mendes, 2014).

2.2. Literature Survey

Analysis methods of masonry structures, such as rigid block analysis, load path method, strut and tie method, equivalent frame method, discrete element method, finite element method and limit analysis method, are studied in the literature by many authors.

Orduña (2017) studied non-linear static analysis which is performed by rigid block approach. He concluded that, some failure types cannot be studied by rigid block analysis and the method is suitable for wall types that are subjected to low stresses, which cause mainly shear failure. Yi et al (2006), obtained the maximum strength of masonry by using this method as an of upper-bound value.

Roca (2006) calculated the ultimate load capacity of masonry structures with simple equilibrium model under load path method. He also studied strut and tie method. The behavior of walls under vertical and horizontal forces was studied with this analysis method. Palmisano et al (2003) also chose load path method to assess the behavior of masonry structures under principal stresses.

Siano et al (2017) studied equivalent frame method in their study as a simplified procedure for structural modeling of masonry constructions with huge achievement

for the great harmony between the integrity of geometric identification and the convenience of mechanical calibration. Besides this, Quagliarini et al (2017) Roca et al (2005) also employed this method to analyze masonry structures.

Discrete element method and finite element method were also used by many researches. Roca et al (2010) studied discrete element method in order to analyze structural failures during static and dynamic loading. Sutcliffe et al (2001) studied finite element and lower bound theorem to calculate collapse load of masonry structure under in-plane loading by the help of Mohr-Coulomb approximation with three-node triangular elements. Mihai and Ainsworth (2009) used finite element procedure to obtain limit loads of linear-elastic blocks. Mohammed (2010) used a Fortran code for finite element analysis of walls and he observed the behavior of the masonry walls under monotonic loading. Senthivel and Lourenço (2009) investigated failure modes of stone masonry walls under combined axial compression and lateral shear load by using finite element analysis with micro modelling strategy. Ali and Page (1988) also studied failure condition of a brick masonry structure with finite element analysis under in-plane loading. In addition to these authors, finite element method was employed for masonry structures by Abdulla et al (2017) and Milani (2008).

In the literature, limit analysis method has also been studied by many authors. Milani et al (2007) studied limit analysis for unreinforced masonry structure under in-plane and out-of-plane loading and obtained collapse loads for the structure. In addition to that, Milani et al (2006.b) combined finite element analysis and limit analysis to obtain failure surfaces by both lower and upper bound limit analysis approach. Orduna and Lourenco (2005) studied limit analysis by modeling a three dimensional rigid block system. In this study, the formulation that was used provide compressive and torsion failures. Portioli et al (2015) also investigated this method in an efficient solution procedure for the crushing failure in 3D limit analysis of masonry block structures with non-associative frictional joints. Beside these studies, Li and Yu (2005) used upper bound limit analysis method to search for an answer to a nonlinear programming

problems. Serviceability of the upper bound theorem was shown in various numerical examples in that study. Kawa et al (2008), studied brick masonry structures by using lower bound analysis. They constructed plastically admissible stress field in accordance with equilibrium and boundary conditions. This method is also investigated by Milani (2015), Jiang (1994), Milani (2011), Livesley (1978), Gilbert et al (2006), Biolzi (1988), Li et al (2017). Limit analysis can also be used in soil stability problems by plasticity theory. Sloan (1988) is one of the authors that used this method for soil mechanics. In addition to that, Drucker and Prager (1951), Michalowski (2000), Chen and Scawthorn (1968) and Lia and Cheng (2012) invoked limit analysis by studying on soil mechanics.

CHAPTER 3

LIMIT ANALYSIS

3.1. Introduction

Theory of elasticity and plasticity are two branches of mechanics to understand the behavior of solid states. Elasticity theory focuses on linear elastic response without irrecoverable changes in strain, which means reforming to its original shape after loading is removed. Basic structural analysis is based on the elastic theory (Chen, 2000). On the contrary, in theory of plasticity, permanent deformations exist, after elastic stage has been exceeded and stresses cause deformation even though loading is removed. Limit analysis is the simplest and most useful method for performing plastic analysis compared to other methods. This theory was first developed in 1952 by Drucker and Prager in Brown University.

The use of limit analysis method for reinforced concrete structures began with Johansen (1930), who was developer of Yield-Line Theory for slab design and used upper bound theory of limit analysis. In the following research, Gvozdev (1960) studied limit analysis for reinforced concrete structure in an innovative manner for the first time. Lower bound theory of limit analysis, then, was investigated by Drucker for reinforced concrete beam design by using stress fields in 1961. Muttoni et al, improved this technique in later years by more practical ways for concrete structures in 1997.

Limit analysis is also used and provide benefit for soil mechanics in stability problems. Limit equilibrium method proposed by Terzaghi (1943) is the most powerful and common technique for the analysis of soil stability in favor of Mohr Coulomb failure criterion. Developments and studies related to soil plasticity was concentrated in 1960s at the University of Cambridge. Critical State Soil Mechanics, published by

Professor Roscoe and his team in 1968, has shed light on soil stability analysis in the coming years. (Schofield and Wroth, 1968).

Although masonry is the oldest construction type and has been existing from the very first centuries to the present time, developments of analysis methods for masonry are not so developed. Limit analysis in masonry structure was investigated first by Galileo and Hooke in 17th century. It is not modern limit analysis method but they used the basics of the theory. Robert Hook stated that "Ut pendet continuum flexile, sic stabit contiguum rigidum inversum" – "As hangs the flexible line, so but inverted will stand the rigid arch" in 1675. This statement was later developed by Poleni. It was used to analyze the cracking in the dome of St. Peter's Church (Orduna, 2003). After Poleni, bearing capacity of masonry arches were calculated with limit analysis method by Coulomb in 1776 which is close to the modern limit analysis theory. Gvozdev and Drucker and Prager are also the developers of limit analysis method for masonry structures. In addition, Heyman (1966) is the most well-known researchers which used and developed limit analysis method based on plasticity theory and limit analysis rules for masonry arches. Limit analysis is the simplest and the most useful method for performing plastic analysis compared to other methods. Limit analysis provides convenience and time saving in the analysis of masonry buildings.

3.2. Basics of Limit Analysis

Elastic analysis does not answer questions about reserve strength after the elastic limit. In other words, if stress exceeds the yield limit, the actual stress cannot be achieved by elastic analysis. Therefore, elastic analysis does not help to learn the total strength of the structure.

As it can be seen in Figure 3.1, when the material exhibits plastic behavior after the elastic limit or in other words the yield point, the analysis should be performed according to the plastic properties of the material. After this point, the reserve strength of the structure after the elastic limit is revealed. Plastic analysis ensures that the

remaining strength is obtained. Thus, the maximum strength of the structure is reached (Karnovsky and Lebed, 2010).

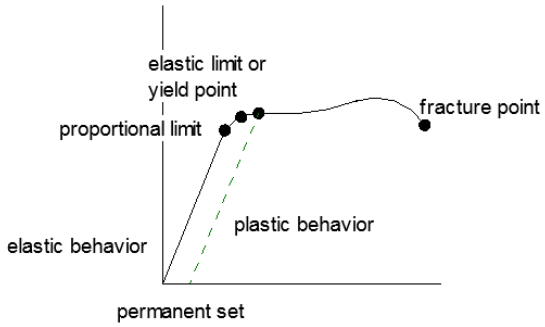

Figure 3.1. Stress-strain curve of ductile material

Since the plastic analysis is used to calculate the maximum load that the structure can take, the classical limit analysis method is defined based on the rigid perfectly plastic model, which is illustrated in Figure 3.2. Thus, the maximum load the structure can take can be calculated and failure mechanism can be determined by using the limit analysis method.

Figure 3.2. Stress-strain curve of rigid - plastic material

If the load applied to the system is less than the elastic limit, i.e. yield point, there will be no deformation and the system will return to its original state. From this point of view, no stress field can be defined for materials with stress values less than the yield stress. If the stress is increased above the yield point to the structure, unlimited deformation is possible even if there is no change in the loading after yielding. The state in which this event occurs is called "collapse by yielding". The last point where the load reaches its ultimate limit is called the "collapse load". It is also defined as the failure load. Since the load corresponds to the maximum load to be carried by the structure, the load carrying capacity of the building is also defined. The term limit analysis comes from this collapse by yielding state (Nielsen and Hoang, 2010).

If the structure is not very complex and/or very large and if the maximum load that the structure can carry is required without detailed calculations, it is best to use the limit analysis method. The limit analysis is based on rigid perfectly plastic behavior and the way to move to the plastic phase is through the yield point. Therefore, yield function φ is used as the basis for the limit analysis method. There are 3 cases in which the yield function can be found;

1) $\varphi < 0$ case, in which the stress value to the system has not yet reached the yield point and the structure is not damaged.

2) $\varphi = 0$ case, in which the load to the system has reached the yield point and the structure is on the verge of plastic deformation.

3) $\varphi > 0$ case, in which the load to the system has exceeded the yield point and the stress condition is not acceptable.

Limit analysis method is composed of three theorems. These are the lower bound or static theorem, the upper bound or kinematic theorem and the uniqueness theorem. In following paragraphs, these theorems are briefly explained.

Assume that, when maximum load level is reached in failure state, the load factor is δ_F. In case the structure remains on the safe side, that is, no collapse occurs, the internal

loads of the system must be in equilibrium with external loads. In addition to that, yield conditions must be provided. Yield condition is the case where the stress level applied to the structure is less than or equal to the strength of the material as described previously. This condition where the equilibrium state and yield condition are provided is called the lower bound or the static theorem. It is also known as the safe theorem. The largest statically admissible load factor is chosen within all the statically admissible load factors of the system and that is the safety factor δ_L. In other words, if the load safety factor δ_L of the system is less than or equal failure load factor δ_F, the system does not collapse as long as equilibrium of the system and yield conditions are maintained. In the lower bound theorem, maximum load factor is sought within the load factors.

In the case the upper bound theorem is applied, the structure becomes a mechanism. For each kinematically admissible mechanism, the load factor δ_U is assumed to be equal to or greater than the safety factor in the upper bound theorem while smallest of the load factor is chosen as safety factor in the lower bound theorem. In other words, if the load safety factor of the system δ_U is equal to or greater than failure load factor δ_F, the system collapses if the external work applied to the system is less than the internal work of the system. In the upper bound theorem, minimum load factor is sought within the load factors (Mendes, 2014).

The third limit analysis approach is the uniqueness theorem. The safety factor for the lower bound theorem can be equal to or less than the failure load factor δ_F. On the other hand, in the upper bound theorem the safety factor can be equal to or greater than the failure load factor. If the load factor of the system δ_L obtained from the lower bound theorem and the load factor δ_U obtained from the upper bound theorem are equal, the system is both in statically admissible stress condition and not on the safe side. In other words, the uniqueness theorem occurs when both mechanisms from the upper bound and the equilibrium equation and yield condition from the lower bound theorem are provided, and the safety factors of the two states are equal to each other and hence equal to the failure load factor δ_F. Failure load factor δ_F in the uniqueness

theorem is obtained by the safety factors obtained from two approaches. In Figure 3.3 three cases of limit analysis and their load factors can be seen.

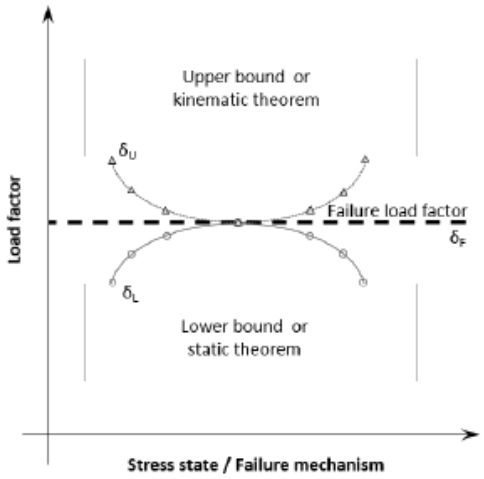

Figure 3.3. Limit analysis methods and load factors (Mendes,2014)

Lower bound and upper bound theorems are powerful methods that have been used for many years. Limit analysis method used in various analyses has provided simplicity and speed of calculation. Limit analysis method employs stress fields or velocity fields in the body, depending on the selected theorem. These fields help to obtain the maximum load that the structure can take or to obtain an approximate result of limit loads (Jiang, 1994).

3.2.1. Yield Surface and the Related Criteria

As mentioned above, if the system is loaded up to the yield level, the system exceeds elastic range and starts to exhibit plastic behavior. In this case, even if the load is completely lifted, the system cannot be completely restored and a permanent deformation is obtained. Any system that exceeds the yield level gets closer to collapse. There are many theorems that explain the concept of yielding. The most well-known of these are the Tresca theorem and the Von-Mises theorem.

According to Trescas's yield theorem, if maximum shear stress that occurs due to external loads acting on a mechanical system reaches to an ultimate value (τ_{yield}), yielding begins and the system shows plastic deformation. Hence all admissible stress fields should satisfy the inequality

$$\tau \leq \tau_{yield} \tag{3.1}$$

On all points of this system, where τ stands for shear stress and calculates as

$$\tau = \frac{\sigma_1 - \sigma_3}{2} \tag{3.2}$$

In the Von Mises theorem, again shear stress is used to provide the yield criteria. However, strain energy of shear deformation is considered instead of maximum shear stress. Accordingly, yielding starts when the strain of energy resulting from the loads applied to the system is equal or greater to the energy at the moment of yield of the system.

$$\frac{1}{2}((\sigma_1 - \sigma_2)^2 + (\sigma_2 - \sigma_3)^2 + (\sigma_3 - \sigma_1)^2) = \sigma_{yield} \tag{3.3}$$

where σ_1, σ_2 and σ_3 are the principal stresses when σ_{yield} is the yield stress. Figure 3.4 shows a comparison of the Tresca and the Von mises yield surfaces.

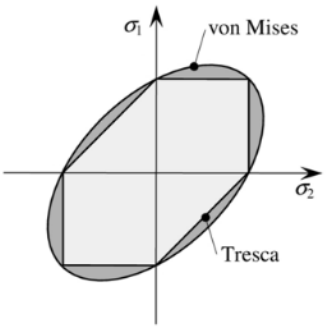

Figure 3.4. Tresca and Von Mises yield criteria (Bocko et al,2017)

3.3. Heyman's Assumptions on Masonry Structures

As mentioned previously, masonry structures are more complex and difficult to analyze than reinforced concrete and steel structures, and certain difficulties may be encountered when applying the limit analysis method to masonry structures. Heyman (1966) has identified three assumptions to be considered when analyzing masonry structures. These assumptions are not absolutely correct for the structure being analyzed, but are based on his previous experience, which should be considered before or during the application to obtain a better result. These three assumptions can be stated as follows;

1) Masonry has no tensile strength: Materials that constitute a masonry wall (i.e. units and mortar) have low tensile strength, which is generally the main cause of failure. Therefore, ignoring the tensile strength is a conservative and reasonable assumption.

2) Masonry has unlimited compressive strength: If the average stress is taken into account, it can be assumed that masonry has unlimited compressive strength. In masonry structure under high compressive forces, damage due to compressive stresses can be formed as splitting or crushing. These types of damage are not as crucial as the damage caused by tension cracks.

3) Sliding failure does not occur in masonry: This statement is not always valid in masonry structures. It has been observed that sliding failures occurs especially in masonry structures constructed using stone units. However, it has been seen that providing a slight prestressing is sufficient to prevent these sliding failures in masonry structures.

3.4. The Lower Bound Theory

In lower bound theorem, some conditions need to be satisfied to ensure that the structure is on the safe side. These conditions can be sorted as;

1) Satisfying equilibrium equations (the internal loads of the system must be in equilibrium with external loads)

2) Satisfying the boundary conditions

3) Any point in the body does not violate the yield condition (yield condition is the case where the stress level applied to the structure is less than or equal to the strength of the material)

As long as these three conditions are provided, the load condition at any point in the system cannot be greater than the actual collapse load. The conditions provided by these conditions are called statically admissible stress field. As it can be realized, the lower bound theory takes into account only the equilibrium and yield. The kinematic state of the system is not the subject of the lower bound theorem. The load on the structure is multiplied with load factor δ which is increased from zero to its final value. Limit load factor is failure load factor δ_F. The largest statically admissible load factor is chosen within the all statically admissible load factors of the system and that is the safety factor is δ_L. In other words, if the load safety factor δ_L of the system is less than or equal failure load factor δ_F, the system does not collapse while equilibrium of the system and yield conditions are provided. If the appropriate statically admissible stress field is provided for the structure, the system is safe (Orduna, 2003).

One of the most important advantages of the lower bound theorem is that complex loads and structures with different geometries can be analyzed easily. Although analysis of such structures normally takes a lot of time with complex methods and programs, lower bound theorem ensures computational time saving. Briefly, lower bound theorem is not only a very simple method in terms of reaching the maximum loads that structures can take, it is also easy and convenient method that minimizes the computational effort.

3.5. The Upper Bound Theory

In the upper bound theorem, some other conditions should be provided to ensure that the structure is on the unsafe side. These conditions can be defined as;

1) Satisfying the velocity conditions

2) Satisfying the strain velocity compatibility conditions which should not be less than the actual collapse value.

As long as these two conditions are provided, the load condition at any point in the system cannot be less than the actual collapse load. In other words, if the work resulting from external loads in the system is equal to or greater than the rate of dissipation in the internal energy, then the collapse occurs. The conditions provided by these conditions are called kinematically admissible deformation field. The theorem takes into account the calculation of velocity and energy dissipation. That means, unlike lower bound theorem, it is not necessary to provide stress dissipation in equilibrium.

The load on the structure is multiplied with load factor δ. Limit load factor is the failure load factor δ_F. The smallest load factor is chosen within all the admissible load factors of the system and that is the safety factor is δ_U. In other words, if the load safety factor of the system δ_U is equal to or greater than failure load factor δ_F, the system collapse if the external work applied to the system is less than the internal work of the system. If the appropriate kinematically admissible stress field is provided for the structure, the maximum load that the system can take is obtained.

3.6. The Uniqueness Theorem

In the uniqueness theorem, if both statically admissible stress field and kinematically admissible velocity field are satisfied at the same time, then the uniqueness theorem takes place.

The load condition necessary for statically admissible stress field must be less than or equal to the collapse load. On the other hand, the load condition necessary for kinematically admissible velocity field must be equal to or greater than the collapse load. In the uniqueness theorem where these two conditions are supplied together, the load is unique and is equal to the collapse load.

In the collapse state, all parts of the system are not deformed and stresses in the non-deformed parts cannot be found using this theorem. With this method, only stresses within or on the yield surface are obtained. It is possible to have different geometric areas of the same load carrying capacity within the system, because both conditions must occur simultaneously for uniqueness theorem to occur. When studying these different geometric fields, there may be situations in which stresses are equal at different places in the body, in which strains are different than zero. So, with this theorem, the load that the system can carry is calculated. However, it is not a suitable theorem to uniquely identify failure mechanism or stress fields (Nielsen and Hoang, 2010).

CHAPTER 4

METHODOLOGY

4.1. Introduction

Limit analysis theorem is a common method used to determine the strength of structures and provides time savings. There are two options for the solution of a problem which are the upper bound method and the lower bound method. The lower bound method is used in this study for analysis of ultimate load on masonry walls. Lower bound theory states that if the stresses that provide the internal equilibrium and boundary conditions of the system do not violate the yield criterion throughout the system, then collapse will not occur as discussed in Chapter 3. An application of lower bound method for analysis of masonry wall is explained in this Chapter.

4.2. Method of Analysis

It is assumed that a masonry wall is exposed to in-plane stresses. So a wall to be analyzed is first divided into an appropriate number of rectangular panels. 3 in-plane stress components σ_X, σ_Y and τ are accepted as internal stresses for each node. The out-of-plane stresses are all taken as zero. After obtaining equilibrium equations for each rectangular panels, boundary conditions are determined. Mohr Coulomb failure theory is implemented in lower bound method. The equations obtained using Mohr Coulomb failure theory are used for each node of the wall in order to obtain ultimate stress conditions of these nodes. A computer program in the language of Matlab2017b (Mathworks, 2017) is developed. Thus the ultimate load that can be applied on a wall before collapse is found.

4.3. Procedure of The Study

For each wall type, the wall was first divided into rectangular panels. The unknowns are stresses on each node located on corners of these panels. It is assumed that any stress component is changing linearly between nodes. Calculations are performed before the analysis of sample wall types into the software environment in order to calculate maximum lateral load which wall sample can carry. The equations to be determined are obtained from the principles of lower bound method described in Chapter 3. These are;

1) satisfying equilibrium equations for each rectangular panels for static equilibrium,

2) satisfying the boundary conditions,

3) satisfying yield condition by applying Mohr Coulomb failure criteria to each nodes.

So the number of equations should be consistent with the number of unknown stresses.

4.3.1. Stresses on Nodes of Rectangular Panels

To analyze masonry walls, each wall should be divided into rectangular panels. Stress condition is assumed at each node of a panel which consists of normal stresses σ_X and σ_Y and shear stress τ, considering only the in-plane stresses of the body. Figure 4.1 presents a sample wall with 4 rectangular panels and an illustration of stresses on node i. Each node on the wall is indicated by a black dot.

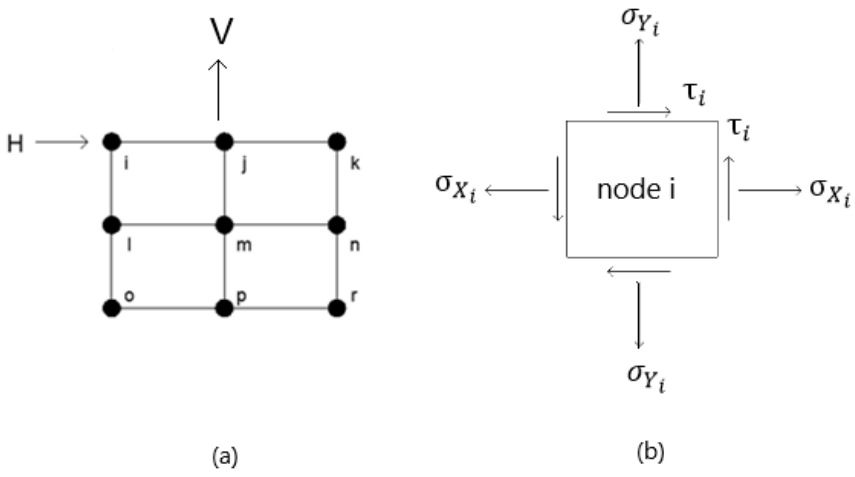

Figure 4.1. Determination of stresses (a) a wall with 2x2 rectangular panels, (b) an illustration of stresses on node i

In a system with three unknown stresses for each node, the total number of unknowns is three times the total number of nodes. These are unknown internal stresses of the wall. In addition, the ultimate lateral load which is indicated by H is considered unknown. The total vertical load on a wall which is shown by V is supposed to be known. In order to find unknowns of the system, a system of equations should be built. In case of linear equations, these equations yield to

$$[A] \cdot \{\sigma\} = \{B\} \tag{4.1}$$

Here, {σ} is a vector consisting of all unknowns. [A] is the coefficient matrix consisting of multipliers for stresses in equations and {B} is the vector consisting of the constant terms in these equations. All available equations will be written on the matrices one by one for each unknown. These equations are explained in the following sections.

4.3.2. Equations for Static Equilibrium

First rule of the lower bound method is satisfying equilibrium equations which is mentioned in Section 3.4. The equilibrium in the x direction and in the y direction must be maintained for each rectangular panel. Positive stress conditions are accepted for each node for the stress distributions. Figure 4.2 shows the stress distribution on the periphery of a rectangular panel which has four nodes, i, j, l and m. The dimension in x direction of the block is shown as 'a' and the dimension in y direction is shown as 'b'. The thickness of the wall in out-of-plane direction is equal to 't'.

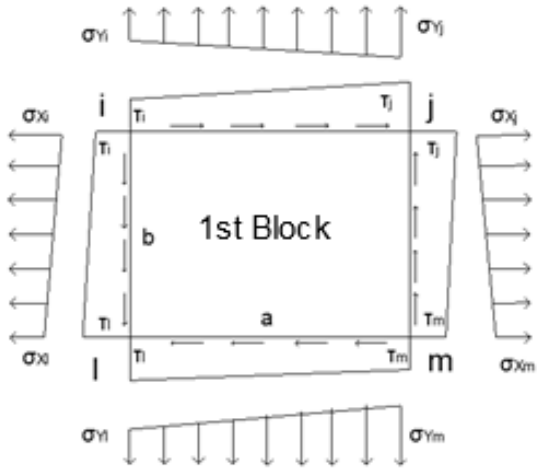

Figure 4.2. General stress distribution for a rectangular panel

The stress change between the two nodes was assumed to be linear. The total force acting on each side was found from the area of the trapezoid. Figure 4.3 presents the resultant forces acting on each side. Formulas for the resultant normal forces and resultant shear forces obtained from normal stresses and shear stress acting on each edge of a panel are as follows;

$$F_{X_{il}} = (\sigma_{Xi} + \sigma_{Xl}) \cdot \left(\frac{b}{2}\right) \cdot t \tag{4.2}$$

$$F_{S_{il}} = (\tau_i + \tau_l) \cdot \left(\frac{b}{2}\right) \cdot t \tag{4.3}$$

where F_{Xil} is resultant normal force and, F_{Sil} resultant shear force acting on the side between nodes i and l.

$$F_{Y_{ij}} = \left(\sigma_{Yi} + \sigma_{Yj}\right) \cdot \left(\frac{a}{2}\right) \cdot t \tag{4.4}$$

$$F_{S_{ij}} = \left(\tau_i + \tau_j\right) \cdot \left(\frac{a}{2}\right) \cdot t \tag{4.5}$$

where F_{Yij} is resultant normal force and, F_{Sij} resultant shear force acting on the side between nodes i and j.

$$F_{X_{jm}} = \left(\sigma_{Xj} + \sigma_{Xm}\right) \cdot \left(\frac{b}{2}\right) \cdot t \tag{4.6}$$

$$F_{S_{jm}} = \left(\tau_j + \tau_m\right) \cdot \left(\frac{b}{2}\right) \cdot t \tag{4.7}$$

where F_{Xjm} is resultant normal force and, F_{Sjm} resultant shear force acting on the side between nodes j and m.

$$F_{Y_{lm}} = (\sigma_{Yl} + \sigma_{Ym}) \cdot \left(\frac{a}{2}\right) \cdot t \tag{4.8}$$

$$F_{S_{lm}} = (\tau_l + \tau_m) \cdot \left(\frac{a}{2}\right) \cdot t \tag{4.9}$$

where F_{Ylm} is resultant normal force and, F_{Slm} resultant shear force acting on the side between nodes l and m.

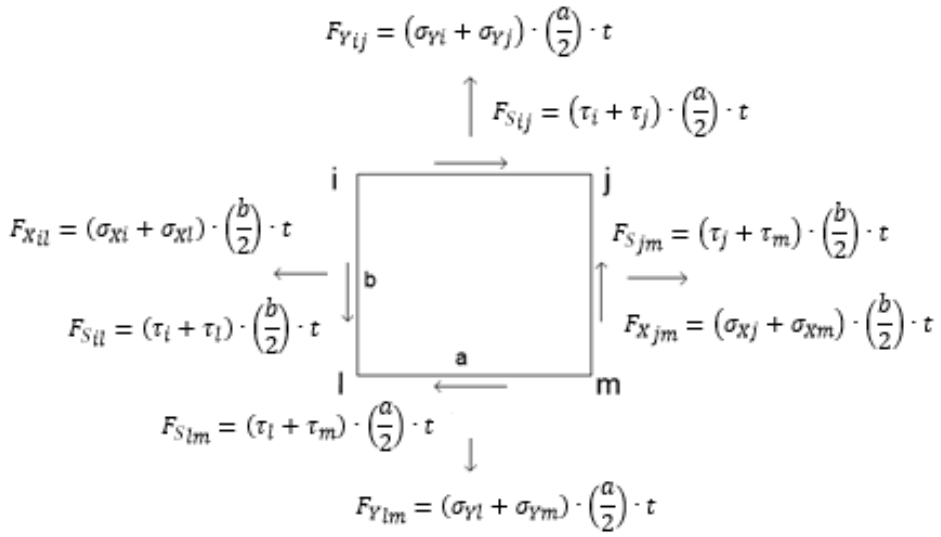

Figure 4.3. The resultant forces acting on each side of a rectangular panel

In order to satisfy equilibrium, the total forces acting in x and y direction must be equal to zero.

$$-F_{X_{il}} + F_{X_{jm}} + F_{S_{ij}} - F_{S_{lm}} = 0 \tag{4.10}$$

$$F_{Y_{ij}} - F_{Y_{lm}} - F_{S_{il}} + F_{S_{jm}} = 0 \tag{4.11}$$

In addition to equilibrium equations of each panels, in order to satisfy equilibrium, total moment created by the forces acting on the wall ∑M should be equal to zero. Figure 4.4 shows the reaction forces at bottom nodes and their moment arms. It is

assumed that the sum of external forces acting on right and left sides of a wall is equal to zero.

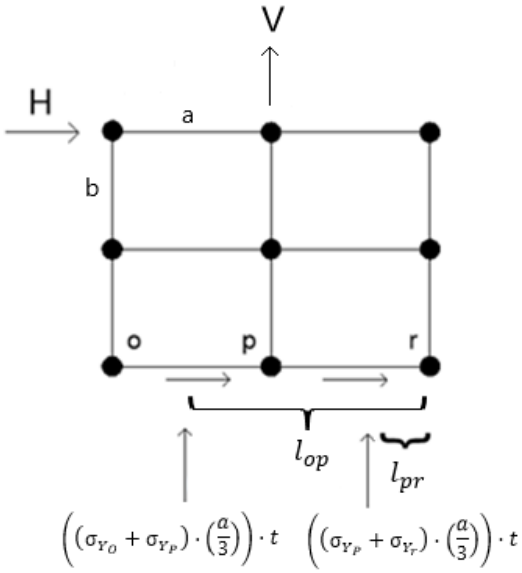

Figure 4.4. Reaction forces and center of gravity of trapezoidal distributed forces

Sum of moments around the node located on the right down corner (r) is calculated. In Figure 4.4 moment arms of forces Fy_{op} which is acting between nodes o and p and Fy_{pr} which is acting between nodes p and r, are l_{op} and l_{pr} respectively. These moment arms are formulated as

$$l_{op} = a + (\frac{a}{3}) \cdot \left(\frac{\sigma_{yp} + 2 \cdot \sigma_{yo}}{\sigma_{yp} + \sigma_{yo}}\right) \tag{4.12}$$

$$l_{pr} = (\frac{a}{3}) \cdot \left(\frac{\sigma_{yr} + 2 \cdot \sigma_{yp}}{\sigma_{yr} + \sigma_{yp}}\right) \tag{4.13}$$

Total moment around node r on Figure 4.4 is;

$$F_{Y_{op}} \cdot l_{op} + F_{Y_{pr}} \cdot l_{pr} + H \cdot (2 \cdot b) + V \cdot a = 0 \quad (4.14)$$

The ultimate lateral load H is calculated by using nodal stresses on top of a wall as explained in Section 4.3.5. This formula is extended for wall models with more rectangular panels. The equations of equilibrium (4.10) and (4.11) are applied to each rectangular panels. Equation (4.14) is also written in terms of stresses so that all equations of equilibrium can be substituted in Equation (4.1).

4.3.3. Equations for Boundary Conditions

The boundary conditions should be satisfied according to the second rule of lower bound method (Section 3.4). Boundary conditions can be divided into three. These are boundary conditions on top of the wall, sides of the wall and around openings. The equations for boundary conditions are applied on each node at sides of a wall.

4.3.3.1. Boundary Conditions on Sides of the Wall

Boundary condition for the sides is based on the forces coming to the right and left sides of the wall. In Figure 4.5 a wall with 2 by 2 rectangular panels is illustrated as an example. The resultant forces due to internal stress distribution between nodes i and l are given at the edges of the wall. The width in x direction of the block is shown as ‘a’ and the dimension of y direction is shown as ‘b’ in the figure. The resultant normal forces are calculated as shown by the Equations (4.2) and (4.6) whereas the resultant shear forces are calculated as shown by Equation (4.3) and (4.7).

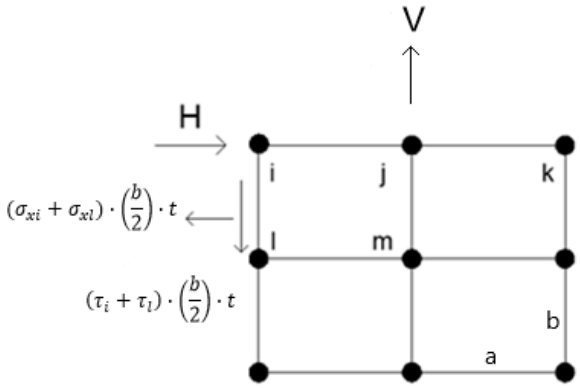

Figure 4.5. Illustration of sample 2x2 meshed wall with internal forces at sides of the wall

In the situation where only lateral load H and vertical load V coming from top of the wall, there is no external axial force in the x direction and external shear force acting on the left and right sides of the wall. Therefore, the resultant forces on right and left side of a wall should be all equal to zero. Total forces equations between every node located at the right and left sides of the wall can be written as;

$$(\sigma_{xi} + \sigma_{xl}) \cdot \left(\frac{b}{2}\right) \cdot t = 0 \tag{4.15}$$

$$(\tau_i + \tau_l) \cdot \left(\frac{b}{2}\right) \cdot t = 0 \tag{4.16}$$

These equations are generic for all rectangular panels located at the right and left boundary of a wall.

4.3.3.2. Boundary Conditions of Top of the Wall

After providing the right and left boundary conditions, the boundary conditions at the top edge of the wall should be considered. Vertical forces acting on top of the wall are

calculated from normal forces acting on the top of the wall between nodes i, j and k. Vertical forces acting on a wall with four rectangular panels are shown in Figure 4.6.

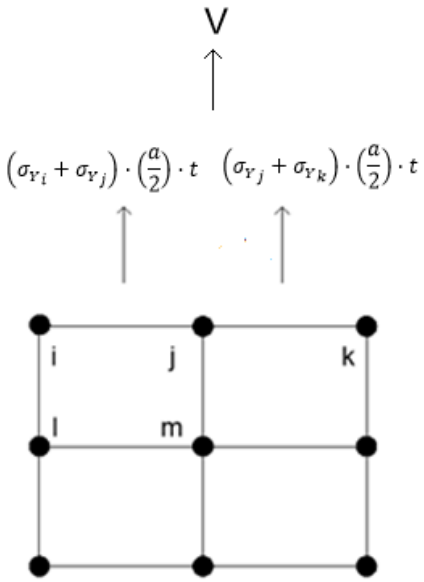

Figure 4.6. Calculation for the external force acting on top of the wall

In order to satisfy equilibrium on top of the wall, total force acting in vertical direction should be equal to vertical load V applied on a wall. Equation of total forces on the top of the wall can be written as;

$$\left(\left(\frac{a}{2}\right) \cdot t\right) \cdot \left(\sigma_{Y_i} + \sigma_{Y_j}\right) + \left(\left(\frac{a}{2}\right) \cdot t\right) \cdot \left(\sigma_{Y_j} + \sigma_{Y_k}\right) = V \tag{4.17}$$

4.3.3.3. Boundary Conditions around Openings

If there are openings on a wall such as windows and doors, the boundary conditions around these openings should be defined. In Figure 4.7, there is an opening between

nodes i, j, k and l. Axial forces on the lines connecting these nodes are calculated by Equation (4.2) and (4.6).

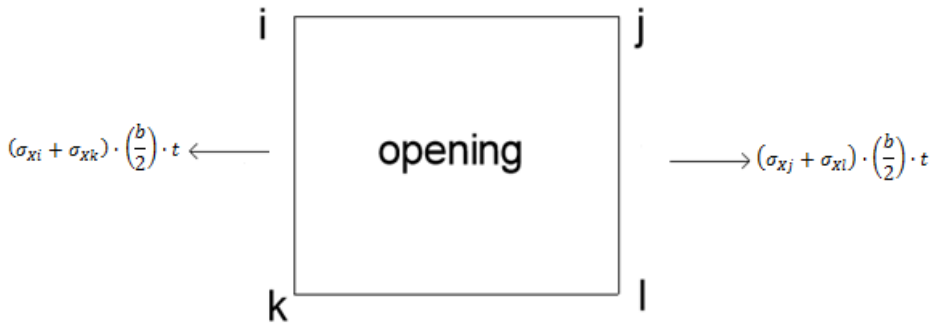

Figure 4.7. Total forces acting on sides of the opening

It is assumed that there is no external normal force on the sides of the window in the x direction. Therefore, the total force between right and left sides of windows should be equal to zero as shown in Equation (4.18a) and (4.18b). Since shear force from the top edge of the window is supposed to be transmitted through the window edges, then shear force acting on left and right side of a window are supposed to be different from zero.

$$(\sigma_{Xi} + \sigma_{XK}) \cdot \frac{b}{2} \cdot t = 0 \tag{4.18a}$$

$$(\sigma_{XJ} + \sigma_{Xl}) \cdot \frac{b}{2} \cdot t = 0 \tag{4.18b}$$

4.3.4. Application of Mohr Coulomb Failure Criterion

The Mohr Coulomb failure criterion is related to maximum principal stresses σ_1 and minimum principal stress σ_3. By ignoring the intermediate principal stress σ_2, it

explains the ultimate stress condition of an isotropic material in a three-dimensional stress space. From Mohr's stress circle principal stresses are obtained as;

$$\sigma_1 = \frac{\sigma_x + \sigma_y}{2} + \sqrt{\left(\frac{\sigma_x - \sigma_y}{2}\right)^2 + \tau_{xy}^2} \tag{4.19}$$

$$\sigma_3 = \frac{\sigma_x + \sigma_y}{2} - \sqrt{\left(\frac{\sigma_x - \sigma_y}{2}\right)^2 + \tau_{xy}^2} \tag{4.20}$$

Mohr Coulomb failure criterion can be explained by using Mohr stress circle. In case diameter of Mohr's circle is tangent to the failure envelope, the stresses on that point in a material has reached to an ultimate condition. A larger stress circle is not admissible. This is illustrated in Figure 4.8.

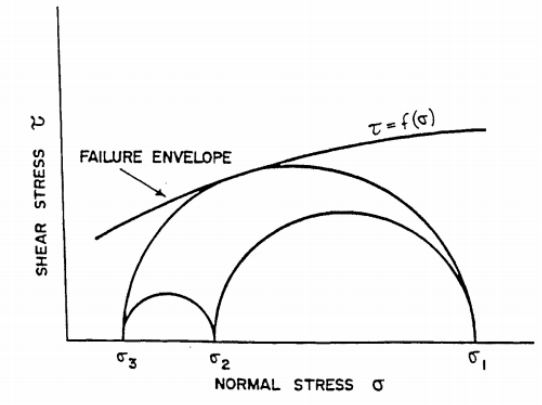

Figure 4.8. Mohr envelope for the soil (Yuen, 2003)

The use of a linear failure envelope simplifies the Mohr-Coulomb equations as shown in Figure 4.9. In that case only two material parameters, the compressive strength (Sc) and the tensile strength (St), are sufficient to define ultimate stress state on a brittle material.

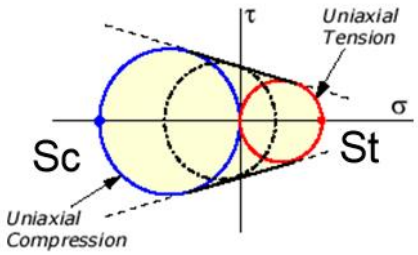

Figure 4.9. Mohr envelope for brittle materials (eFunda, 2019)

Consequently, there are 3 cases that describe the ultimate stress states during failure of a brittle materials on Mohr's circle envelope.

1) Case 1

If principal stresses σ_1 and σ_3 are both in tension state ($\sigma_1 > 0$ and $\sigma_3 > 0$), then failure will occur when principal stress σ_1 becomes equal to the tensile strength of material (S_t).

$$\frac{\sigma_1}{S_T} = 1 \tag{4.21}$$

After substitution of Equation (4.19), the ultimate state for this case is expressed as;

$$\frac{\frac{\sigma_x + \sigma_y}{2} + \sqrt{\left(\frac{\sigma_x - \sigma_y}{2}\right)^2 + \tau_{xy}^2}}{S_T} = 1 \tag{4.22}$$

2) Case 2

If σ_1 is in tension state and σ_3 is in compression state ($\sigma_1 > 0$ and $\sigma_3 < 0$), then failure will occur when principal stresses satisfy

$$\frac{\sigma_1}{S_t} - \frac{\sigma_3}{S_c} = 1 \tag{4.23}$$

After substitution of Equations (4.19) and (4.20), the ultimate state for this case is expressed as;

$$\frac{\frac{\sigma_x + \sigma_y}{2} + \sqrt{\left(\frac{\sigma_x - \sigma_y}{2}\right)^2 + \tau_{xy}^2}}{S_T} - \frac{\frac{\sigma_x + \sigma_y}{2} - \sqrt{\left(\frac{\sigma_x - \sigma_y}{2}\right)^2 + \tau_{xy}^2}}{S_C} = 1 \tag{4.24}$$

3) Case 3

If principal stresses σ_1 and σ_3 are both in compression state ($\sigma_1 < 0$ and $\sigma_3 < 0$), then failure will occur when principal stress σ_3 equals to the negative of compressive strength of material ($-S_c$).

$$\frac{\sigma_3}{S_C} = -1 \tag{4.25}$$

After substitution of Equation (4.20), the ultimate state for this case is expressed as;

$$\frac{\frac{\sigma_x + \sigma_y}{2} - \sqrt{\left(\frac{\sigma_x - \sigma_y}{2}\right)^2 + \tau_{xy}^2}}{S_C} = -1 \tag{4.26}$$

Figure 4.10 shows the allowable range of principal stresses according to Mohr Coulomb failure equations (4.22), (4.24) and (4.26).

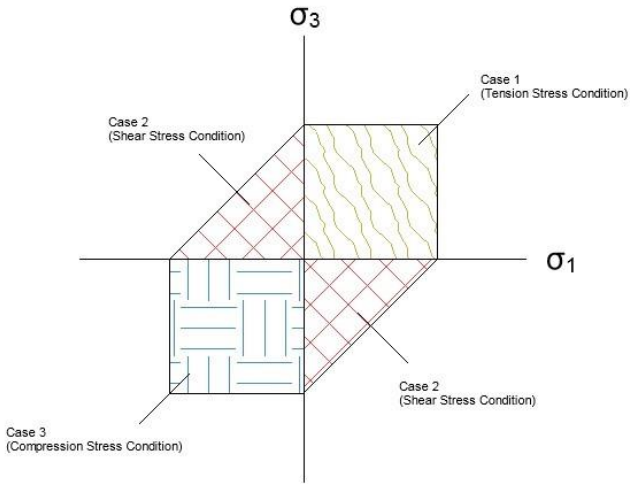

Figure 4.10. Envelopes for stresses according to Mohr-Coulomb failure criterion

Third rule of the lower bound theory is that any point on a wall does not violate yield condition. In order to satisfy this rule, Mohr coulomb failure criterion is applied to stresses conditions on each node of a wall in order to obtain ultimate stress state on these nodes. This assumption is similar to the Rankine's solution (1857) in soil mechanics. According to Rankine's solution for active earth pressure on a retaining wall, the stresses on soil retained is assumed to be completely in failure state. This assumption yields a simple yet reliable formula for estimation on ultimate load on a retaining wall.

The equations obtained from Mohr Coulomb function should be linearized in order to be used in system of Equation (4.1) for a numerical solution. Thereafter Taylor series

expansion was used for converting these nonlinear equations to approximate linear equations. The solution for the system of nonlinear (Mohr-Coulomb) equations were determined iteratively by using a Newton-Raphson algorithm. While σ_x, σ_y and τ are the newest approximation for the stresses on a node, σ_{x0}, σ_{y0} and τ_0 are the initial approximation for them. The first order approximation by Taylor Series expansion yields;

$$f(\sigma_x,\sigma_y,\tau) = f(\sigma_{x0},\sigma_{y0},\tau_0) + \frac{df}{d\sigma x}(\sigma_{x0},\sigma_{y0},\tau_0)\cdot(\sigma_x-\sigma_{x0}) + \frac{df}{d\sigma y}(\sigma_{x0},\sigma_{y0},\tau_0) \cdot(\sigma_y-\sigma_{y0}) + \frac{df}{d\tau}(\sigma_{x0},\sigma_{y0},\tau_0)\cdot(\tau-\tau_0)$$

or,

$$\frac{df}{d\sigma x}(\sigma_{x0},\sigma_{y0},\tau_0)\cdot(\sigma_x) + \frac{df}{d\sigma y}(\sigma_{x0},\sigma_{y0},\tau_0)\cdot(\sigma_y) + \frac{df}{d\tau}(\sigma_{x0},\sigma_{y0},\tau_0)\cdot(\tau) = f(\sigma_x,\sigma_y,\tau) - f(\sigma_{x0},\sigma_{y0},\tau_0) + \frac{df}{d\sigma x}(\sigma_{x0},\sigma_{y0},\tau_0)\cdot(\sigma_{x0}) + \frac{df}{d\sigma y}(\sigma_{x0},\sigma_{y0},\tau_0)\cdot(\sigma_{y0}) + \frac{df}{d\tau}(\sigma_{x0},\sigma_{y0},\tau_0)\cdot(\tau_0) \quad (4.27)$$

The terms in Equation (4.27) for Case 1 are given as follows;

$$f(\sigma_x,\sigma_y,\tau) = \frac{\frac{\sigma_x+\sigma_y}{2} + \sqrt{\left(\frac{\sigma_x-\sigma_y}{2}\right)^2+\tau_{xy}^2}}{S_T} \quad (4.28a)$$

$$f(\sigma_{x0},\sigma_{y0},\tau_0) = \frac{\frac{\sigma_{x0}+\sigma_{y0}}{2} + \sqrt{\left(\frac{\sigma_{x0}-\sigma_{y0}}{2}\right)^2+\tau_0^2}}{S_T} \quad (4.28b)$$

$$\frac{df}{d\sigma_x}(\sigma_{x0},\sigma_{y0},\tau_0)=\frac{\frac{1}{2}+\frac{\sigma_{x0}-\sigma_{y0}}{4\cdot\sqrt{\left(\frac{\sigma_{x0}-\sigma_{y0}}{2}\right)^2+\tau_0^2}}}{S_T} \tag{4.28c}$$

$$\frac{df}{d\sigma_y}(\sigma_{x0},\sigma_{y0},\tau_0)=\frac{\frac{1}{2}-\frac{\sigma_{x0}-\sigma_{y0}}{4\cdot\sqrt{\left(\frac{\sigma_{x0}-\sigma_{y0}}{2}\right)^2+\tau_0^2}}}{S_T} \tag{4.28d}$$

$$\frac{df}{d\tau}(\sigma_{x0},\sigma_{y0},\tau_0)=\frac{\frac{\tau_0}{\sqrt{\left(\frac{\sigma_{x0}-\sigma_{y0}}{2}\right)^2+\tau_0^2}}}{S_T} \tag{4.28e}$$

It should be noted that Equation (4.28a) is equal to 1 from Equation (4.22). Equation (4.28c-e) are elements of the coefficient matrix [A] as given in Equation (4.1). The right side of the Equation (4.27) is the element of vector {B}.

The terms in Equation (4.27) for Case 2 are given as follows;

$$f(\sigma_x,\sigma_y,\tau)=\frac{\frac{\sigma_x+\sigma_y}{2}+\sqrt{\left(\frac{\sigma_x-\sigma_y}{2}\right)^2+\tau_{xy}^2}}{S_T}-\frac{\frac{\sigma_x+\sigma_y}{2}-\sqrt{\left(\frac{\sigma_x-\sigma_y}{2}\right)^2+\tau_{xy}^2}}{S_C} \tag{4.29a}$$

$$f(\sigma_{x0},\sigma_{y0},\tau_0)=\frac{\frac{\sigma_{x0}+\sigma_{y0}}{2}+\sqrt{\left(\frac{\sigma_{x0}-\sigma_{y0}}{2}\right)^2+\tau_0^2}}{S_T}-\frac{\frac{\sigma_{x0}+\sigma_{y0}}{2}-\sqrt{\left(\frac{\sigma_{x0}-\sigma_{y0}}{2}\right)^2+\tau_0^2}}{S_C} \tag{4.29b}$$

$$\frac{df}{d\sigma_x}(\sigma_{x0},\sigma_{y0},\tau_0) \tag{4.29c}$$
$$= \frac{1}{2\cdot S_T} + \frac{\sigma_{x0}-\sigma_{y0}}{4\cdot S_T\cdot\left(\sqrt{\left(\frac{\sigma_{x0}-\sigma_{y0}}{2}\right)^2+\tau_0^2}\right)} - \frac{1}{2\cdot S_C}$$
$$+ \frac{\sigma_{x0}-\sigma_{y0}}{4\cdot S_C\cdot\left(\sqrt{\left(\frac{\sigma_{x0}-\sigma_{y0}}{2}\right)^2+\tau_0^2}\right)}$$

$$\frac{df}{d\sigma_y}(\sigma_{x0},\sigma_{y0},\tau_0) \tag{4.29d}$$
$$= \frac{1}{2\cdot S_T} - \frac{\sigma_{x0}-\sigma_{y0}}{4\cdot S_T\cdot\left(\sqrt{\left(\frac{\sigma_{x0}-\sigma_{y0}}{2}\right)^2+\tau_0^2}\right)} - \frac{1}{2\cdot S_C}$$
$$- \frac{\sigma_{x0}-\sigma_{y0}}{4\cdot S_C\cdot\left(\sqrt{\left(\frac{\sigma_{x0}-\sigma_{y0}}{2}\right)^2+\tau_0^2}\right.}$$

$$\frac{df}{d\tau}(\sigma_{x0},\sigma_{y0},\tau_0) = \frac{\tau_0}{S_T\cdot\sqrt{\left(\frac{\sigma_{x0}-\sigma_{y0}}{2}\right)^2+\tau_0^2}} - \frac{\tau_0}{S_C\cdot\sqrt{\left(\frac{\sigma_{x0}-\sigma_{y0}}{2}\right)^2+\tau_0^2}} \tag{4.29e}$$

Equation (4.29a) is equal to 1 from Equation (4.24). Equation (4.29c-e) are elements of the coefficient matrix [A] as given in Equation (4.1). The right side of the Equation (4.27) is the element of vector {B}.

Finally, the terms in Equation (4.27) for Case 3 are given as follows;

$$f(\sigma_x,\sigma_y,\tau) = \frac{\frac{\sigma_x+\sigma_y}{2} - \sqrt{\left(\frac{\sigma_x-\sigma_y}{2}\right)^2+\tau_{xy}^2}}{S_c} \tag{4.30a}$$

$$f(\sigma_{x0}, \sigma_{y0}, \tau_0) = \frac{\frac{\sigma_{x0} + \sigma_{y0}}{2} - \sqrt{\left(\frac{\sigma_{x0} - \sigma_{y0}}{2}\right)^2 + \tau_0^2}}{S_c} \tag{4.30b}$$

$$\frac{df}{d\sigma_x}(\sigma_{x0}, \sigma_{y0}, \tau_0) = \frac{\frac{1}{2} - \frac{\sigma_{x0} - \sigma_{y0}}{4 \cdot \sqrt{\left(\frac{\sigma_{x0} - \sigma_{y0}}{2}\right)^2 + \tau_0^2}}}{S_C} \tag{4.30c}$$

$$\frac{df}{d\sigma_Y}(\sigma_{x0}, \sigma_{y0}, \tau_0) = \frac{\frac{1}{2} + \frac{\sigma_{x0} - \sigma_{y0}}{4 \cdot \sqrt{\left(\frac{\sigma_{x0} - \sigma_{y0}}{2}\right)^2 + \tau_0^2}}}{S_C} \tag{4.30d}$$

$$\frac{df}{d\tau}(\sigma_{x0}, \sigma_{y0}, \tau_0) = -\frac{\frac{\tau_0}{\sqrt{\left(\frac{\sigma_{x0} - \sigma_{y0}}{2}\right)^2 + \tau_0^2}}}{S_C} \tag{4.30e}$$

Equation (4.30a) is equal to -1 from Equation (4.26). Equation (4.30c-e) are elements of the coefficient matrix [A] as given in Equation (4.1). The right side of the Equation (4.27) is the element of vector {B}. The stresses should be solved recursively as explained in next section.

4.3.5. Solution for Nodal Stresses

The equilibrium equations obtained from Equations (4.10), (4.11) and (4.14) and boundary conditions equations obtained from Equations (4.15) to (4.18b) are substituted in linear system of equations shown as equation (4.1).

The equations for Mohr Coulomb failure criterion are substituted for each node. Since Mohr Coulomb equations are nonlinear, the approximations due to equation (4.27) are used. The solution for stresses are found by recursive calculation such that

$$[A(\sigma_0)] \cdot \{\sigma\} = \{B(\sigma_0)\} \tag{4.31}$$

where subscript 0 denotes function evaluations due to previous approximations for nodal stresses, and {σ} denotes new approximations for nodal stresses. The initial estimations for stresses are all set to 1. Then the principal stresses for each node σ_1 and σ_3 are calculated. This is followed by recalculation of [A] and {B} before the next approximate solution.

The approximate relative error ε_σ for any approximate stress {σ} is calculated by

$$\varepsilon_\sigma = \frac{[\sigma] - [\sigma_0]}{[\sigma]} \tag{4.32}$$

A computer program employing the algorithm shown in Figure 4.11 is developed by using the language of Matlab (Mathworks, 2017). The recursive solution for {σ} is stopped when ε_σ for each unknown stress becomes less than ε_s for all nodal stresses. ε_s is the tolerable (satisfactory) level of relative error, ε_σ, and it is chosen as 10^{-5} in this study.

Then ultimate lateral load H acting on top of a wall can be calculated by using the sum of shear stresses on the top of the wall as shown in Figure (4.12) for a wall with 2 x 2 rectangular panels. Hence, for this wall the ultimate lateral load is computed by

$$\left(\left(\frac{a}{2}\right) \cdot t\right) \cdot (\tau_i + \tau_j) + \left(\left(\frac{a}{2}\right) \cdot t\right) \cdot (\tau_j + \tau_k) = H \tag{4.33}$$

This equation is generic for all types of walls used in this study.

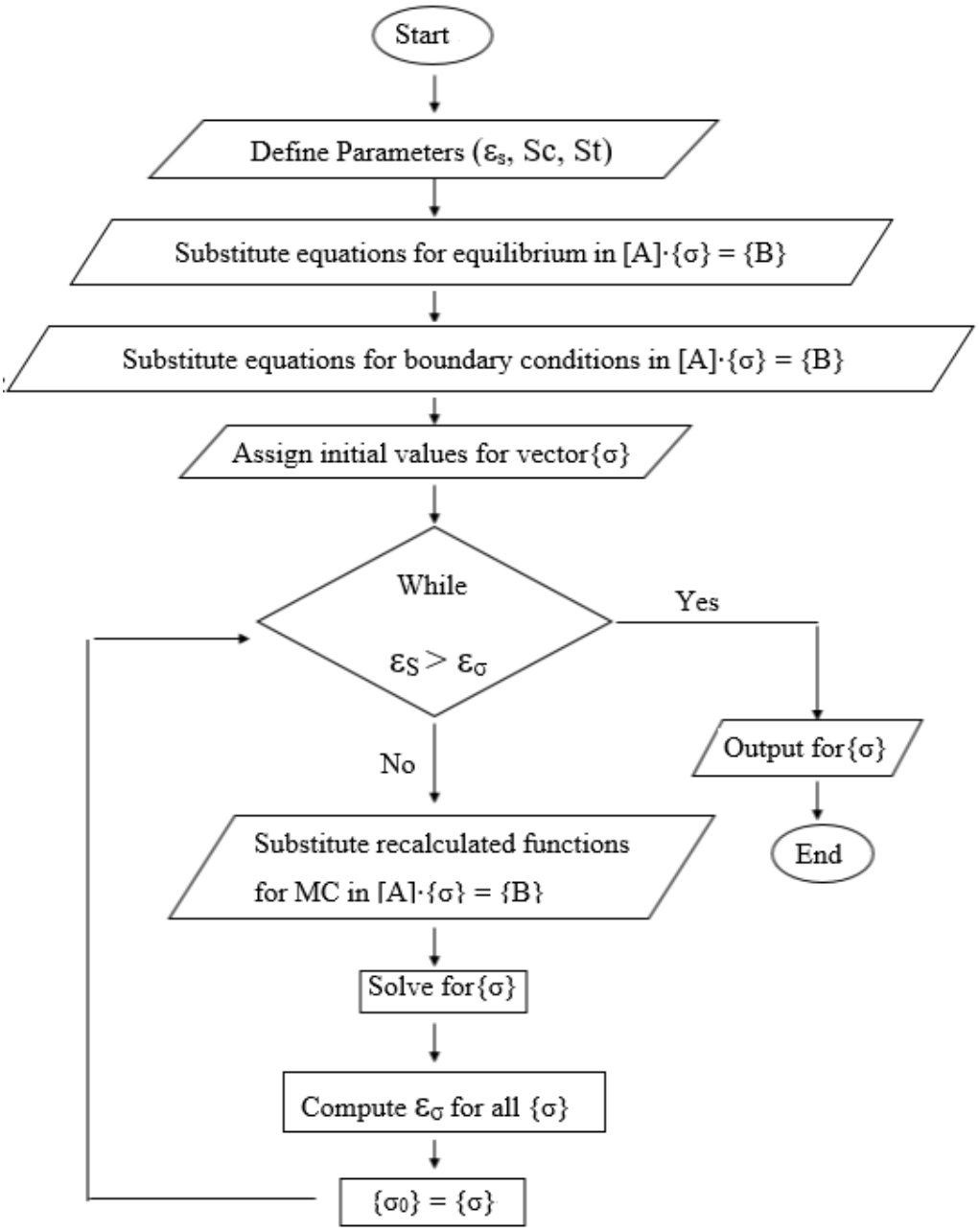

Figure 4.11. Algorithm for calculations

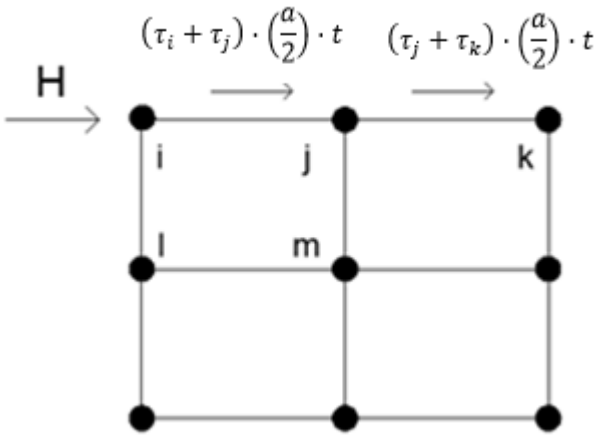

Figure 4.12. Calculation for the ultimate horizontal load on top of the wall

CHAPTER 5

VERIFICATION OF THE PROPOSED ANALYSIS METHOD

5.1. General Information About the Verification Study

Verification of the analysis method proposed by using the lower bound theorem is performed in two stages. First, the method is verified by comparing the results with the experimental findings from the literature. In order to prove the accuracy and reliability of the analysis method, the results obtained by modeling the experimental specimens in the literature using the analysis method are compared with the experimental results. Second, parametric studies are performed for verification of the known physical effects of different parameters on the lateral load capacity of masonry walls. The analysis method is applied to a reference masonry wall and then the maximum lateral load that the wall can take is estimated. While selecting the wall types, the answers of the following questions are sought and results are assessed accordingly. These questions are;

- Do different types of walls with different dimensions behave differently under the same stress conditions? How does the collapse load vary by wall dimensions?
- If the total vertical stress applied to the wall changes, how is the lateral load capacity of the wall affected?
- If a material with different tensile strength is used, how does the lateral load capacity of the wall change?
- How does the size of the openings contribute to the load bearing capacity of the wall?

For the following case study walls, maximum lateral load indicated by H is calculated under a given value of vertical compressive load indicated by V. The proposed macro-modeling approach is employed for specific values of material strength by dividing the walls into macro panels. The main assumption is that all ingredients of the wall, i.e. masonry units, mortar and unit-mortar interface, are homogenized into a macro wall panel characterized by its compressive and tensile strength.

5.2. Application of the Macro-Model Approach to Masonry Walls

The proposed method was explained in detail in the previous Chapter. In this section some different wall types have been used for verification analysis (i.e solid wall, wall with window opening, wall with door opening and wall with window and door opening). The analysis procedure for these wall types can be explained as follows: First the wall is divided into a number of rectangular panels. The mesh size does not have to be fine, i.e for a solid wall, a 3x3 mesh can be sufficient to estimate the lateral load capacity of the wall. In the case of walls with openings, the mesh size and location should be arranged in accordance with this specific geometry. As explained in Section 4.3.1, there are three unknowns in terms of normal and shear stresses at each corner of the wall panels, from which the total number of unknowns is determined. In order to solve for these unknowns, equilibrium conditions in the panels (with the exception of areas of window and door openings) and the overturning moment equation for the wall should be written as stated in Section 4.3.2. The next step is to identify the boundary conditions. These include the side boundary conditions and the top boundary conditions of the wall as explained in Sections 4.3.3.1 and 4.3.3.2. In the case of window and door openings, boundary conditions are obtained for the left and right sides of the openings, which is presented in Section 4.3.3.3. After establishing all the equilibrium and boundary conditions for the selected wall, Mohr-Coulomb failure criterion is defined at each node of the wall panels in order to solve the set of equations for the ultimate condition of failure (see Section 4.3.4). Matlab codes have been written separately for solid wall, wall with window opening, wall with door opening, wall with window and door openings and they are presented in Appendices A, B, C

and D, respectively. After the set of equations are solved by the help of computer codes in terms of internal stresses, these values are used in order to find the horizontal load H. For this purpose, the lateral equilibrium in the wall panels is taken into account.

5.3. Comparison of Analysis Results with Experimental Studies

The analysis method proposed in this study is compared with various experimental results in the literature for verification purposes. The experiments used include solid wall, unreinforced masonry wall with a single window opening and unreinforced masonry wall with a single door opening.

5.3.1. Masonry Wall with No Opening (Solid Wall)

Lourenço et al (2005), studied structural behavior of dry joint masonry walls and the analysis of in-plane capacity under compressive and shear loading. During the experimental campaign, seven dry joint masonry walls are tested to obtain their lateral load capacities under different level of compressive loading with 30, 100, 200 and 250 kN. In this study, one of the square-shaped masonry wall specimens with no openings has been selected. Its dimensions are 100x100 cm with a thickness of 20 cm (Figure 5.1). The compressive and tensile strengths of the wall specimen were reported as 82.7 MPa and 3.7 MPa, respectively. The considered level of vertical load is 100 kN. After the specimen was tested, the maximum lateral load is obtained for the wall was 49 kN (Lourenço et al, 2005).

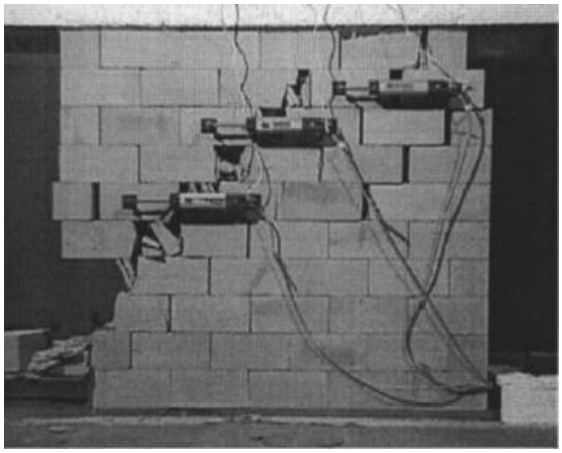

Figure 5.1. Masonry wall specimen with no opening (Lourenço, 2005)

In order to analyze the specimen with proposed approach, first 3x3 mesh size is used for the wall. Totally 48 stresses are identified at 16 nodes. This means, there are 48 stress unknowns at the nodes as opposed to the known value of vertical load (100 kN). In order to satisfy equilibrium for 9 rectangular panels, 18 equilibrium equations are obtained by using Equation (4.10) and (4.11) and 1 moment equation is obtained from Equation (4.14). For ensuring the boundary conditions, 6 normal force equations are obtained by using Equation (4.15) and whereas 6 shear force equations are obtained by using Equation (4.16). In addition to that, 1 boundary condition for vertical external force is provided through Equation (4.17). For 16 nodes, 16 Mohr-Coulomb points are placed and 16 equations are procured. At the end, for the 48 unknowns, 48 equations are obtained and solved by the written Matlab code.

At the end of the analysis, maximum lateral load H is obtained as 55.2 kN from the obtained internal stresses by using Equation (4.33). The maximum lateral load obtained from the experiment is 49 kN, while the maximum lateral load obtained from the analysis is 55.2 kN. The error percentage of 11% indicates that the analysis results is consistent with the physical behavior obtained through testing.

5.3.2. Masonry Wall with Window Opening

Kalali and Kabir (2012) studied the behavior of six masonry wall specimens with window openings before and after retrofit in order to investigate their capacity under in-plane loading. In the experimental campaign, one unreinforced masonry wall was tested in addition to 5 masonry walls strengthened with glass fiber reinforced polymers. The wall specimen which is investigated in this study has dimensions with 194x143 cm with 16 cm thickness and a window opening at its center, which has a dimension of 52x47 cm. For unreinforced masonry wall, compressive masonry wall strength of 11.7 MPa is reported while tensile strength of material is 5% of compressive strength, which is 0.585 MPa. When 41.2 kN was applied to unreinforced masonry wall specimen, maximum horizontal load was obtained as 26.1 kN. Wall specimen investigated is illustrated in Figure 5.2.

Figure 5.2. Unreinforced masonry wall specimen with window opening (Kalali and Kabir, 2012)

In order to analyze this wall with the proposed method, first it is divided into macro panels. After applying a 3x3 mesh size, a total of 48 stress parameters are introduced at 16 nodes. This means, there are 48 stress at the nodes as opposed to the known value of vertical load (41.2 kN). In order to satisfy equilibrium for 8 rectangular panels, 16 equilibrium equations are obtained by using Equation (4.10) and (4.11) and 1 moment

equation is obtained from Equation (4.14). For ensuring the boundary conditions, 6 normal force equations are obtained by using Equation (4.15) and whereas 6 shear force equations are obtained by using Equation (4.16). In addition to that, 1 boundary condition for vertical external force is provided through Equation (4.17). Since one of the panels is replaced with a window opening, 2 boundary conditions are obtained by using Equation (4.18a) and (4.18b) for this opening. For 16 nodes, 16 Mohr-Coulomb points are placed and 16 equations are procured. At the end, for the 48 unknowns, 48 equations are obtained and solved by the written Matlab code.

Maximum lateral load H is obtained as 28.13 kN as a result of analysis from obtained internal stresses by using Equation (4.33). The maximum lateral load obtained from the experiment was 26.1 kN, while the maximum lateral load obtained from the analysis is 28.13 kN. It can be seen that results are very close to each other. The error percentage of 8% indicates that the analysis result is consistent with the physical behavior obtained through testing.

5.3.3. Masonry Wall with Door Opening

Allen et al (2016), conducted the experiment of three different unreinforced masonry walls with door opening. These wall types were investigated in order to obtain force displacement relationships. In this study, one of the wall specimens has been used with dimensions 36x24 cm and 11 cm thickness. The door opening is in the middle of the wall with dimensions 12x18 cm (Figure 5.3). The compressive and tensile strength of the specimen were reported as 9.6 MPa and 1.85 MPa, respectively. The considered value of vertical load is 79.2 kN. After specimen was tested, the maximum lateral load obtained for the wall was 39 kN (Allen et al, 2016).

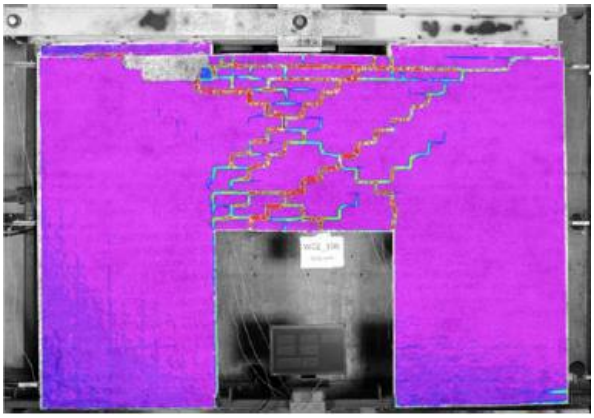

Figure 5.3. Unreinforced masonry wall specimen with door opening (Allen et al, 2016)

In order to analyze the specimen with the proposed approach, first 3x3 mesh size is used for the wall. Totally 48 stresses are identified at 16 nodes. This means, there are 48 stress at the nodes as opposed to the known value of vertical load (41.2 kN). In order to satisfy equilibrium for 7 rectangular panels, 14 equilibrium equations are obtained by using Equation (4.10) and (4.11) and 1 moment equation is obtained from Equation (4.14). For ensuring the boundary conditions, 6 normal force equations are obtained by using Equation (4.15) and whereas 6 shear force equations are obtained by using Equation (4.16). In addition to that, 1 boundary condition for vertical external force is provided through Equation (4.17). Since one of the panels is replaced with a door opening, 4 boundary conditions are obtained by using Equation (4.18a) and (4.18b) for this opening. For 16 nodes, 16 Mohr-Coulomb points are placed and 16 equations are procured. At the end, for the 48 unknowns, 48 equations are obtained and solved by the written Matlab code.

Maximum lateral load H is obtained as 45.7 kN as a result of analysis from the obtained internal stresses by using Equation (4.33). The maximum lateral load obtained from the experiment was 39 kN, while the maximum lateral load obtained from the analysis is 45.7 kN. The error percentage of 17% indicates that the analysis result is still valid after considering all the gross assumptions and simplifications of the method.

5.4. Parametric Studies for the Verification of the Method

In the last phase of the study, parametric studies have also been conducted to evaluate the influence of different parameters for masonry wall types for the purpose of verification. First, the effect of change in wall dimensions on horizontal capacity for a masonry wall without opening under a certain vertical load is investigated. Second, the effect of change in the vertical load applied to the wall on the horizontal capacity is investigated using the masonry wall with and without window opening case study. Then, masonry wall with and without door opening case studies are assessed and the effect of the change in tensile strength of the material on the lateral capacity of the wall is evaluated. Finally, starting from a masonry wall without opening, various opening sizes are used on this wall and the effect of the change in opening size on the lateral capacity of the wall is observed.

5.4.1. Effect of Change in Dimension on Lateral Capacity of the Wall

In order to examine the effect of the change of wall dimensions on the lateral strength of the wall, a masonry wall without opening is studied. The dimensions of this wall, which can be varied arbitrarily, are 500x300 cm as the reference values in study and thickness of the wall is chosen as 30 cm. This wall type is meshed into 3x3 and therefore 9 rectangular panels are obtained as illustrated in Figure 5.4. Compressive and tensile strength values are used as 11 MPa and 0.55 MPa, respectively according to the study of Kalali and Kabir (2012). As the wall is subjected to a vertical compressive load of 300 kN, the aim is to calculate how much lateral horizontal load the wall can withstand.

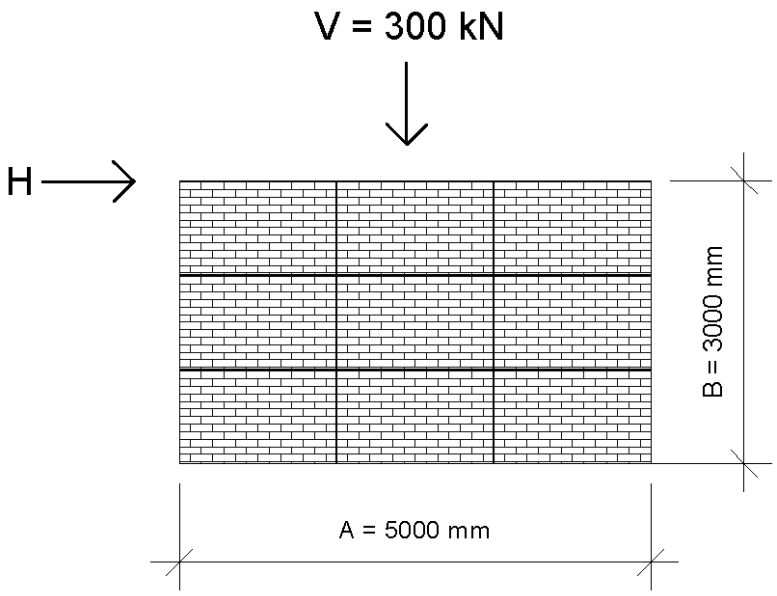

Figure 5.4. Masonry wall with no opening under vertical stress (500x300 cm)

The case study wall, which is divided into rectangular panels, is solved as described in Section 5.2. The corresponding stress values at the nodes are obtained by using the Matlab code. As a result, the maximum horizontal load is calculated as 66.7 kN / m.

Then, the dimension of the wall is varied by increasing the horizontal dimension with increment of 30 cm while the vertical load of 300 kN remains constant. The maximum lateral load values obtained as a result of analyses by changing dimensions of the wall are shown in Figure 5.5.

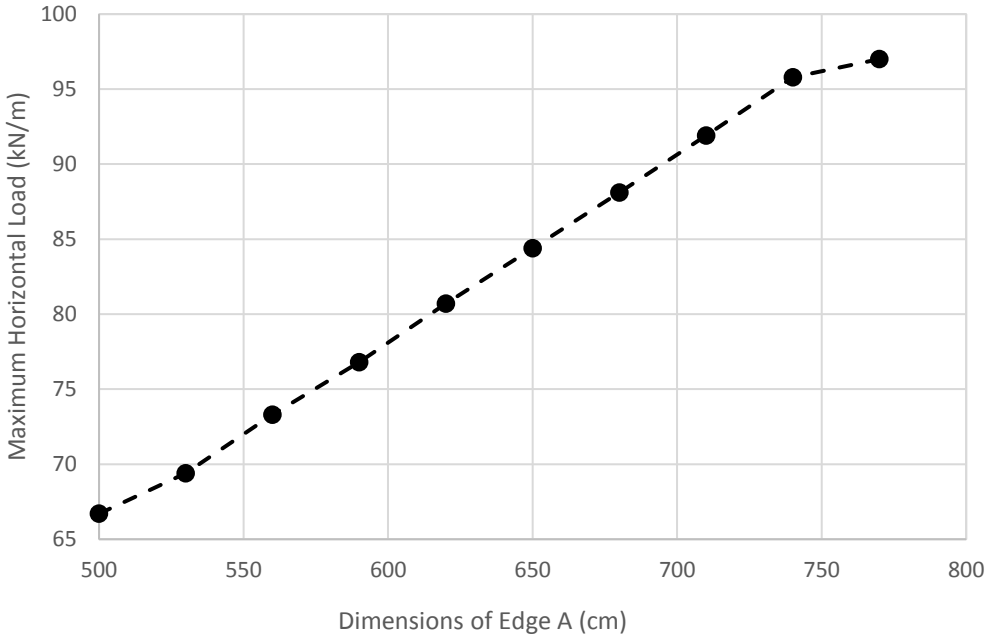

Figure 5.5. Masonry wall without opening with changing dimension

The maximum lateral load of the wall has been found as 66.7 kN/m under 300 kN vertical load before changing the horizontal dimension. Subsequently, the increase in dimension results in a 6% increase in the area ratio at each increment. It is expected that this increase contributes to the maximum horizontal load change in the same rate. As a result of the analysis, 6% increase in total area resulted in 7% increase in the horizontal load capacity, which is consistent with the expected behavior.

5.4.2. Effect of Change in Vertical Load on Lateral Capacity of the Wall

In order to see the effect of the change in vertical load on the horizontal capacity of the wall, first masonry wall without opening and then masonry wall with window opening are studied.

The case study solid wall is divided into rectangular panels and it is solved as described in Section 5.2. The corresponding stress values at the nodes are obtained by using the Matlab code. As a result, the maximum horizontal load is obtained as 66.7

kN / m under 300 kN vertical load. Sample internal stress values and distribution plots are presented in Appendix E for the ultimate condition of the considered wall.

After examining the solid wall, masonry wall with window opening is studied. The wall dimensions for this example have been kept constant (i.e 500x300 cm) and thickness of the wall is chosen as 30 cm. A window opening is located at the middle of the wall with a dimension of 100x100 cm and the wall is divided into 9 rectangular panels as illustrated in Figure 5.6. While the wall is subjected to a vertical compressive load of 300 kN, the aim is to calculate the maximum lateral load.

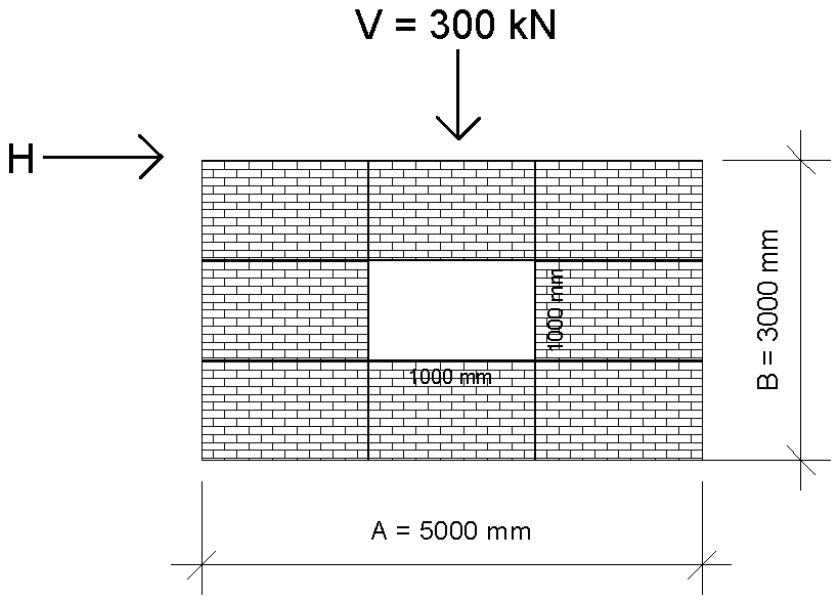

Figure 5.6. Masonry wall with window opening

The case study wall, which is divided into panels, is solved as described in Section 5.2. The corresponding stress values at the nodes are obtained by using the Matlab code. As a result, the maximum horizontal load is calculated as 58.4 kN / m.

Then, the vertical load value is changed by keeping the wall dimensions and strength values constant for solid wall and wall with window opening case studies. The maximum lateral load values obtained as a result of analyses by changing in vertical

load are shown in Figure 5.7 where σ/f_m is the ratio of axial stress to compressive strength of masonry.

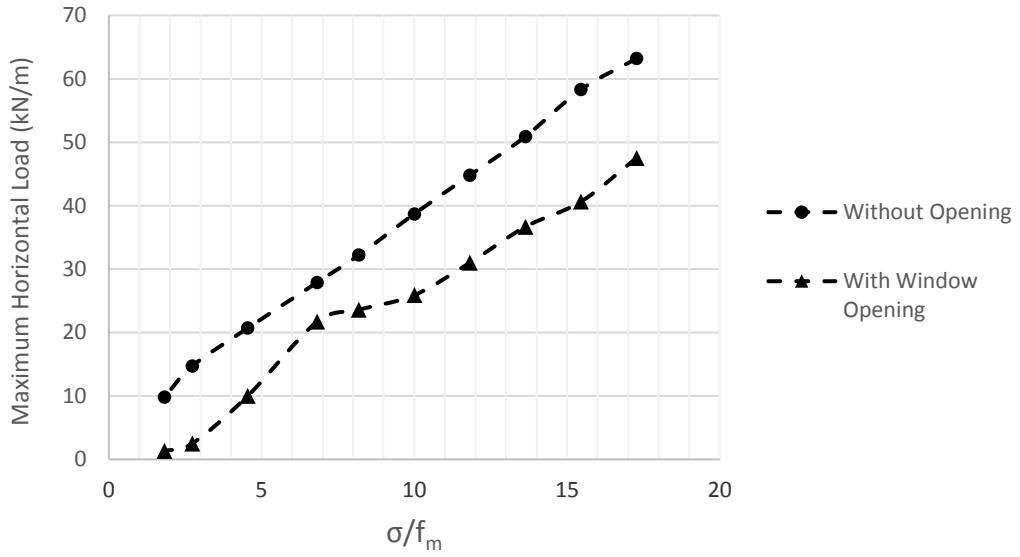

Figure 5.7. Masonry wall with and without window opening under changing vertical load

It has been predicted that the maximum lateral load value decreases if the vertical compressive load on the masonry wall is decreased. Decrease in vertical load cause reduction in lateral capacity because of the decrease in friction between mortar and unit. When vertical load increases then the friction also increases, so the wall can resist more lateral load. As shown in the graph, decrease in the vertical load causes a decrease in the maximum lateral load capacity of the wall. In masonry wall without opening, the effect of the change in vertical load on horizontal capacity is more linear, whereas in masonry wall with window opening, the change is more scattered. This is caused by the non-uniform stress distribution around the opening so that the increase in horizontal capacity may not be linearly proportional to an increase in vertical load. Overall, the trends seem to be reasonable in terms of physical behavior.

5.4.3. Effect of Change in Tensile Strength on Lateral Capacity of the Wall

In order to see the effect of the change in tensile strength on the horizontal capacity of the wall, first masonry wall without opening and then masonry wall with door opening are studied.

For both cases, the same dimensions (500x300 cm), thickness (30 cm), compressive strength (11 MPa) and vertical load (300 kN) are used as illustrated in Figure 5.8. In the case with door opening, the door is located in the middle of the wall with dimensions 210x100 cm. In both cases the wall is divided into 9 rectangular panels for analysis.

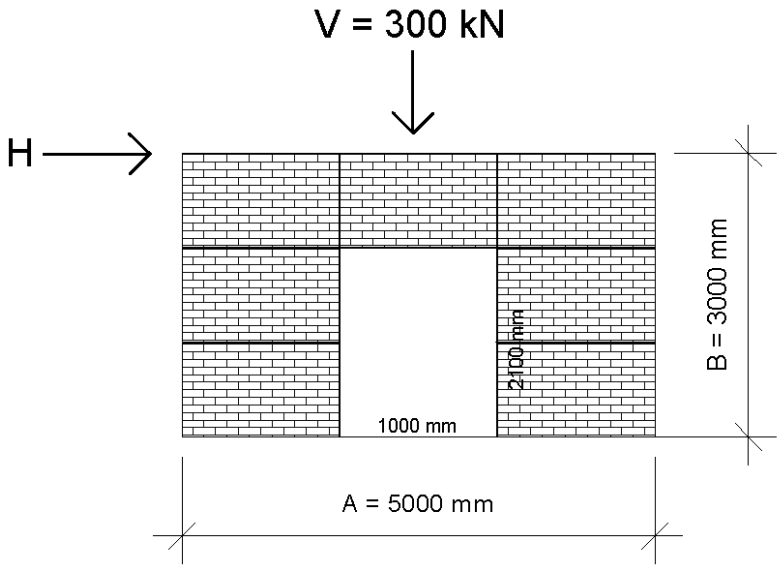

Figure 5.8. Masonry wall with door opening

Then, the wall dimensions and vertical load are kept constant and tensile strength value is varied between 0.20 MPa to 1 MPa. The maximum lateral load values obtained as a result of the analyses by varying the in tensile strength values for two types of wall are shown in Figure 5.9.

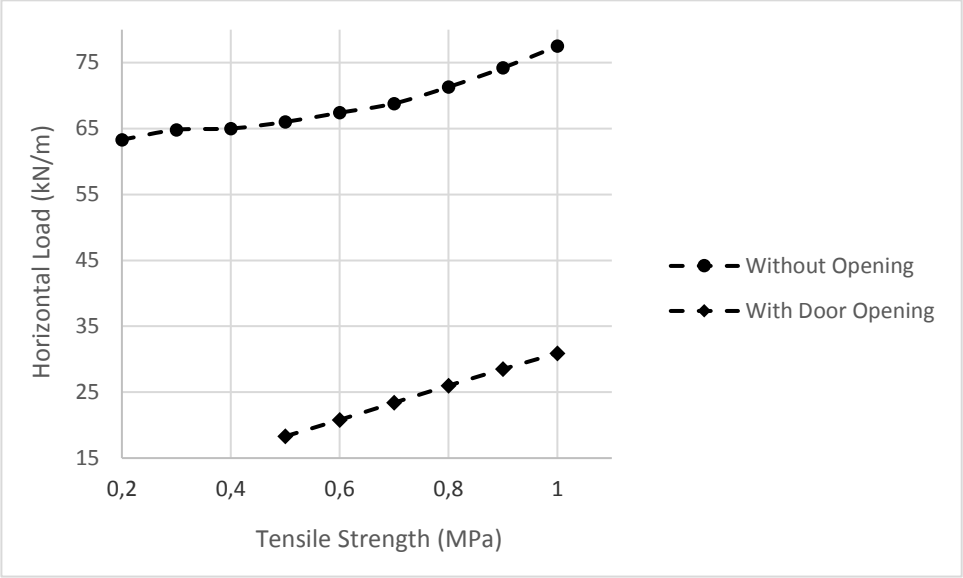

Figure 5.9. Masonry wall with and without door opening with changing tensile strength

Maximum lateral load of masonry wall without opening by a tensile strength value of 0.20 MPa is 63.3 kN/m while it is obtained as 77.5 kN/m for a tensile strength value of 1 MPa. On the other hand, there is no solution for the wall with opening when tensile strength values are 0.2-0.4 MPa. This means that the wall with door opening cannot withstand 300 kN vertical load with these values of tensile strength. It is also observed that, the effect of the increase in tensile strength on the horizontal capacity of the wall is higher in the masonry wall with door opening, while it does not cause a significant increase in the masonry wall without opening. The reason is that the nodes on the wall without opening are more likely to fail in shear (tension-compression state). The increase in tensile strength does not cause a significant increase in wall which fails in shear. However, as the number of failing nodes in tension is greater in the wall with door opening than the wall without opening, the increase in tensile strength has a greater effect on the lateral capacity of the wall. As a result, since the tension capacity of the masonry wall is known to be less than the compression capacity and the cause of failure is due to tension and/or shear, the compression strength value

is kept constant and the tension strength value is increased. It has been predicted that the maximum lateral load value would change with tensile strength and results confirm this prediction.

5.4.4. Effect of Change in Opening Size on Lateral Capacity of the Wall

A window or door opening on a masonry wall has a significant effect on the lateral capacity of the wall. In order to observe this, various openings are located on the wall by considering the solid masonry wall as reference and analyses are performed. Wall dimensions are kept constant as 500x300 cm with thickness of 30 cm. The vertical stress value is 300 kN and the compressive and tensile strength values are 11 and 0.55 MPa respectively. First, masonry wall without opening is analyzed as described in Section 5.2. Then, masonry wall with window opening is considered and the opening dimensions are taken as 100x100 cm, 100x125 cm, 120x125 cm and 125x125 cm respectively. After the wall with window opening, the opening size has been further enlarged and the next step is to examine the single-door wall example with door dimensions accepted as 95x210 cm and 100x210 cm. After examining the case studies with single-window and single-door opening, the last step is to examine the behavior of wall with a door and window openings together. For this type of wall, a window opening of 100x100 cm and a door opening of 100x210 cm have been assumed on the wall as illustrated in Figure 5.10. Maximum lateral load is obtained by using the proposed analysis method. Then dimensions of window and door openings in this example have also been increased as 105x100 cm and 105x210 cm respectively.

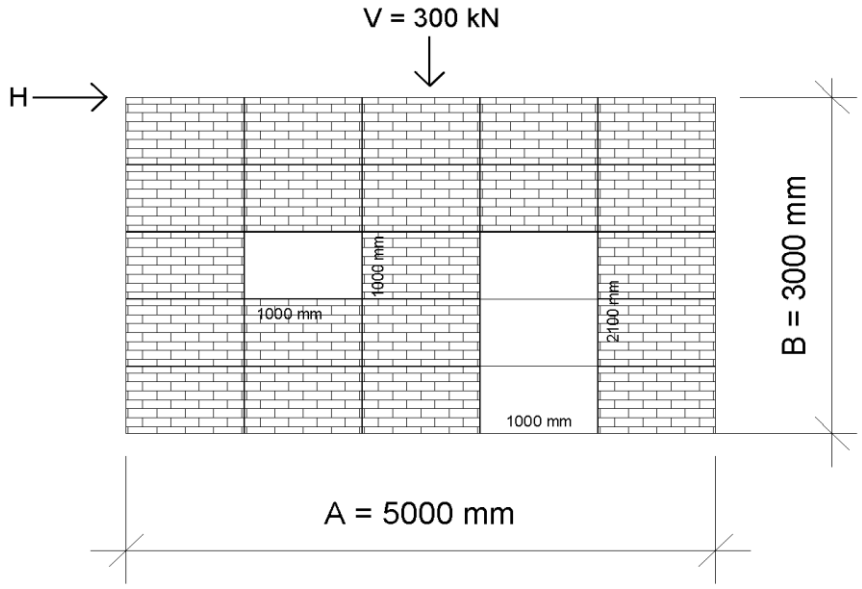

Figure 5.10. Masonry wall with one window and one door openings

The maximum lateral load values obtained as a result of the analysis of the wall by changing the opening sizes are given in Table 5.1. The change in the lateral load capacity of the wall as a result of increase of openings size in percentage is also shown in the plot given in Figure 5.11.

Table 5.1. *Analysis results of walls with changing opening area*

Wall Type	Window Opening (cm)	Door Opening (cm)	Maximum Lateral Load (kN/m)
Without opening	–	–	66.7
With window opening	100x100	_	58.4
	100x125	_	35.9
	120x125	_	34.9
	125x125	_	30.4
With door opening	–	95x210	23.2
	_	100x210	19.6
With single window and single door	100x100	100x210	17.7
	105x100	105x210	8.9

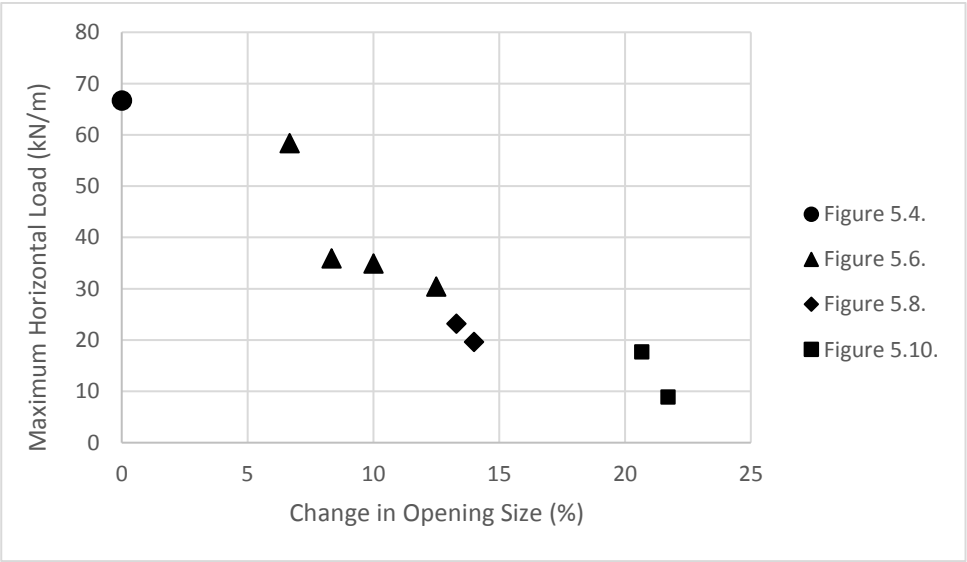

Figure 5.11. Relationship between maximum lateral load and change in opening size for the case study wall

These examples and the obtained values show the effect of the gradual increase in opening sizes for the same wall type on the maximum lateral load. The opening size are gradually increased and it has been observed that the maximum lateral load decreases. The lateral load capacity of the wall is minimized when the opening size has its maximum value. This trend verifies that the openings in unreinforced masonry structures cause serious reductions in lateral load capacity of the wall. For unreinforced masonry structures, it is not possible to quantify the effect of openings explicitly. Although decrease and increase in percentage are not the same as shown in the graph, it is obvious that as the dimensions of the openings increase, the strength capacity of the masonry wall decreases noticeably.

CHAPTER 6

SUMMARY AND CONCLUSIONS

Masonry structures are still used as dwellings in rural areas. There are several challenges for the analysis of these buildings. First, masonry walls are composite structures. Bearing elements are units (such as brick, blocks, etc) and mortar, in which the complexity is formed by the combination of these two ingredients. The main reason for the difficulties in the analysis of masonry structures comes from this heterogeneity. In addition to that, lack of structural drawings, design specifications, technical reports and lack of knowledge about the materials used in construction make structural analysis of these masonry structures extremely difficult. Analysis methods and modeling strategies are mainly different from reinforced concrete and steel structures that cannot be approached with the same criteria. Moreover, using a computer program for the analysis of masonry buildings is often difficult and irrelevant. Because there is a need for structural and mechanical parameters to be used as input in software programs that are developed for the analysis of such structures, which is often not available and/or missing. In addition, the lack of the mentioned design regulations also makes it difficult to model these deficient structures as regular systems with well-defined load paths.

Although there are many methods of analysis for masonry buildings, the majority of these methods are complex and time consuming. However, detailed and complex analysis methods become irrelevant since these structures do not even have a consistent structural system and in most of the cases, it is not possible to estimate material properties to be used in complex analysis. Therefore, simple and practical analysis should be used in order to obtain seismic response of especially non-engineered masonry structures.

Limit analysis is a simple and useful method for performing plastic analysis compared to other methods. Limit analysis which provides convenience and time saving in the analysis of masonry buildings, is composed of three approaches which are the lower bound theorem, the upper bound theorem and the uniqueness theorem. The lower bound theorem is a static theorem based on the equilibrium of the system, while the upper bound theorem is a kinematic theorem based on the energy of the system. The uniqueness theorem occurs when both the mechanism from the upper bound and the equilibrium equation plus the yield condition from the lower bound theorem are provided.

In this study, masonry walls are analyzed by using the lower bound theorem. The aim is to estimate how much lateral load the masonry walls can withstand under a certain vertical load. The rules of the lower bound theorem are applied for these calculations. First, the internal equilibrium and moment equilibrium of the wall are provided, then the assumptions are taken into account to provide boundary conditions. Finally, yield conditions are implemented. For this, Mohr Coulomb failure criterion has been used which assists in presuming the failure state of brittle materials and it is applied on the 2D stress conditions. There are 3 cases that describe the allowable stress states without failure on Mohr's circle envelope, which are tension state, tension-compression state and compression state. At each node of the rectangular panels, when these stress conditions are not exceeded, the third rule of the lower bound theorem is activated which states that any point in the body does not violate yield condition. After obtaining the statically admissible stress field for all conditions of the lower bound theorem, Matlab codes are used to solve the linear system of equations.

First of all, the results of the experiments with different masonry wall types in the literature are compared with the results from the proposed method for the same wall types. The close match in the results reveals the reliability of the analysis method in comparison with the physical behavior. Afterwards, a parametric study is conducted, in which various wall types are employed to estimate the maximum lateral load of case study walls. These types of masonry walls are wall without opening (solid wall),

wall with window opening, wall with door opening and wall with both window and door opening. These wall types are also arranged according to various assumptions and the results are obtained.

Consequently, the most important product of this study is the use of lower bound theorem for simple failure analyses of masonry walls. The proposed lower-bound limit analysis method is simple and easy to apply. It does not require too many input parameters or fine meshes like the Finite Element Method. Although it has many simplifications and gross assumptions, the obtained results seem to be consistent with the physical behavior from the experimental findings. In addition, the variation of some major parameters have been observed to give consistent results with the expected behavior of a typical masonry wall. Overall, these results encourage the use of the proposed method especially for non-engineered masonry structures for which the use of detailed analysis tools is not feasible.

Other conclusions obtained according to the analyses employing the proposed method are:

- Changing the dimensions of the wall causes a change in the maximum lateral load of the wall. The lateral load capacity of the wall is parallel to the change in wall dimensions.
- As the vertical load applied to the wall increases, the maximum lateral load also increases because of the friction between mortar and unit. The lateral capacity of the wall varies directly proportional with the value of the vertical load applied. This facilitates the comparison between the lower and upper floors in a multi-story building. Since the vertical loads at the lower floors of the building are higher, the in-plane wall resistance of the lower floors to the lateral load is more than the upper floors. This is verified after parametric analysis by using the proposed approach.
- Since the stress concentration in the wall with window opening is not uniform on the window edges, the increase in the horizontal capacity with vertical load

is not proportional as in the wall without opening. The openings formed on the wall adversely affect the lateral capacity of the wall.

- Since the compression strength of masonry walls is higher than the tension strength, the in-plane failures of masonry walls are usually caused by tension and/or tension-compression states. This means the change in the tension strength value of the wall affects the capacity of the wall. Increasing the tension strength value of the wall causes the lateral load capacity of the wall to increase.

- Increase in tension strength does not affect horizontal capacity significantly because nodes on the wall without opening showed mostly shear failure. On the other hand, as nodes showing tension failure on the wall with door opening is greater, the increase in horizontal capacity is more significant and higher than the wall without opening by increase in tensile strength.

- As the openings on the wall increase in number and size, the maximum lateral load that the wall can carry decreases. This has been verified during parametric analyses. However, the method should be used with caution in cases where there are too many openings on the wall. In such cases, stress concentrations and non-uniform stresses are the main issues that may cause deviations in the results of the proposed method.

Some recommendations can be presented for future studies. In this study, the lower bound limit analysis method was performed for single walls instead of entire building exposed to in-plane stress. By combining these walls, an entire building can be analyzed with this method for low-rise buildings. In addition, since lower bound theorem is used in this study, if the upper bound theorem is calculated for the same wall types in the future studies, the most appropriate result for the lateral load capacity of the wall can be reached in accordance with the results of these two studies.

REFERENCES

Abdulla KF, Cunningham LS, Gillie M. (2017). Simulating masonry wall behavior using a simplified micro-model approach. Engineering Structures 151:349–365.

Ali SS, Page AW (1988). Finite element model for masonry subjected to concentrated loads. Journal of Structural Engineering 114(8):1761-1784.

Allen C, Masia M.J, Page A.W, Griffith M.C, Derakshan H, Mojsilovic N. (2016). Experimental testing of unreinforced masonry walls with openings subject to cyclin in-plane shear. 16th International Brick and Block Masonry Conference. Padova, Italy.

Bhattacharya S, Nayak S, Dutta SC. (2014). A critical review of retrofitting methods for unreinforced masonry structures. International Journal of Disaster Risk Reduction 7:51–67.

Biolzi L. (1988). Evaluation of Compressive Strength of Masonry Walls by Limit Analysis. Journal of Structural Engineering, 114(10).

Bocko J, Delyová I, Sivák P, Tomko M. (2017). Selection of a significant numerical model of plasticity for the purpose of numerical analysis of plastic reinforcement. American Journal of Mechanical Engineering, 5(6):334-340.

Bower AF. (2009). Applied Mechanics of Solids. CRC Press.

Chen WF, Scawthorn CR. (1968). Soil mechanics and theories of plasticity, Limit analysis and limit equilibrium solutions in soil mechanics. Fritz Engineering Laboratory Report No. 355.3, Fritz Engineering, Laboratory Department of Civil Engineering, Lehigh University Bethlehem, Pennsylvania.

Chen WF. (2000). Plasticity, limit analysis and structural design. International Journal of Solids and Structures 37:81-92.

Churilov S, Dumova-Jovanoska E. (2010). In plane shear behavior of unreinforced masonry walls. 14th European Conference on Earthquake Eng. Ohrid, Macedonia.

Davis RO, Selvadurai APS. (2009). Plasticity and geomechanics. Cambridge University Press.

Drucker DC, Prager W. (1952). Soil mechanics and plastic analysis on limit design. Journal of applied mathematics. 10:157-165.

Drucker DC. (1961). On structural concrete and the theorems of limit analysis. International Association for Bridge and Structural Engineering. Zurich.

Gilbert M, Casapulla C, Ahmed HM. (2006). Limit analysis of masonry block structures with non-associative frictional joints using linear programming. Computers and Structures 84:873–887.

Giordano N, Crespi P, Franchi A. (2017). Flexural strength-ductility assessment of unreinforced masonry cross-sections: analytical expressions. Engineering Structures 148:399–409.

Gvozdev AA. (1960). The determination of the value of the collapse load for statically indeterminate system undergoing plastic deformation. International Journal of Mechanical Sciences 1:322-335

Heyman J. (1966). The stone skeleton. International Journal of Solids Structures 2:249–279.

Jiang GL. (1994). Regularized Method in Limit Analysis. Journal of Engineering Mechanics, 120(6).

Johansen, KW. (1930). Styrekeforholden i stobeskel i beton (The strength of joints in concrete). Bygningsstat. Medd. 2:67-68.

Kalali A, Kabir MZ. (2012). Cyclic behavior of perforated masonry walls with strengthened with glass fiber reinforced polymers. Scientia Iranica 19 (2):151-1665.

Kamal OA, Hamdy GA, El-Salakawy TS. (2013). Nonlinear analysis of historic and contemporary vaulted masonry assemblages. Housing and Building National Research Center Journal (10):235-246.

Karnovsky IA, Lebed O. (2010). Advanced methods of structural analysis. Springer US, Springer-Verlag US.

Kawa M, Pietruszczak S, Shieh-Beygi B. (2008). Limit states for brick masonry based on homogenization approach. International Journal of Solids and Structures 45:998–1016.

Labuz JF, Zang A. (2012). Rock mechanics and rock engineering. Volume 45, Issue 6:975-979.

Li C, Sun C, Li Cuihua, Zheng H. (2017). Lower bound limit analysis by quadrilateral elements. Journal of Computational and Applied Mathematics 315:319–326.

Li HX, Yu HS. (2005). Kinematic limit analysis of frictional materials using nonlinear programming. International Journal of Solids and Structures 42:4058–4076.

Lia D, Cheng Y. (2012). Lower bound limit analysis using nonlinear failure criteria, Procedia Earth and Planetary Science 5:170–174.

Livesley RK. (1978). Limit analysis of structures formed from rigid blocks. International Journal for Numerical Methods in Engineering 12:1853-1871.

Lourenço PB (1996). Computational strategies for masonry structures. Dissertation. Civil Engineering Department, Delft University of Technology.

MathWorks, Inc. (2017). MATLAB. (version 2017b). Natick, Massachusetts, United States.

Mendes N, Lourenço PB (2014). Sensitivity analysis of the seismic performance of existing masonry buildings. Engineering Structures 80:137–146

Mendes, N. (2015). Masonry macro-block analysis. In Encyclopedia of Earthquake Engineering 1-10. Springer Berlin Heidelberg

Michalowski RL. (2000). Plasticity based analysis of reinforced soil structures. Geotechnical Special Publication 345-349.

Mihai AL, Ainsworth M. (2009). A finite element procedure for rigorous numerical enclosures on the limit load in the analysis of multibody structures. Computer Methods in Applied Mechanics and Engineering. 199:48–60

Milani G, Lourenço PB, Tralli A. (2006.a). Homogenization Approach for the Limit Analysis of Out-of-Plane Loaded Masonry Walls. Journal of Structural Engineering 132:1650-1663.

Milani G, Lourenço PB, Tralli A (2006.b). Homogenised limit analysis of masonry walls, Part I: Failure surfaces. Computers and Structures 84:166–180

Milani G, Zuccarello FA, Olivito RS, Tralli A (2007). Heterogeneous upper-bound finite element limit analysis of masonry walls out-of-plane loaded. Computer Mechanics 40:911–931.

Milani G. (2008). 3D upper bound limit analysis of multi-leaf masonry walls. International Journal of Mechanical Sciences 50:817–836.

Milani G. (2011). Simple lower bound limit analysis homogenization model for in- and out-of-plane loaded masonry walls. Construction and Building Materials 25:4426–4443

Milani G. (2015). Upper bound sequential linear programming mesh adaptation scheme for collapse analysis of masonry vaults. Advances in Engineering Software 79:91–110.

Mojsilovic N. (2011). Strength of masonry subjected to in-plane loading: A contribution. International Journal of Solids and Structures 48:865–873.

Mourad SH, El-Hakim AF (1996). Evaluation of structural integrity of damaged masonry building. Journal of Performance of Constructed Facilities 10(2):73-78.

MS Mohammed. (2010). Finite element analysis of unreinforced masonry walls. Al Rafdain Engineering Journal 18(4):55-68.

Muttoni, A., Schwartz, J., Thurlimann, B. (1997). Design of concrete structures with stress fields. Birkhauser, Berlin.

Nayak S, Dutta SC. (2015). Improving seismic performance of masonry structures with openings by polypropylene bands and L-shaped reinforcing bars. Journal of Performance of Constructed Facilities 30(2), 04015003.

Nielsen MP, Hoang LC. (2010). Limit analysis and concrete plasticity. CRC Press, Taylor&Francis Group.

Orduna A, Lourenço PB. (2005). Three-dimensional limit analysis of rigid blocks assemblages. Part I: Torsion failure on frictional interfaces and limit analysis formulation. International Journal of Solids and Structures 42:5140–5160.

Orduna A. (2003). Seismic assessment of ancient masonry structures by rigid block limit analysis. Dissertation. Department of Civil Engineering. University of Minho, Guimaraes, Portugal.

Orduna A. (2017). Non-linear static analysis of rigid block models for structural assessment of ancient masonry constructions. International Journal of Solids and Structures 128:23–35.

Oyguc, R, Oyguc E. (2017). 2011 Van earthquakes: Lessons from damaged masonry structures. Journal of Performance of Constructed Facilities 31(5).

Palmisano F, Vitone A, Vitona C. (2003) From load path method to classical models of structural analysis. Journal of system-based vision for strategic and creative design 1:589-596

Palmisano F. (2016). Rapid diagnosis of crack patterns of masonry buildings subjected to landslide-induced settlements by using the load path method. International Journal of Architectural Heritage 10(4):438–456.

Portioli F, Casapulla C, Cascini L. (2015). An efficient solution procedure for crushing failure in 3D limit analysis of masonry block structures with non-associative frictional joints. International Journal of Solids and Structures 69–70:252–266.

Quagliarini E, Maracchini G, Clementi F. (2017). Uses and limits of the equivalent frame model on existing unreinforced masonry buildings for assessing their seismic risk: A review. Journal of Building Engineering 10:166–182.

Rankine, W. (1857) On the stability of loose earth. Philosophical Transactions of the Royal Society of London, Vol. 147.

Roca P, Cervera M, Gariup G, Pela L (2010). Structural analysis of masonry historical constructions classical and advanced approaches. Archives of Computational Methods in Engineering 17:299–325.

Roca P, Molins C, Mari AR. (2005). Strength capacity of masonry wall structures by the equivalent frame method. Journal of Structural Engineering. 131(10):1601-1610

Roca P. (2006). Assessment of masonry shear-walls by simple equilibrium models. Construction and Building Materials 20:229–238.

Salmanpour AH, Mojsilovic N, Schwartz J. (2013). Deformation capacity of unreinforced masonry walls subjected to in-plane loading: a state-of-the-art review. International Journal of Advanced Structural Engineering, 5:22.

Schofield, MA, Wroth CP. (1968). Critical state soil mechanics. McGraw-Hill, London.

Senthivel R, Lourenço PB (2009). Finite element modeling of deformation characteristics of historical stone masonry shear wall. Engineering Structures 31:1930-1943

Siano R, Sepe V, Camata G, Spacone E, Roca P, Pela L. (2017). Analysis of the performance in the linear field of equivalent-frame models for regular and irregular masonry walls. Engineering Structures 145:190–210.

Sloan SW. (1988). Lower bound limit analysis using finite elements and linear programming. International Journal for Numerical and Analytical Methods in Geomechanis, 12:61-77.

Sutcliffe DJ, Yu HS, Page AW (2001). Lower bound limit analysis of unreinforced masonry shear walls. Computers and Structures 79:1295-1312.

Terzaghi, K. (1943). Theoretical soil mechanics. Wiley, New York.

Yi T, Moon FL, Leon RT, Kahn LF. (2006). Analyses of a two-story unreinforced masonry building. Journal of Structural Engineering 132(5).

Yi T. (2004). Experimental investigation and numerical simulation of an unreinforced masonry structure with flexible diaphragms. Dissertation. Civil and Environmental Engineering, Georgia Institute of Technology.

Yu HS. (2006). Plasticity and geotechnics. Springer.

Yu MH (2004). Unified strength theory and its applications. Springer.

APPENDICES

A. MATLAB Code for Masonry Wall without Opening

```
%unknowns
Sigmax_A=1;Sigmay_A=1;Tao_A=1;      %Node A
Sigmax_B=1;Sigmay_B=1;Tao_B=1;      %Node B
Sigmax_C=1;Sigmay_C=1;Tao_C=1;      %Node C
Sigmax_D=1;Sigmay_D=1;Tao_D=1;      %Node D
Sigmax_E=1;Sigmay_E=1;Tao_E=1;      %Node E
Sigmax_F=1;Sigmay_F=1;Tao_F=1;      %Node F
Sigmax_G=1;Sigmay_G=1;Tao_G=1;      %Node G
Sigmax_H=1;Sigmay_H=1;Tao_H=1;      %Node H
Sigmax_I=1;Sigmay_I=1;Tao_I=1;      %Node I
Sigmax_J=1;Sigmay_J=1;Tao_J=1;      %Node J
Sigmax_K=1;Sigmay_K=1;Tao_K=1;      %Node K
Sigmax_L=1;Sigmay_L=1;Tao_L=1;      %Node L
Sigmax_M=1;Sigmay_M=1;Tao_M=1;      %Node M
Sigmax_N=1;Sigmay_N=1;Tao_N=1;      %Node N
Sigmax_O=1;Sigmay_O=1;Tao_O=1;      %Node O
Sigmax_P=1;Sigmay_P=1;Tao_P=1;      %Node P
H=1;

%number indices of nodes for each block
B1=[1,2,3,4,5,6,13,14,15,16,17,18];
B2=[4,5,6,7,8,9,16,17,18,19,20,21];
B3=[7,8,9,10,11,12,19,20,21,22,23,24];
B4=[13,14,15,16,17,18,25,26,27,28,29,30];
B5=[16,17,18,19,20,21,28,29,30,31,32,33];
B6=[19,20,21,22,23,24,31,32,33,34,35,36];
B7=[25,26,27,28,29,30,37,38,39,40,41,42];
B8=[28,29,30,31,32,33,40,41,42,43,44,45];
B9=[31,32,33,34,35,36,43,44,45,46,47,48];
BLOCK=[B1;B2;B3;B4;B5;B6;B7;B8;B9];

A=zeros(49,49);
for X=1:9, BLOCK(X,:);
    %equilibrium equation in x direction
     A((3*X-2),BLOCK(X,1))=-b/2;
     A((3*X-2),BLOCK(X,4))=b/2;
     A((3*X-2),BLOCK(X,7))=-b/2;
     A((3*X-2),BLOCK(X,10))=b/2;
     A((3*X-2),BLOCK(X,3))=a/2;
     A((3*X-2),BLOCK(X,6))=a/2;
     A((3*X-2),BLOCK(X,9))=-a/2;
     A((3*X-2),BLOCK(X,12))=-a/2;
     %equilibrium equation in y direction
     A((3*X-1),BLOCK(X,2))=a/2;
     A((3*X-1),BLOCK(X,5))=a/2;
     A((3*X-1),BLOCK(X,8))=-a/2;
     A((3*X-1),BLOCK(X,11))=-a/2;
     A((3*X-1),BLOCK(X,3))=-b/2;
     A((3*X-1),BLOCK(X,6))=b/2;
     A((3*X-1),BLOCK(X,9))=-b/2;
     A((3*X-1),BLOCK(X,12))=b/2;
End
```

```
%Boundary conditions Sigma_x
A(28,1)=b/2;
A(28,13)=b/2;
A(29,13)=b/2;
A(29,25)=b/2;

A(31,25)=b/2;
A(31,37)=b/2;
A(32,10)=b/2;
A(32,22)=b/2;

A(34,22)=b/2;
A(34,34)=b/2;
A(35,34)=b/2;
A(35,46)=b/2;

%Boundary conditions Tao
A(37,3)=b/2;
A(37,15)=b/2;
A(38,15)=b/2;
A(38,27)=b/2;

A(40,27)=b/2;
A(40,39)=b/2;
A(41,12)=b/2;
A(41,24)=b/2;

A(43,24)=b/2;
A(43,36)=b/2;
A(44,36)=b/2;
A(44,48)=b/2;

%External forces equilibrium H
A(46,3)=(a*t)/2;
A(46,6)=a*t;
A(46,9)=a*t;
A(46,12)=(a*t)/2;
A(46,49)=-1*(3*a);

%Boundary condition external forces equilibrium V
A(47,2)=(a/2);
A(47,5)=a;
A(47,8)=a;
A(47,11)=(a/2);

%Total moment
A(49,38)=((4*(a^2)*t)/3);
A(49,41)=(2*(a^2)*t);
A(49,44)=((a^2)*t);
A(49,47)=(((a^2)*t)/6);
A(49,49)=9*a*b;


B=zeros(49,1);
B(47,1)=(V)*(3*a);
B(49,1)=(-1)*(V)*t*((9*(a^2))/2);

Errmax=1;
Xnew=zeros(49,1);
%Initial values of principal stresses
```

```
SigmaA1=0;SigmaA3=0;
SigmaB1=0;SigmaB3=0;
SigmaC1=0;SigmaC3=0;
SigmaD1=0;SigmaD3=0;
SigmaE1=0;SigmaE3=0;
SigmaF1=0;SigmaF3=0;
SigmaG1=0;SigmaG3=0;
SigmaH1=0;SigmaH3=0;
SigmaI1=0;SigmaI3=0;
SigmaJ1=0;SigmaJ3=0;
SigmaK1=0;SigmaK3=0;
SigmaL1=0;SigmaL3=0;
SigmaM1=0;SigmaM3=0;
SigmaN1=0;SigmaN3=0;
SigmaO1=0;SigmaO3=0;
SigmaP1=0;SigmaP3=0;


while Errmax>0.00001


[A(3,1),A(3,2),A(3,3),B(3,1)]=mohr(SigmaA1,SigmaA3,Sigmax_A,Sigmay_A,Tao_A,
Sc,St);

[A(6,4),A(6,5),A(6,6),B(6,1)]=mohr(SigmaB1,SigmaB3,Sigmax_B,Sigmay_B,Tao_B,
Sc,St);

[A(9,7),A(9,8),A(9,9),B(9,1)]=mohr(SigmaC1,SigmaC3,Sigmax_C,Sigmay_C,Tao_C,
Sc,St);

[A(12,10),A(12,11),A(12,12),B(12,1)]=mohr(SigmaD1,SigmaD3,Sigmax_D,Sigmay_D
,Tao_D,Sc,St);

[A(15,13),A(15,14),A(15,15),B(15,1)]=mohr(SigmaE1,SigmaE3,Sigmax_E,Sigmay_E
,Tao_E,Sc,St);

[A(18,16),A(18,17),A(18,18),B(18,1)]=mohr(SigmaF1,SigmaF3,Sigmax_F,Sigmay_F
,Tao_F,Sc,St);

[A(21,19),A(21,20),A(21,21),B(21,1)]=mohr(SigmaG1,SigmaG3,Sigmax_G,Sigmay_G
,Tao_G,Sc,St);

[A(24,22),A(24,23),A(24,24),B(24,1)]=mohr(SigmaH1,SigmaH3,Sigmax_H,Sigmay_H
,Tao_H,Sc,St);

[A(27,25),A(27,26),A(27,27),B(27,1)]=mohr(SigmaI1,SigmaI3,Sigmax_I,Sigmay_I
,Tao_I,Sc,St);

[A(30,28),A(30,29),A(30,30),B(30,1)]=mohr(SigmaJ1,SigmaJ3,Sigmax_J,Sigmay_J
,Tao_J,Sc,St);

[A(33,31),A(33,32),A(33,33),B(33,1)]=mohr(SigmaK1,SigmaK3,Sigmax_K,Sigmay_K
,Tao_K,Sc,St);

[A(36,34),A(36,35),A(36,36),B(36,1)]=mohr(SigmaL1,SigmaL3,Sigmax_L,Sigmay_L
,Tao_L,Sc,St);

[A(39,37),A(39,38),A(39,39),B(39,1)]=mohr(SigmaM1,SigmaM3,Sigmax_M,Sigmay_M
,Tao_M,Sc,St);
```

```
[A(42,40),A(42,41),A(42,42),B(42,1)]=mohr(SigmaN1,SigmaN3,Sigmax_N,Sigmay_N
,Tao_N,Sc,St);

[A(45,43),A(45,44),A(45,45),B(45,1)]=mohr(SigmaO1,SigmaO3,Sigmax_O,Sigmay_O
,Tao_O,Sc,St);

[A(48,46),A(48,47),A(48,48),B(48,1)]=mohr(SigmaP1,SigmaP3,Sigmax_P,Sigmay_P
,Tao_P,Sc,St);



Xold=[Sigmax_A;Sigmay_A;Tao_A;Sigmax_B;Sigmay_B;Tao_B;Sigmax_C;Sigmay_C;Tao
_C;Sigmax_D;Sigmay_D;Tao_D;Sigmax_E;Sigmay_E;Tao_E;Sigmax_F;Sigmay_F;Tao_F;
Sigmax_G;Sigmay_G;Tao_G;Sigmax_H;Sigmay_H;Tao_H;Sigmax_I;Sigmay_I;Tao_I;Sig
max_J;Sigmay_J;Tao_J;Sigmax_K;Sigmay_K;Tao_K;Sigmax_L;Sigmay_L;Tao_L;Sigmax
_M;Sigmay_M;Tao_M;Sigmax_N;Sigmay_N;Tao_N;Sigmax_O;Sigmay_O;Tao_O;Sigmax_P;
Sigmay_P;Tao_P;H];

       Xnew=A\B;
            Delta=Xnew-Xold;
            Err=Delta./Xnew;
            Errmax=max(abs(Err));
            Sigmax_A=Xnew(1,1);
            Sigmay_A=Xnew(2,1);
            Tao_A=Xnew(3,1);
            Sigmax_B=Xnew(4,1);
            Sigmay_B=Xnew(5,1);
            Tao_B=Xnew(6,1);
            Sigmax_C=Xnew(7,1);
            Sigmay_C=Xnew(8,1);
            Tao_C=Xnew(9,1);
            Sigmax_D=Xnew(10,1);
            Sigmay_D=Xnew(11,1);
            Tao_D=Xnew(12,1);
            Sigmax_E=Xnew(13,1);
            Sigmay_E=Xnew(14,1);
            Tao_E=Xnew(15,1);
            Sigmax_F=Xnew(16,1);
            Sigmay_F=Xnew(17,1);
            Tao_F=Xnew(18,1);
            Sigmax_G=Xnew(19,1);
            Sigmay_G=Xnew(20,1);
            Tao_G=Xnew(21,1);
            Sigmax_H=Xnew(22,1);
            Sigmay_H=Xnew(23,1);
            Tao_H=Xnew(24,1);
            Sigmax_I=Xnew(25,1);
            Sigmay_I=Xnew(26,1);
            Tao_I=Xnew(27,1);
            Sigmax_J=Xnew(28,1);
            Sigmay_J=Xnew(29,1);
            Tao_J=Xnew(30,1);
            Sigmax_K=Xnew(31,1);
            Sigmay_K=Xnew(32,1);
            Tao_K=Xnew(33,1);
            Sigmax_L=Xnew(34,1);
            Sigmay_L=Xnew(35,1);
            Tao_L=Xnew(36,1);
            Sigmax_M=Xnew(37,1);
```

```
            Sigmay_M=Xnew(38,1);
            Tao_M=Xnew(39,1);
            Sigmax_N=Xnew(40,1);
            Sigmay_N=Xnew(41,1);
            Tao_N=Xnew(42,1);
            Sigmax_O=Xnew(43,1);
            Sigmay_O=Xnew(44,1);
            Tao_O=Xnew(45,1);
            Sigmax_P=Xnew(46,1);
            Sigmay_P=Xnew(47,1);
            Tao_P=Xnew(48,1);
            H=Xnew(49,1);
end
```

B. MATLAB Code for Masonry Wall with Window Opening

```
%unknowns
Sigmax_A=1;Sigmay_A=1;Tao_A=1;       %Node A
Sigmax_B=1;Sigmay_B=1;Tao_B=1;       %Node B
Sigmax_C=1;Sigmay_C=1;Tao_C=1;       %Node C
Sigmax_D=1;Sigmay_D=1;Tao_D=1;       %Node D
Sigmax_E=1;Sigmay_E=1;Tao_E=1;       %Node E
Sigmax_F=1;Sigmay_F=1;Tao_F=1;       %Node F
Sigmax_G=1;Sigmay_G=1;Tao_G=1;       %Node G
Sigmax_H=1;Sigmay_H=1;Tao_H=1;       %Node H
Sigmax_I=1;Sigmay_I=1;Tao_I=1;       %Node I
Sigmax_J=1;Sigmay_J=1;Tao_J=1;       %Node J
Sigmax_K=1;Sigmay_K=1;Tao_K=1;       %Node K
Sigmax_L=1;Sigmay_L=1;Tao_L=1;       %Node L
Sigmax_M=1;Sigmay_M=1;Tao_M=1;       %Node M
Sigmax_N=1;Sigmay_N=1;Tao_N=1;       %Node N
Sigmax_O=1;Sigmay_O=1;Tao_O=1;       %Node O
Sigmax_P=1;Sigmay_P=1;Tao_P=1;       %Node P
H=1;

%number indices of nodes for each block
B1=[1,2,3,4,5,6,13,14,15,16,17,18];
B2=[4,5,6,7,8,9,16,17,18,19,20,21];
B3=[7,8,9,10,11,12,19,20,21,22,23,24];
B4=[13,14,15,16,17,18,25,26,27,28,29,30];
B5=[16,17,18,19,20,21,28,29,30,31,32,33];
B6=[19,20,21,22,23,24,31,32,33,34,35,36];
B7=[25,26,27,28,29,30,37,38,39,40,41,42];
B8=[28,29,30,31,32,33,40,41,42,43,44,45];
B9=[31,32,33,34,35,36,43,44,45,46,47,48];
BLOCK=[B1;B2;B3;B4;B5;B6;B7;B8;B9];

A=zeros(49,49);
for X=1:9, BLOCK(X,:);
    if X==5;
        continue
    end
    if X==1 || X==3 || X==7 || X==9;
        x=a;
        y=b;
    end
    if X==2 || X==8;
        x=c;
        y=b;
    end
    if X==4 || X==6;
        x=a;
        y=d;
    end

    %equilibrium equation in x direction
     A((3*X-2),BLOCK(X,1))=-y/2;
     A((3*X-2),BLOCK(X,4))=y/2;
     A((3*X-2),BLOCK(X,7))=-y/2;
     A((3*X-2),BLOCK(X,10))=y/2;
     A((3*X-2),BLOCK(X,3))=x/2;
     A((3*X-2),BLOCK(X,6))=x/2;
     A((3*X-2),BLOCK(X,9))=-x/2;
```

```
     A((3*X-2),BLOCK(X,12))=-x/2;
     %equilibrium equation in y direction
     A((3*X-1),BLOCK(X,2))=x/2;
     A((3*X-1),BLOCK(X,5))=x/2;
     A((3*X-1),BLOCK(X,8))=-x/2;
     A((3*X-1),BLOCK(X,11))=-x/2;
     A((3*X-1),BLOCK(X,3))=-y/2;
     A((3*X-1),BLOCK(X,6))=y/2;
     A((3*X-1),BLOCK(X,9))=-y/2;
     A((3*X-1),BLOCK(X,12))=y/2;
end


%Boundary conditions around opening
A(13,16)=d/2;
A(13,28)=d/2;
A(14,19)=d/2;
A(14,31)=d/2;

%Boundary conditions Sigma_x
A(28,1)=b/2;
A(28,13)=b/2;
A(29,13)=d/2;
A(29,25)=d/2;

A(31,25)=b/2;
A(31,37)=b/2;
A(32,10)=b/2;
A(32,22)=b/2;

A(34,22)=d/2;
A(34,34)=d/2;
A(35,34)=b/2;
A(35,46)=b/2;


%Boundary conditions Tao
A(37,3)=b/2;
A(37,15)=b/2;
A(38,15)=d/2;
A(38,27)=d/2;

A(40,27)=b/2;
A(40,39)=b/2;
A(41,12)=b/2;
A(41,24)=b/2;

A(43,24)=d/2;
A(43,36)=d/2;
A(44,36)=b/2;
A(44,48)=b/2;

%External forces equilibrium H
A(46,3)=(a*t)/2;
A(46,6)=((a*t)/2)+((c*t)/2);
A(46,9)=((a*t)/2)+((c*t)/2);
A(46,12)=(a*t)/2;
A(46,49)=-1*((2*a)+c);

%Boundary condition external forces equilibrium V
```

```
A(47,2)=a/2;
A(47,5)=(a/2)+(c/2);
A(47,8)=(a/2)+(c/2);
A(47,11)=a/2;

%Total moment
A(49,38)=((5*t*(a^2))/6)+((a*c*t)/2);
A(49,41)=((2*(a^2)*t)/3)+(a*c*t)+((t*(c^2))/3);
A(49,44)=((a*c*t)/2)+((t*(c^2))/6)+((t*(a^2))/3);
A(49,47)=(t*(a^2))/6;
A(49,49)=(2*a+c)*(2*b+d);

B=zeros(49,1);
B(47,1)=V*(2*a+c);
B(49,1)=-V*t*(((2*a+c)^2)/2);


Errmax=1;
Xnew=zeros(49,1);
%Initial values of principal stresses
SigmaA1=0;SigmaA3=0;
SigmaB1=0;SigmaB3=0;
SigmaC1=0;SigmaC3=0;
SigmaD1=0;SigmaD3=0;
SigmaE1=0;SigmaE3=0;
SigmaF1=0;SigmaF3=0;
SigmaG1=0;SigmaG3=0;
SigmaH1=0;SigmaH3=0;
SigmaI1=0;SigmaI3=0;
SigmaJ1=0;SigmaJ3=0;
SigmaK1=0;SigmaK3=0;
SigmaL1=0;SigmaL3=0;
SigmaM1=0;SigmaM3=0;
SigmaN1=0;SigmaN3=0;
SigmaO1=0;SigmaO3=0;
SigmaP1=0;SigmaP3=0;


while Errmax>0.00001


[A(3,1),A(3,2),A(3,3),B(3,1)]=mohr(SigmaA1,SigmaA3,Sigmax_A,Sigmay_A,Tao_A,
Sc,St);

[A(6,4),A(6,5),A(6,6),B(6,1)]=mohr(SigmaB1,SigmaB3,Sigmax_B,Sigmay_B,Tao_B,
Sc,St);

[A(9,7),A(9,8),A(9,9),B(9,1)]=mohr(SigmaC1,SigmaC3,Sigmax_C,Sigmay_C,Tao_C,
Sc,St);

[A(12,10),A(12,11),A(12,12),B(12,1)]=mohr(SigmaD1,SigmaD3,Sigmax_D,Sigmay_D
,Tao_D,Sc,St);

[A(15,13),A(15,14),A(15,15),B(15,1)]=mohr(SigmaE1,SigmaE3,Sigmax_E,Sigmay_E
,Tao_E,Sc,St);

[A(21,19),A(21,20),A(21,21),B(21,1)]=mohr(SigmaG1,SigmaG3,Sigmax_G,Sigmay_G
,Tao_G,Sc,St);
```

```
[A(24,22),A(24,23),A(24,24),B(24,1)]=mohr(SigmaH1,SigmaH3,Sigmax_H,Sigmay_H
,Tao_H,Sc,St);

[A(18,16),A(18,17),A(18,18),B(18,1)]=mohr(SigmaF1,SigmaF3,Sigmax_F,Sigmay_F
,Tao_F,Sc,St);

[A(27,25),A(27,26),A(27,27),B(27,1)]=mohr(SigmaI1,SigmaI3,Sigmax_I,Sigmay_I
,Tao_I,Sc,St);

[A(30,28),A(30,29),A(30,30),B(30,1)]=mohr(SigmaJ1,SigmaJ3,Sigmax_J,Sigmay_J
,Tao_J,Sc,St);

[A(33,31),A(33,32),A(33,33),B(33,1)]=mohr(SigmaK1,SigmaK3,Sigmax_K,Sigmay_K
,Tao_K,Sc,St);

[A(36,34),A(36,35),A(36,36),B(36,1)]=mohr(SigmaL1,SigmaL3,Sigmax_L,Sigmay_L
,Tao_L,Sc,St);

[A(39,37),A(39,38),A(39,39),B(39,1)]=mohr(SigmaM1,SigmaM3,Sigmax_M,Sigmay_M
,Tao_M,Sc,St);

[A(42,40),A(42,41),A(42,42),B(42,1)]=mohr(SigmaN1,SigmaN3,Sigmax_N,Sigmay_N
,Tao_N,Sc,St);

[A(45,43),A(45,44),A(45,45),B(45,1)]=mohr(SigmaO1,SigmaO3,Sigmax_O,Sigmay_O
,Tao_O,Sc,St);

[A(48,46),A(48,47),A(48,48),B(48,1)]=mohr(SigmaP1,SigmaP3,Sigmax_P,Sigmay_P
,Tao_P,Sc,St);



Xold=[Sigmax_A;Sigmay_A;Tao_A;Sigmax_B;Sigmay_B;Tao_B;Sigmax_C;Sigmay_C;Tao
_C;Sigmax_D;Sigmay_D;Tao_D;Sigmax_E;Sigmay_E;Tao_E;Sigmax_F;Sigmay_F;Tao_F;
Sigmax_G;Sigmay_G;Tao_G;Sigmax_H;Sigmay_H;Tao_H;Sigmax_I;Sigmay_I;Tao_I;Sig
max_J;Sigmay_J;Tao_J;Sigmax_K;Sigmay_K;Tao_K;Sigmax_L;Sigmay_L;Tao_L;Sigmax
_M;Sigmay_M;Tao_M;Sigmax_N;Sigmay_N;Tao_N;Sigmax_O;Sigmay_O;Tao_O;Sigmax_P;
Sigmay_P;Tao_P;H];

       Xnew=A\B;
            Delta=Xnew-Xold;
            Err=Delta./Xnew;
            Errmax=max(abs(Err));
            Sigmax_A=Xnew(1,1);
            Sigmay_A=Xnew(2,1);
            Tao_A=Xnew(3,1);
            Sigmax_B=Xnew(4,1);
            Sigmay_B=Xnew(5,1);
            Tao_B=Xnew(6,1);
            Sigmax_C=Xnew(7,1);
            Sigmay_C=Xnew(8,1);
            Tao_C=Xnew(9,1);
            Sigmax_D=Xnew(10,1);
            Sigmay_D=Xnew(11,1);
            Tao_D=Xnew(12,1);
            Sigmax_E=Xnew(13,1);
            Sigmay_E=Xnew(14,1);
            Tao_E=Xnew(15,1);
            Sigmax_F=Xnew(16,1);
```

```
                Sigmay_F=Xnew(17,1);
                Tao_F=Xnew(18,1);
                Sigmax_G=Xnew(19,1);
                Sigmay_G=Xnew(20,1);
                Tao_G=Xnew(21,1);
                Sigmax_H=Xnew(22,1);
                Sigmay_H=Xnew(23,1);
                Tao_H=Xnew(24,1);
                Sigmax_I=Xnew(25,1);
                Sigmay_I=Xnew(26,1);
                Tao_I=Xnew(27,1);
                Sigmax_J=Xnew(28,1);
                Sigmay_J=Xnew(29,1);
                Tao_J=Xnew(30,1);
                Sigmax_K=Xnew(31,1);
                Sigmay_K=Xnew(32,1);
                Tao_K=Xnew(33,1);
                Sigmax_L=Xnew(34,1);
                Sigmay_L=Xnew(35,1);
                Tao_L=Xnew(36,1);
                Sigmax_M=Xnew(37,1);
                Sigmay_M=Xnew(38,1);
                Tao_M=Xnew(39,1);
                Sigmax_N=Xnew(40,1);
                Sigmay_N=Xnew(41,1);
                Tao_N=Xnew(42,1);
                Sigmax_O=Xnew(43,1);
                Sigmay_O=Xnew(44,1);
                Tao_O=Xnew(45,1);
                Sigmax_P=Xnew(46,1);
                Sigmay_P=Xnew(47,1);
                Tao_P=Xnew(48,1);
                H=Xnew(49,1);
end
```

C. MATLAB Code for Masonry Wall with Door Opening

```
%unknowns
Sigmax_A=1;Sigmay_A=1;Tao_A=1;      %Node A
Sigmax_B=1;Sigmay_B=1;Tao_B=1;      %Node B
Sigmax_C=1;Sigmay_C=1;Tao_C=1;      %Node C
Sigmax_D=1;Sigmay_D=1;Tao_D=1;      %Node D
Sigmax_E=1;Sigmay_E=1;Tao_E=1;      %Node E
Sigmax_F=1;Sigmay_F=1;Tao_F=1;      %Node F
Sigmax_G=1;Sigmay_G=1;Tao_G=1;      %Node G
Sigmax_H=1;Sigmay_H=1;Tao_H=1;      %Node H
Sigmax_I=1;Sigmay_I=1;Tao_I=1;      %Node I
Sigmax_J=1;Sigmay_J=1;Tao_J=1;      %Node J
Sigmax_K=1;Sigmay_K=1;Tao_K=1;      %Node K
Sigmax_L=1;Sigmay_L=1;Tao_L=1;      %Node L
Sigmax_M=1;Sigmay_M=1;Tao_M=1;      %Node M
Sigmax_N=1;Sigmay_N=1;Tao_N=1;      %Node N
Sigmax_O=1;Sigmay_O=1;Tao_O=1;      %Node O
Sigmax_P=1;Sigmay_P=1;Tao_P=1;      %Node P
H=1;

%number indices of nodes for each block
B1=[1,2,3,4,5,6,13,14,15,16,17,18];
B2=[4,5,6,7,8,9,16,17,18,19,20,21];
B3=[7,8,9,10,11,12,19,20,21,22,23,24];
B4=[13,14,15,16,17,18,25,26,27,28,29,30];
B5=[16,17,18,19,20,21,28,29,30,31,32,33];
B6=[19,20,21,22,23,24,31,32,33,34,35,36];
B7=[25,26,27,28,29,30,37,38,39,40,41,42];
B8=[28,29,30,31,32,33,40,41,42,43,44,45];
B9=[31,32,33,34,35,36,43,44,45,46,47,48];
BLOCK=[B1;B2;B3;B4;B5;B6;B7;B8;B9];

A=zeros(49,49);
for X=1:9, BLOCK(X,:);
    if X==5 || X==8;
        continue
    end
    if X==1 || X==3;
        x=a;
        y=b;
    end
    if X==2;
        x=c;
        y=b;
    end
    if X==4 || X==6 || X==7 || X==9;
        x=a;
        y=d;
    end

    %equilibrium equation in x direction
     A((3*X-2),BLOCK(X,1))=-y/2;
     A((3*X-2),BLOCK(X,4))=y/2;
     A((3*X-2),BLOCK(X,7))=-y/2;
     A((3*X-2),BLOCK(X,10))=y/2;
     A((3*X-2),BLOCK(X,3))=x/2;
     A((3*X-2),BLOCK(X,6))=x/2;
     A((3*X-2),BLOCK(X,9))=-x/2;
```

```
     A((3*X-2),BLOCK(X,12))=-x/2;
     %equilibrium equation in y direction
     A((3*X-1),BLOCK(X,2))=x/2;
     A((3*X-1),BLOCK(X,5))=x/2;
     A((3*X-1),BLOCK(X,8))=-x/2;
     A((3*X-1),BLOCK(X,11))=-x/2;
     A((3*X-1),BLOCK(X,3))=-y/2;
     A((3*X-1),BLOCK(X,6))=y/2;
     A((3*X-1),BLOCK(X,9))=-y/2;
     A((3*X-1),BLOCK(X,12))=y/2;
end


%Boundary conditions around opening
A(13,16)=d/2;
A(13,28)=d/2;
A(14,19)=d/2;
A(14,31)=d/2;

A(22,28)=d/2;
A(22,40)=d/2;
A(23,31)=d/2;
A(23,43)=d/2;

%Boundary conditions Sigma_x
A(28,1)=b/2;
A(28,13)=b/2;
A(29,13)=d/2;
A(29,25)=d/2;

A(31,25)=d/2;
A(31,37)=d/2;
A(32,10)=b/2;
A(32,22)=b/2;

A(34,22)=d/2;
A(34,34)=d/2;
A(35,34)=d/2;
A(35,46)=d/2;

%Boundary conditions Tao
A(37,3)=b/2;
A(37,15)=b/2;
A(38,15)=d/2;
A(38,27)=d/2;

A(40,27)=d/2;
A(40,39)=d/2;
A(41,12)=b/2;
A(41,24)=b/2;

A(43,24)=d/2;
A(43,36)=d/2;
A(44,36)=d/2;
A(44,48)=d/2;

%External forces equilibrium H
A(46,3)=(a*t)/2;
A(46,6)=((a*t)/2)+((c*t)/2);
A(46,9)=((a*t)/2)+((c*t)/2);
```

```
A(46,12)=(a*t)/2;
A(46,49)=-1*((2*a)+c);

%Boundary condition external forces equilibrium V
A(47,2)=a/2;
A(47,5)=(a/2)+(c/2);
A(47,8)=(a/2)+(c/2);
A(47,11)=a/2;

%Total moment
A(49,38)=((5*(a^2*t))/6)+((a*c*t)/2);
A(49,41)=((2*(a^2*t))/3)+((a*c*t)/2);
A(49,44)=((a^2*t)/3);
A(49,47)=(a^2*t)/6;
A(49,49)=(2*a+c)*(2*d+b);


B=zeros(49,1);
B(47,1)=V*(2*a+c);
B(49,1)=-V*(((2*a+c)^2)/2)*t;

Errmax=1;
Xnew=zeros(49,1);
%Initial values of principal stresses
SigmaA1=0;SigmaA3=0;
SigmaB1=0;SigmaB3=0;
SigmaC1=0;SigmaC3=0;
SigmaD1=0;SigmaD3=0;
SigmaE1=0;SigmaE3=0;
SigmaF1=0;SigmaF3=0;
SigmaG1=0;SigmaG3=0;
SigmaH1=0;SigmaH3=0;
SigmaI1=0;SigmaI3=0;
SigmaJ1=0;SigmaJ3=0;
SigmaK1=0;SigmaK3=0;
SigmaL1=0;SigmaL3=0;
SigmaM1=0;SigmaM3=0;
SigmaN1=0;SigmaN3=0;
SigmaO1=0;SigmaO3=0;
SigmaP1=0;SigmaP3=0;

while Errmax>0.00001


[A(3,1),A(3,2),A(3,3),B(3,1)]=mohr(SigmaA1,SigmaA3,Sigmax_A,Sigmay_A,Tao_A,
Sc,St);

[A(6,4),A(6,5),A(6,6),B(6,1)]=mohr(SigmaB1,SigmaB3,Sigmax_B,Sigmay_B,Tao_B,
Sc,St);

[A(9,7),A(9,8),A(9,9),B(9,1)]=mohr(SigmaC1,SigmaC3,Sigmax_C,Sigmay_C,Tao_C,
Sc,St);

[A(12,10),A(12,11),A(12,12),B(12,1)]=mohr(SigmaD1,SigmaD3,Sigmax_D,Sigmay_D
,Tao_D,Sc,St);

[A(15,13),A(15,14),A(15,15),B(15,1)]=mohr(SigmaE1,SigmaE3,Sigmax_E,Sigmay_E
,Tao_E,Sc,St);
```

```
[A(18,16),A(18,17),A(18,18),B(18,1)]=mohr(SigmaF1,SigmaF3,Sigmax_F,Sigmay_F
,Tao_F,Sc,St);

[A(21,19),A(21,20),A(21,21),B(21,1)]=mohr(SigmaG1,SigmaG3,Sigmax_G,Sigmay_G
,Tao_G,Sc,St);

[A(24,22),A(24,23),A(24,24),B(24,1)]=mohr(SigmaH1,SigmaH3,Sigmax_H,Sigmay_H
,Tao_H,Sc,St);

[A(27,25),A(27,26),A(27,27),B(27,1)]=mohr(SigmaI1,SigmaI3,Sigmax_I,Sigmay_I
,Tao_I,Sc,St);

[A(30,28),A(30,29),A(30,30),B(30,1)]=mohr(SigmaJ1,SigmaJ3,Sigmax_J,Sigmay_J
,Tao_J,Sc,St);

[A(33,31),A(33,32),A(33,33),B(33,1)]=mohr(SigmaK1,SigmaK3,Sigmax_K,Sigmay_K
,Tao_K,Sc,St);

[A(36,34),A(36,35),A(36,36),B(36,1)]=mohr(SigmaL1,SigmaL3,Sigmax_L,Sigmay_L
,Tao_L,Sc,St);

[A(39,37),A(39,38),A(39,39),B(39,1)]=mohr(SigmaM1,SigmaM3,Sigmax_M,Sigmay_M
,Tao_M,Sc,St);

[A(42,40),A(42,41),A(42,42),B(42,1)]=mohr(SigmaN1,SigmaN3,Sigmax_N,Sigmay_N
,Tao_N,Sc,St);

[A(45,43),A(45,44),A(45,45),B(45,1)]=mohr(SigmaO1,SigmaO3,Sigmax_O,Sigmay_O
,Tao_O,Sc,St);

[A(48,46),A(48,47),A(48,48),B(48,1)]=mohr(SigmaP1,SigmaP3,Sigmax_P,Sigmay_P
,Tao_P,Sc,St);



Xold=[Sigmax_A;Sigmay_A;Tao_A;Sigmax_B;Sigmay_B;Tao_B;Sigmax_C;Sigmay_C;Tao
_C;Sigmax_D;Sigmay_D;Tao_D;Sigmax_E;Sigmay_E;Tao_E;Sigmax_F;Sigmay_F;Tao_F;
Sigmax_G;Sigmay_G;Tao_G;Sigmax_H;Sigmay_H;Tao_H;Sigmax_I;Sigmay_I;Tao_I;Sig
max_J;Sigmay_J;Tao_J;Sigmax_K;Sigmay_K;Tao_K;Sigmax_L;Sigmay_L;Tao_L;Sigmax
_M;Sigmay_M;Tao_M;Sigmax_N;Sigmay_N;Tao_N;Sigmax_O;Sigmay_O;Tao_O;Sigmax_P;
Sigmay_P;Tao_P;H];

       Xnew=A\B;
            Delta=Xnew-Xold;
            Err=Delta./Xnew;
            Errmax=max(abs(Err));
            Sigmax_A=Xnew(1,1);
            Sigmay_A=Xnew(2,1);
            Tao_A=Xnew(3,1);
            Sigmax_B=Xnew(4,1);
            Sigmay_B=Xnew(5,1);
            Tao_B=Xnew(6,1);
            Sigmax_C=Xnew(7,1);
            Sigmay_C=Xnew(8,1);
            Tao_C=Xnew(9,1);
            Sigmax_D=Xnew(10,1);
            Sigmay_D=Xnew(11,1);
            Tao_D=Xnew(12,1);
            Sigmax_E=Xnew(13,1);
```

```
                Sigmay_E=Xnew(14,1);
                Tao_E=Xnew(15,1);
                Sigmax_F=Xnew(16,1);
                Sigmay_F=Xnew(17,1);
                Tao_F=Xnew(18,1);
                Sigmax_G=Xnew(19,1);
                Sigmay_G=Xnew(20,1);
                Tao_G=Xnew(21,1);
                Sigmax_H=Xnew(22,1);
                Sigmay_H=Xnew(23,1);
                Tao_H=Xnew(24,1);
                Sigmax_I=Xnew(25,1);
                Sigmay_I=Xnew(26,1);
                Tao_I=Xnew(27,1);
                Sigmax_J=Xnew(28,1);
                Sigmay_J=Xnew(29,1);
                Tao_J=Xnew(30,1);
                Sigmax_K=Xnew(31,1);
                Sigmay_K=Xnew(32,1);
                Tao_K=Xnew(33,1);
                Sigmax_L=Xnew(34,1);
                Sigmay_L=Xnew(35,1);
                Tao_L=Xnew(36,1);
                Sigmax_M=Xnew(37,1);
                Sigmay_M=Xnew(38,1);
                Tao_M=Xnew(39,1);
                Sigmax_N=Xnew(40,1);
                Sigmay_N=Xnew(41,1);
                Tao_N=Xnew(42,1);
                Sigmax_O=Xnew(43,1);
                Sigmay_O=Xnew(44,1);
                Tao_O=Xnew(45,1);
                Sigmax_P=Xnew(46,1);
                Sigmay_P=Xnew(47,1);
                Tao_P=Xnew(48,1);
                H=Xnew(49,1);
end
```

D. MATLAB Code for Masonry Wall with Single Window and Single Door Opening

```
%Unknowns
Sigmax_A=1;Sigmay_A=1;Tao_A=1;       %Node A
Sigmax_B=1;Sigmay_B=1;Tao_B=1;       %Node B
Sigmax_C=1;Sigmay_C=1;Tao_C=1;       %Node C
Sigmax_D=1;Sigmay_D=1;Tao_D=1;       %Node D
Sigmax_E=1;Sigmay_E=1;Tao_E=1;       %Node E
Sigmax_F=1;Sigmay_F=1;Tao_F=1;       %Node F
Sigmax_G=1;Sigmay_G=1;Tao_G=1;       %Node G
Sigmax_H=1;Sigmay_H=1;Tao_H=1;       %Node H
Sigmax_I=1;Sigmay_I=1;Tao_I=1;       %Node I
Sigmax_J=1;Sigmay_J=1;Tao_J=1;       %Node J
Sigmax_K=1;Sigmay_K=1;Tao_K=1;       %Node K
Sigmax_L=1;Sigmay_L=1;Tao_L=1;       %Node L
Sigmax_M=1;Sigmay_M=1;Tao_M=1;       %Node M
Sigmax_N=1;Sigmay_N=1;Tao_N=1;       %Node N
Sigmax_O=1;Sigmay_O=1;Tao_O=1;       %Node O
Sigmax_P=1;Sigmay_P=1;Tao_P=1;       %Node P
Sigmax_R=1;Sigmay_R=1;Tao_R=1;       %Node R
Sigmax_S=1;Sigmay_S=1;Tao_S=1;       %Node S
Sigmax_T=1;Sigmay_T=1;Tao_T=1;       %Node T
Sigmax_U=1;Sigmay_U=1;Tao_U=1;       %Node U
Sigmax_V=1;Sigmay_V=1;Tao_V=1;       %Node V
Sigmax_W=1;Sigmay_W=1;Tao_W=1;       %Node W
Sigmax_Y=1;Sigmay_Y=1;Tao_Y=1;       %Node Y
Sigmax_Z=1;Sigmay_Z=1;Tao_Z=1;       %Node Z
Sigmax_AA=1;Sigmay_AA=1;Tao_AA=1;    %Node AA
Sigmax_BB=1;Sigmay_BB=1;Tao_BB=1;    %Node BB
Sigmax_CC=1;Sigmay_CC=1;Tao_CC=1;    %Node CC
Sigmax_DD=1;Sigmay_DD=1;Tao_DD=1;    %Node DD
Sigmax_EE=1;Sigmay_EE=1;Tao_EE=1;    %Node EE
Sigmax_FF=1;Sigmay_FF=1;Tao_FF=1;    %Node FF
Sigmax_GG=1;Sigmay_GG=1;Tao_GG=1;    %Node GG
Sigmax_HH=1;Sigmay_HH=1;Tao_HH=1;    %Node HH
Sigmax_II=1;Sigmay_II=1;Tao_II=1;    %Node II
Sigmax_JJ=1;Sigmay_JJ=1;Tao_JJ=1;    %Node JJ
Sigmax_KK=1;Sigmay_KK=1;Tao_KK=1;    %Node KK
Sigmax_LL=1;Sigmay_LL=1;Tao_LL=1;    %Node LL
H=1;

%number indices of nodes for each block
B1=[1,2,3,4,5,6,19,20,21,22,23,24];
B2=[4,5,6,7,8,9,22,23,24,25,26,27];
B3=[7,8,9,10,11,12,25,26,27,28,29,30];
B4=[10,11,12,13,14,15,28,29,30,31,32,33];
B5=[13,14,15,16,17,18,31,32,33,34,35,36];
B6=[19,20,21,22,23,24,37,38,39,40,41,42];
B7=[22,23,24,25,26,27,40,41,42,43,44,45];
B8=[25,26,27,28,29,30,43,44,45,46,47,48];
B9=[28,29,30,31,32,33,46,47,48,49,50,51];
B10=[31,32,33,34,35,36,49,50,51,52,53,54];
B11=[37,38,39,40,41,42,55,56,57,58,59,60];
B12=[40,41,42,43,44,45,58,59,60,61,62,63];
B13=[43,44,45,46,47,48,61,62,63,64,65,66];
B14=[46,47,48,49,50,51,64,65,66,67,68,69];
B15=[49,50,51,52,53,54,67,68,69,70,71,72];
```

```
B16=[55,56,57,58,59,60,73,74,75,76,77,78];
B17=[58,59,60,61,62,63,76,77,78,79,80,81];
B18=[61,62,63,64,65,66,79,80,81,82,83,84];
B19=[64,65,66,67,68,69,82,83,84,85,86,87];
B20=[67,68,69,70,71,72,85,86,87,88,89,90];
B21=[73,74,75,76,77,78,91,92,93,94,95,96];
B22=[76,77,78,79,80,81,94,95,96,97,98,99];
B23=[79,80,81,82,83,84,97,98,99,100,101,102];
B24=[82,83,84,85,86,87,100,101,102,103,104,105];
B25=[85,86,87,88,89,90,103,104,105,106,107,108];
BLOCK=[B1;B2;B3;B4;B5;B6;B7;B8;B9;B10;B11;B12;B13;B14;B15;B16;B17;B18;B19;B
20;B21;B22;B23;B24;B25];

A=zeros(109,109);
for X=1:25, BLOCK(X,:);
    if X==12 || X==14 || X==19 || X==24;
        continue
    end
    if X==1 || X==5 || X==6 || X==10;
        x=a;
        y=b;
    end
    if X==2 || X==4 || X==7 || X==9;
        x=c;
        y=b;
    end
    if X==3 || X==8;
        x=e;
        y=b;
    end
    if X==11 || X==15;
        x=a;
        y=f;
    end
    if X==13;
        x=e;
        y=f;
    end
    if X==16 || X==20 || X==21 || X==25;
        x=a;
        y=d;
    end
    if X==17 || X==22;
        x=c;
        y=d;
    end
    if X==18 || X==23;
        x=e;
        y=d;
    end

    %equilibrium equation in x direction
     A((3*X-2),BLOCK(X,1))=-y/2;
     A((3*X-2),BLOCK(X,4))=y/2;
     A((3*X-2),BLOCK(X,7))=-y/2;
     A((3*X-2),BLOCK(X,10))=y/2;
     A((3*X-2),BLOCK(X,3))=x/2;
     A((3*X-2),BLOCK(X,6))=x/2;
     A((3*X-2),BLOCK(X,9))=-x/2;
     A((3*X-2),BLOCK(X,12))=-x/2;
```

```
    %equilibrium equation in y direction
    A((3*X-1),BLOCK(X,2))=x/2;
    A((3*X-1),BLOCK(X,5))=x/2;
    A((3*X-1),BLOCK(X,8))=-x/2;
    A((3*X-1),BLOCK(X,11))=-x/2;
    A((3*X-1),BLOCK(X,3))=-y/2;
    A((3*X-1),BLOCK(X,6))=y/2;
    A((3*X-1),BLOCK(X,9))=-y/2;
    A((3*X-1),BLOCK(X,12))=y/2;
end

%Boundary conditions around opening
A(34,40)=f/2;
A(34,58)=f/2;
A(35,43)=f/2;
A(35,61)=f/2;

A(40,46)=f/2;
A(40,64)=f/2;
A(41,49)=f/2;
A(41,67)=f/2;

A(55,64)=d/2;
A(55,82)=d/2;
A(56,67)=d/2;
A(56,85)=d/2;

A(70,82)=d/2;
A(70,100)=d/2;
A(71,85)=d/2;
A(71,103)=d/2;

%Boundary conditions Sigma_x
A(76,1)=b/2;
A(76,19)=b/2;
A(77,19)=b/2;
A(77,37)=b/2;

A(79,37)=d/2;
A(79,55)=d/2;
A(80,55)=d/2;
A(80,73)=d/2;

A(82,73)=d/2;
A(82,91)=d/2;
A(83,16)=b/2;
A(83,34)=b/2;

A(85,34)=b/2;
A(85,52)=b/2;
A(86,52)=d/2;
A(86,70)=d/2;

A(88,70)=d/2;
A(88,88)=d/2;
A(89,80)=d/2;
A(89,106)=d/2;

%Boundary conditions Tao
A(91,3)=b/2;
```

```
A(91,21)=b/2;
A(92,21)=b/2;
A(92,39)=b/2;

A(94,39)=d/2;
A(94,57)=d/2;
A(95,57)=d/2;
A(95,75)=d/2;

A(97,75)=d/2;
A(97,93)=d/2;
A(98,18)=b/2;
A(98,36)=b/2;

A(100,36)=b/2;
A(100,54)=b/2;
A(101,54)=d/2;
A(101,72)=d/2;

A(103,72)=d/2;
A(103,90)=d/2;
A(104,90)=d/2;
A(104,108)=d/2;

%External forces equilibrium H
A(106,3)=(a/2)*t;
A(106,6)=((a+c)*t)/2;
A(106,9)=((c+e)*t)/2;
A(106,12)=((c+e)*t)/2;
A(106,15)=((a+c)*t)/2;
A(106,18)=(a*t)/2;
A(106,109)=-((2*a)+(2*c)+e);

%Boundary condition external forces equilibrium V
A(107,2)=a/2;
A(107,5)=(a+c)/2;
A(107,8)=(c+e)/2;
A(107,11)=(c+e)/2;
A(107,14)=(a+c)/2;
A(107,17)=a/2;

%Total moment
A(109,92)=(((a*(a+2*c+e))/2)+((a^2)/3))*t;
A(109,95)=(((a*(a+2*c+e))/2)+((c^2)/6)+((e*(a+c))/2)+((e^2)/3))*t;
A(109,98)=(((c*(a+c+e))/2)+((c^2)/6)+((e*(a+c))/2)+((e^2)/3))*t;
A(109,101)=(((e*(a+c))/2)+((e^2)/6))*t;
A(109,104)=((a^2)/3)*t;
A(109,107)=((a^2)/6)*t;
A(109,109)=(2*a+2*c+e)*(3*d+2*b);


B=zeros(109,1);
B(107,1)=V*(2*a+2*c+e);
B(109,1)=-V*t*(((2*a+2*c+e)^2)/2);

Errmax=1;
Xnew=zeros(109,1);
%Initial values of principal stresses
SigmaA1=0;SigmaA3=0;
SigmaB1=0;SigmaB3=0;
```

```
SigmaC1=0;SigmaC3=0;
SigmaD1=0;SigmaD3=0;
SigmaE1=0;SigmaE3=0;
SigmaF1=0;SigmaF3=0;
SigmaG1=0;SigmaG3=0;
SigmaH1=0;SigmaH3=0;
SigmaI1=0;SigmaI3=0;
SigmaJ1=0;SigmaJ3=0;
SigmaK1=0;SigmaK3=0;
SigmaL1=0;SigmaL3=0;
SigmaM1=0;SigmaM3=0;
SigmaN1=0;SigmaN3=0;
SigmaO1=0;SigmaO3=0;
SigmaP1=0;SigmaP3=0;
SigmaR1=0;SigmaR3=0;
SigmaS1=0;SigmaS3=0;
SigmaT1=0;SigmaT3=0;
SigmaU1=0;SigmaU3=0;
SigmaV1=0;SigmaV3=0;
SigmaW1=0;SigmaW3=0;
SigmaY1=0;SigmaY3=0;
SigmaZ1=0;SigmaZ3=0;
SigmaAA1=0;SigmaAA3=0;
SigmaBB1=0;SigmaBB3=0;
SigmaCC1=0;SigmaCC3=0;
SigmaDD1=0;SigmaDD3=0;
SigmaEE1=0;SigmaEE3=0;
SigmaFF1=0;SigmaFF3=0;
SigmaGG1=0;SigmaGG3=0;
SigmaHH1=0;SigmaHH3=0;
SigmaII1=0;SigmaII3=0;
SigmaJJ1=0;SigmaJJ3=0;
SigmaKK1=0;SigmaKK3=0;
SigmaLL1=0;SigmaLL3=0;

while Errmax>0.00001


[A(3,1),A(3,2),A(3,3),B(3,1)]=mohr(SigmaA1,SigmaA3,Sigmax_A,Sigmay_A,Tao_A,
Sc,St);

[A(6,4),A(6,5),A(6,6),B(6,1)]=mohr(SigmaB1,SigmaB3,Sigmax_B,Sigmay_B,Tao_B,
Sc,St);

[A(9,7),A(9,8),A(9,9),B(9,1)]=mohr(SigmaC1,SigmaC3,Sigmax_C,Sigmay_C,Tao_C,
Sc,St);

[A(12,10),A(12,11),A(12,12),B(12,1)]=mohr(SigmaD1,SigmaD3,Sigmax_D,Sigmay_D
,Tao_D,Sc,St);

[A(15,13),A(15,14),A(15,15),B(15,1)]=mohr(SigmaE1,SigmaE3,Sigmax_E,Sigmay_E
,Tao_E,Sc,St);

[A(18,16),A(18,17),A(18,18),B(18,1)]=mohr(SigmaF1,SigmaF3,Sigmax_F,Sigmay_F
,Tao_F,Sc,St);

[A(21,19),A(21,20),A(21,21),B(21,1)]=mohr(SigmaG1,SigmaG3,Sigmax_G,Sigmay_G
,Tao_G,Sc,St);
```

```
[A(24,22),A(24,23),A(24,24),B(24,1)]=mohr(SigmaH1,SigmaH3,Sigmax_H,Sigmay_H
,Tao_H,Sc,St);

[A(27,25),A(27,26),A(27,27),B(27,1)]=mohr(SigmaI1,SigmaI3,Sigmax_I,Sigmay_I
,Tao_I,Sc,St);

[A(30,28),A(30,29),A(30,30),B(30,1)]=mohr(SigmaJ1,SigmaJ3,Sigmax_J,Sigmay_J
,Tao_J,Sc,St);

[A(33,31),A(33,32),A(33,33),B(33,1)]=mohr(SigmaK1,SigmaK3,Sigmax_K,Sigmay_K
,Tao_K,Sc,St);

[A(36,34),A(36,35),A(36,36),B(36,1)]=mohr(SigmaL1,SigmaL3,Sigmax_L,Sigmay_L
,Tao_L,Sc,St);

[A(39,37),A(39,38),A(39,39),B(39,1)]=mohr(SigmaM1,SigmaM3,Sigmax_M,Sigmay_M
,Tao_M,Sc,St);

[A(42,40),A(42,41),A(42,42),B(42,1)]=mohr(SigmaN1,SigmaN3,Sigmax_N,Sigmay_N
,Tao_N,Sc,St);

[A(45,43),A(45,44),A(45,45),B(45,1)]=mohr(SigmaO1,SigmaO3,Sigmax_O,Sigmay_O
,Tao_O,Sc,St);

[A(48,46),A(48,47),A(48,48),B(48,1)]=mohr(SigmaP1,SigmaP3,Sigmax_P,Sigmay_P
,Tao_P,Sc,St);

[A(51,49),A(51,50),A(51,51),B(51,1)]=mohr(SigmaR1,SigmaR3,Sigmax_R,Sigmay_R
,Tao_R,Sc,St);

[A(54,52),A(54,53),A(54,54),B(54,1)]=mohr(SigmaS1,SigmaS3,Sigmax_S,Sigmay_S
,Tao_S,Sc,St);

[A(57,55),A(57,56),A(57,57),B(57,1)]=mohr(SigmaT1,SigmaT3,Sigmax_T,Sigmay_T
,Tao_T,Sc,St);

[A(60,58),A(60,59),A(60,60),B(60,1)]=mohr(SigmaU1,SigmaU3,Sigmax_U,Sigmay_U
,Tao_U,Sc,St);

[A(63,61),A(63,62),A(63,63),B(63,1)]=mohr(SigmaV1,SigmaV3,Sigmax_V,Sigmay_V
,Tao_V,Sc,St);

[A(66,64),A(66,65),A(66,66),B(66,1)]=mohr(SigmaW1,SigmaW3,Sigmax_W,Sigmay_W
,Tao_W,Sc,St);

[A(69,67),A(69,68),A(69,69),B(69,1)]=mohr(SigmaY1,SigmaY3,Sigmax_Y,Sigmay_Y
,Tao_Y,Sc,St);

[A(72,70),A(72,71),A(72,72),B(72,1)]=mohr(SigmaZ1,SigmaZ3,Sigmax_Z,Sigmay_Z
,Tao_Z,Sc,St);

[A(75,73),A(75,74),A(75,75),B(75,1)]=mohr(SigmaAA1,SigmaAA3,Sigmax_AA,Sigma
y_AA,Tao_AA,Sc,St);

[A(78,76),A(78,77),A(78,78),B(78,1)]=mohr(SigmaBB1,SigmaBB3,Sigmax_BB,Sigma
y_BB,Tao_BB,Sc,St);

[A(81,79),A(81,80),A(81,81),B(81,1)]=mohr(SigmaCC1,SigmaCC3,Sigmax_CC,Sigma
y_CC,Tao_CC,Sc,St);
```

```
[A(84,82),A(84,83),A(84,84),B(84,1)]=mohr(SigmaDD1,SigmaDD3,Sigmax_DD,Sigma
y_DD,Tao_DD,Sc,St);

[A(87,85),A(87,86),A(87,87),B(87,1)]=mohr(SigmaEE1,SigmaEE3,Sigmax_EE,Sigma
y_EE,Tao_EE,Sc,St);

[A(90,88),A(90,89),A(90,90),B(90,1)]=mohr(SigmaFF1,SigmaFF3,Sigmax_FF,Sigma
y_FF,Tao_FF,Sc,St);

[A(93,91),A(93,92),A(93,93),B(93,1)]=mohr(SigmaGG1,SigmaGG3,Sigmax_GG,Sigma
y_GG,Tao_GG,Sc,St);

[A(96,94),A(96,95),A(96,96),B(96,1)]=mohr(SigmaHH1,SigmaHH3,Sigmax_HH,Sigma
y_HH,Tao_HH,Sc,St);

[A(99,97),A(99,98),A(99,99),B(99,1)]=mohr(SigmaII1,SigmaII3,Sigmax_II,Sigma
y_II,Tao_II,Sc,St);

[A(102,100),A(102,101),A(102,102),B(102,1)]=mohr(SigmaJJ1,SigmaJJ3,Sigmax_J
J,Sigmay_JJ,Tao_JJ,Sc,St);

[A(105,103),A(105,104),A(105,105),B(105,1)]=mohr(SigmaKK1,SigmaKK3,Sigmax_K
K,Sigmay_KK,Tao_KK,Sc,St);

[A(108,106),A(108,107),A(108,108),B(108,1)]=mohr(SigmaLL1,SigmaLL3,Sigmax_L
L,Sigmay_LL,Tao_LL,Sc,St);



Xold=[Sigmax_A;Sigmay_A;Tao_A;Sigmax_B;Sigmay_B;Tao_B;Sigmax_C;Sigmay_C;Tao
_C;Sigmax_D;Sigmay_D;Tao_D;Sigmax_E;Sigmay_E;Tao_E;Sigmax_F;Sigmay_F;Tao_F;
Sigmax_G;Sigmay_G;Tao_G;Sigmax_H;Sigmay_H;Tao_H;Sigmax_I;Sigmay_I;Tao_I;Sig
max_J;Sigmay_J;Tao_J;Sigmax_K;Sigmay_K;Tao_K;Sigmax_L;Sigmay_L;Tao_L;Sigmax
_M;Sigmay_M;Tao_M;Sigmax_N;Sigmay_N;Tao_N;Sigmax_O;Sigmay_O;Tao_O;Sigmax_P;
Sigmay_P;Tao_P;Sigmax_R;Sigmay_R;Tao_R;Sigmax_S;Sigmay_S;Tao_S;Sigmax_T;Sig
may_T;Tao_T;Sigmax_U;Sigmay_U;Tao_U;Sigmax_V;Sigmay_V;Tao_V;Sigmax_W;Sigmay
_W;Tao_W;Sigmax_Y;Sigmay_Y;Tao_Y;Sigmax_Z;Sigmay_Z;Tao_Z;Sigmax_AA;Sigmay_A
A;Tao_AA;Sigmax_BB;Sigmay_BB;Tao_BB;Sigmax_CC;Sigmay_CC;Tao_CC;Sigmax_DD;Si
gmay_DD;Tao_DD;Sigmax_EE;Sigmay_EE;Tao_EE;Sigmax_FF;Sigmay_FF;Tao_FF;Sigmax
_GG;Sigmay_GG;Tao_GG;Sigmax_HH;Sigmay_HH;Tao_HH;Sigmax_II;Sigmay_II;Tao_II;
Sigmax_JJ;Sigmay_JJ;Tao_JJ;Sigmax_KK;Sigmay_KK;Tao_KK;Sigmax_LL;Sigmay_LL;T
ao_LL;H];

          Xnew=A\B;
            Delta=Xnew-Xold;
            Err=Delta./Xnew;
            Errmax=max(abs(Err));
            Sigmax_A=Xnew(1,1);
            Sigmay_A=Xnew(2,1);
            Tao_A=Xnew(3,1);
            Sigmax_B=Xnew(4,1);
            Sigmay_B=Xnew(5,1);
            Tao_B=Xnew(6,1);
            Sigmax_C=Xnew(7,1);
            Sigmay_C=Xnew(8,1);
            Tao_C=Xnew(9,1);
            Sigmax_D=Xnew(10,1);
            Sigmay_D=Xnew(11,1);
            Tao_D=Xnew(12,1);
```

```
Sigmax_E=Xnew(13,1);
Sigmay_E=Xnew(14,1);
Tao_E=Xnew(15,1);
Sigmax_F=Xnew(16,1);
Sigmay_F=Xnew(17,1);
Tao_F=Xnew(18,1);
Sigmax_G=Xnew(19,1);
Sigmay_G=Xnew(20,1);
Tao_G=Xnew(21,1);
Sigmax_H=Xnew(22,1);
Sigmay_H=Xnew(23,1);
Tao_H=Xnew(24,1);
Sigmax_I=Xnew(25,1);
Sigmay_I=Xnew(26,1);
Tao_I=Xnew(27,1);
Sigmax_J=Xnew(28,1);
Sigmay_J=Xnew(29,1);
Tao_J=Xnew(30,1);
Sigmax_K=Xnew(31,1);
Sigmay_K=Xnew(32,1);
Tao_K=Xnew(33,1);
Sigmax_L=Xnew(34,1);
Sigmay_L=Xnew(35,1);
Tao_L=Xnew(36,1);
Sigmax_M=Xnew(37,1);
Sigmay_M=Xnew(38,1);
Tao_M=Xnew(39,1);
Sigmax_N=Xnew(40,1);
Sigmay_N=Xnew(41,1);
Tao_N=Xnew(42,1);
Sigmax_O=Xnew(43,1);
Sigmay_O=Xnew(44,1);
Tao_O=Xnew(45,1);
Sigmax_P=Xnew(46,1);
Sigmay_P=Xnew(47,1);
Tao_P=Xnew(48,1);
Sigmax_R=Xnew(49,1);
Sigmay_R=Xnew(50,1);
Tao_R=Xnew(51,1);
Sigmax_S=Xnew(52,1);
Sigmay_S=Xnew(53,1);
Tao_S=Xnew(54,1);
Sigmax_T=Xnew(55,1);
Sigmay_T=Xnew(56,1);
Tao_T=Xnew(57,1);
Sigmax_U=Xnew(58,1);
Sigmay_U=Xnew(59,1);
Tao_U=Xnew(60,1);
Sigmax_V=Xnew(61,1);
Sigmay_V=Xnew(62,1);
Tao_V=Xnew(63,1);
Sigmax_W=Xnew(64,1);
Sigmay_W=Xnew(65,1);
Tao_W=Xnew(66,1);
Sigmax_Y=Xnew(67,1);
Sigmay_Y=Xnew(68,1);
Tao_Y=Xnew(69,1);
Sigmax_Z=Xnew(70,1);
Sigmay_Z=Xnew(71,1);
Tao_Z=Xnew(72,1);
```

```
            Sigmax_AA=Xnew(73,1);
            Sigmay_AA=Xnew(74,1);
            Tao_AA=Xnew(75,1);
            Sigmax_BB=Xnew(76,1);
            Sigmay_BB=Xnew(77,1);
            Tao_BB=Xnew(78,1);
            Sigmax_CC=Xnew(79,1);
            Sigmay_CC=Xnew(80,1);
            Tao_CC=Xnew(81,1);
            Sigmax_DD=Xnew(82,1);
            Sigmay_DD=Xnew(83,1);
            Tao_DD=Xnew(84,1);
            Sigmax_EE=Xnew(85,1);
            Sigmay_EE=Xnew(86,1);
            Tao_EE=Xnew(87,1);
            Sigmax_FF=Xnew(88,1);
            Sigmay_FF=Xnew(89,1);
            Tao_FF=Xnew(90,1);
            Sigmax_GG=Xnew(91,1);
            Sigmay_GG=Xnew(92,1);
            Tao_GG=Xnew(93,1);
            Sigmax_HH=Xnew(94,1);
            Sigmay_HH=Xnew(95,1);
            Tao_HH=Xnew(96,1);
            Sigmax_II=Xnew(97,1);
            Sigmay_II=Xnew(98,1);
            Tao_II=Xnew(99,1);
            Sigmax_JJ=Xnew(100,1);
            Sigmay_JJ=Xnew(101,1);
            Tao_JJ=Xnew(102,1);
            Sigmax_KK=Xnew(103,1);
            Sigmay_KK=Xnew(104,1);
            Tao_KK=Xnew(105,1);
            Sigmax_LL=Xnew(106,1);
            Sigmay_LL=Xnew(107,1);
            Tao_LL=Xnew(108,1);
            H=Xnew(109,1);
            Xnew;
end
```

E. Internal Stresses and Stress Distribution of Masonry Wall without Opening

Solid masonry wall case study is analyzed for the ultimate condition which is 897 kN vertical load as presented in Figure 0.1 with dimension 500x300 cm and thickness as 30 cm. Compressive and tensile strength values are 11 MPa and 0.55 MPa respectively. As a result, sample internal stress values are given in Table 0.1 and distribution plots for normal and shear stresses are illustrated in Figure 0.2, Figure 0.3 and Figure 0.4, respectively.

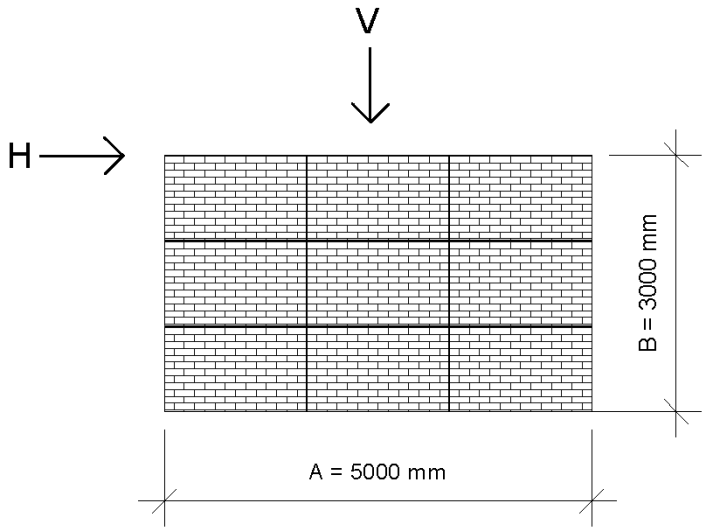

Figure 0.1. Solid masonry wall under ultimate condition

Table 0.1. *Results of internal stresses of masonry wall without opening under maximum vertical load according to Matlab2017b*

NODE	σ_X (MPa)	σ_Y (MPa)	τ (MPa)
A	0.48047	-1.16594	0.13316
B	-0.45814	-1.64320	1.35012
C	-0.58265	0.17844	0.59545
D	-0.48047	0.50746	-0.13316
E	-0.48047	0.50746	-0.13316
F	-0.22832	-1.78636	1.20539
G	-0.10381	-0.40886	0.74018
H	0.48047	0.29498	0.13316
I	0.48047	0.29498	0.13316
J	-0.10381	-0.40886	0.74018
K	-0.22832	-1.78636	1.20539
L	-0.48047	0.50746	-0.13316
M	-0.48047	0.50746	-0.13316
N	-0.58265	0.17844	0.59545
O	-0.45814	-1.64320	1.35012
P	0.48047	-1.16594	0.13316

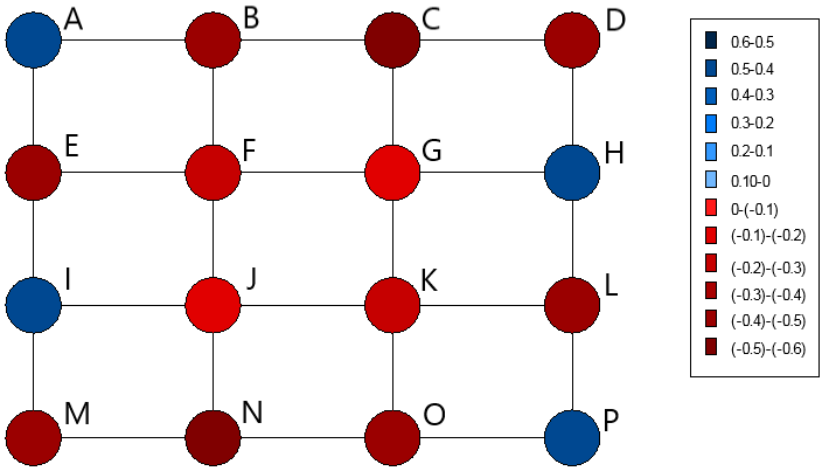

Figure 0.2. Distribution of σ_x on nodes of the wall

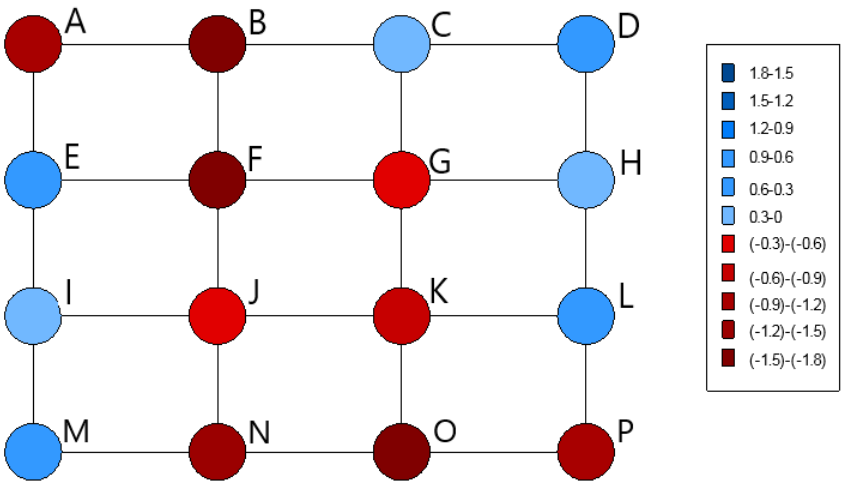

Figure 0.3. Distribution of σ_y on nodes of the wall

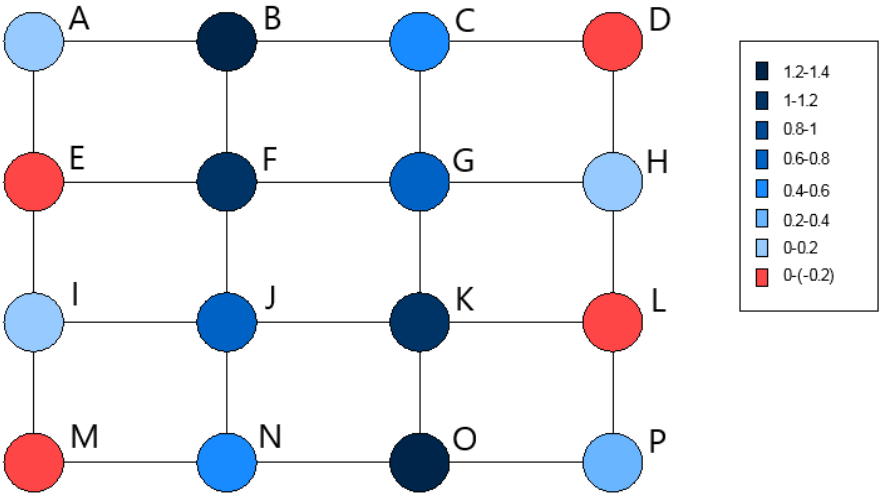

Figure 0.4. Distribution of τ on nodes of the wall